ENHANCEMENT OF AGRICULTURAL RESIDUE ASH REACTIVITY IN CONCRETE THROUGH THE USE OF BIOFUEL PRETREATMENTS

by

FERAIDON FARAHMAND ATAIE

B.Sc., KABUL UNIVERSITY, AFGHANISTAN, 2006
M.Sc., KANSAS STATE UNIVERSITY, USA, 2010

AN ABSTRACT OF A DISSERTATION

submitted in partial fulfillment of the requirements for the degree

DOCTOR OF PHILOSOPHY

DEPARTMENT OF CIVIL ENGINEERING
COLLEGE OF ENGINEERING

KANSAS STATE UNIVERSITY
Manhattan, Kansas

2013

Abstract

The cement industry is an important component in the quest to reduce global greenhouse gas emissions because of vast amounts of cement used annually. Incorporating supplementary cementitious materials (SCMs) into concrete is one alternative to reduce cement production and thereby reduce greenhouse gas emissions. This study investigated three types of agricultural residues, namely corn stover, wheat straw, and rice straw, in addition to bioethanol byproducts as potential resources for SCM production for concrete applications. Pretreatments, commonly used in bioethanol production, were used to improve pozzolanic reactivity of corn stover ash (CSA), wheat straw ash (WSA), and rice straw ash (RSA) in cementitious systems.

In the first part of this research, the impact of distilled water and dilute hydrochloric acid pretreatments on pozzolanic reactivity of WSA, RSA, and CSA were studied. Results showed that pretreatments, particularly dilute acid, improved pozzolanic properties of CSA, WSA, and RSA by removing potassium and phosphorous from the biomass prior to ashing. In addition, WSA and RSA were shown to have similar pozzolanic reactivity to that of silica fume.

In the second part of this study, suitability of high lignin residue (HLR), a bioethanol byproduct, for SCM production was investigated. It was shown that burning high lignin residue produces HLR ash that is very reactive in cementitious materials and can be used as a reactive SCM in concrete.

The impact of each step in the production of bioethanol on the quality of bioethanol byproduct for subsequent burning and use in concrete was also studied. Sodium hydroxide and sulfuric acid pretreatments and enzymatic hydrolysis were used. Results revealed that sodium hydroxide pretreatment of the biomass have negative impact on biomass ash properties for concrete use because sodium hydroxide pretreatment did not remove phosphorous and other crystalline phases out of the biomass. However, sulfuric acid pretreatment of biomass greatly improved ash properties. It was also shown that enzymatic hydrolysis could have beneficial impact on ash properties because, during enzymatic hydrolysis, some phosphorous was leached out of the biomass.

ENHANCEMENT OF AGRICULTURAL RESIDUE ASH REACTIVITY IN CONCRETE THROUGH THE USE OF BIOFUEL PRETREATMENTS

by

FERAIDON FARAHMAND ATAIE

B.Sc., KABUL UNIVERSITY, AFGHANISTAN, 2006
M.Sc., KANSAS STATE UNIVERSITY, USA, 2010

A DISSERTATION

submitted in partial fulfillment of the requirements for the degree

DOCTOR OF PHILOSOPHY

DEPARTMENT OF CIVIL ENGINEERING
COLLEGE OF ENGINEERING

KANSAS STATE UNIVERSITY
Manhattan, Kansas

2013

Approved by:

Major Professor
Dr. Kyle A. Riding

Copyright

Abstract

The cement industry is an important component in the quest to reduce global greenhouse gas emissions because of vast amounts of cement used annually. Incorporating supplementary cementitious materials (SCMs) into concrete is one alternative to reduce cement production and thereby reduce greenhouse gas emissions. This study investigated three types of agricultural residues, namely corn stover, wheat straw, and rice straw, in addition to bioethanol byproducts as potential resources for SCM production for concrete applications. Pretreatments, commonly used in bioethanol production, were used to improve pozzolanic reactivity of corn stover ash (CSA), wheat straw ash (WSA), and rice straw ash (RSA) in cementitious systems.

In the first part of this research, the impact of distilled water and dilute hydrochloric acid pretreatments on pozzolanic reactivity of WSA, RSA, and CSA were studied. Results showed that pretreatments, particularly dilute acid, improved pozzolanic properties of CSA, WSA, and RSA by removing potassium and phosphorous from the biomass prior to ashing. In addition, WSA and RSA were shown to have similar pozzolanic reactivity to that of silica fume.

In the second part of this study, suitability of high lignin residue (HLR), a bioethanol byproduct, for SCM production was investigated. It was shown that burning high lignin residue produces HLR ash that is very reactive in cementitious materials and can be used as a reactive SCM in concrete.

The impact of each step in the production of bioethanol on the quality of bioethanol byproduct for subsequent burning and use in concrete was also studied. Sodium hydroxide and sulfuric acid pretreatments and enzymatic hydrolysis were used. Results revealed that sodium hydroxide pretreatment of the biomass have negative impact on biomass ash properties for concrete use because sodium hydroxide pretreatment did not remove phosphorous and other crystalline phases out of the biomass. However, sulfuric acid pretreatment of biomass greatly improved ash properties. It was also shown that enzymatic hydrolysis could have beneficial impact on ash properties because, during enzymatic hydrolysis, some phosphorous was leached out of the biomass.

Table of Contents

List of Figures

List of Tables

Acknowledgements

I would like to acknowledge the National Science Foundation for providing financial support for this study.

I would like to express my sincere appreciation to my academic advisor, Kyle A. Riding, for his continuous academic guidance and financial support. Without his help and persistent patience, I would have not been able to finish this dissertation. It was my pleasure to work in a mutually respective research environment provided by Dr. Riding. I am also grateful to Dr. Riding for providing me the financial support for a one year research associate position in the civil engineering department at Kansas State University.

I thank all the staff and faculty members of the civil engineering department at Kansas State University. I am thankful to Antoine Borden for his assistance throughout this research. I am grateful for Dr. Maria Juenger from The University of Texas department of civil, architectural and environmental engineering for her academic advice throughout my Ph.D. research.

Special thanks go to my wife, Atia, for all the sacrifices she made for me to finish this degree. Her support and encouragements were priceless. I am indebted to her patience and efforts. I am also grateful to my supportive and persuasive parents; without their support, I would not be the person I am today.

Dedication

To my wife, Atia.

Chapter 1 - Introduction

1.1 Background:

Concrete is the most commonly used construction material worldwide, and second only to water in terms of resource usage on Earth [1.1]. Widespread use of concrete compared to other building materials is attributed to its excellent fire and water resistance, ease of transporting and shaping to desired forms, and wide availability at low cost [1.2]. Concrete consists of three main ingredients: portland cement, water, and aggregate. Portland cement comprises 10-15% of concrete by weight and strengthens the concrete through hydration, a chemical reaction with water.

Portland cement is produced by heating calcium and silica-bearing minerals, such as limestone and clay, to approximately 1450^{o}C in a kiln. The calcium-bearing mineral, usually limestone, is heated to drive off carbon dioxide (CO_2) from the raw material, leaving calcium oxide. The material feeds into a rotating kiln and is heated up to 1450°C. The material is then sintered together, forming nodules of clinker that are cooled rapidly upon exiting the kiln. The most important phases of clinker are tricalcium silicate ($3CaO.SiO_2$), dicalcium silicate ($2CaO.SiO_2$), tricalcium aluminate ($3CaO.Al_2O_3$), and tetracalcium aluminoferrite ($4CaO.\ Al_2O_3.\ Fe_2O_3$). Proportions of these phases depend on the proportion of raw materials and kiln temperatures. Finally, the clinker is mixed with gypsum, ground to become portland cement, and distributed for use. The cement manufacturing process is summarized in Figure 1.1.

The process of cement production is an energy intensive process. Production of one tonne of cement in the United States generates nearly one tonne of CO_2 [1.3]. Approximately 50% to 60% of this carbon dioxide originates from calcination of raw materials, while the remainder is

produced from manufacturing and fossil fuel burning to heat raw materials [1.3]. Because of the vast amount of cement used worldwide, the cement industry is responsible for the release of large quantities of CO_2 into the atmosphere. The industry, however, is currently seeking strategies to mitigate CO_2 emissions from cement production. Incorporating supplementary cementitious materials (SCMs) into concrete is a potential viable alternative to reduce portland cement use and, hence, reduce CO_2 emissions [1.4].

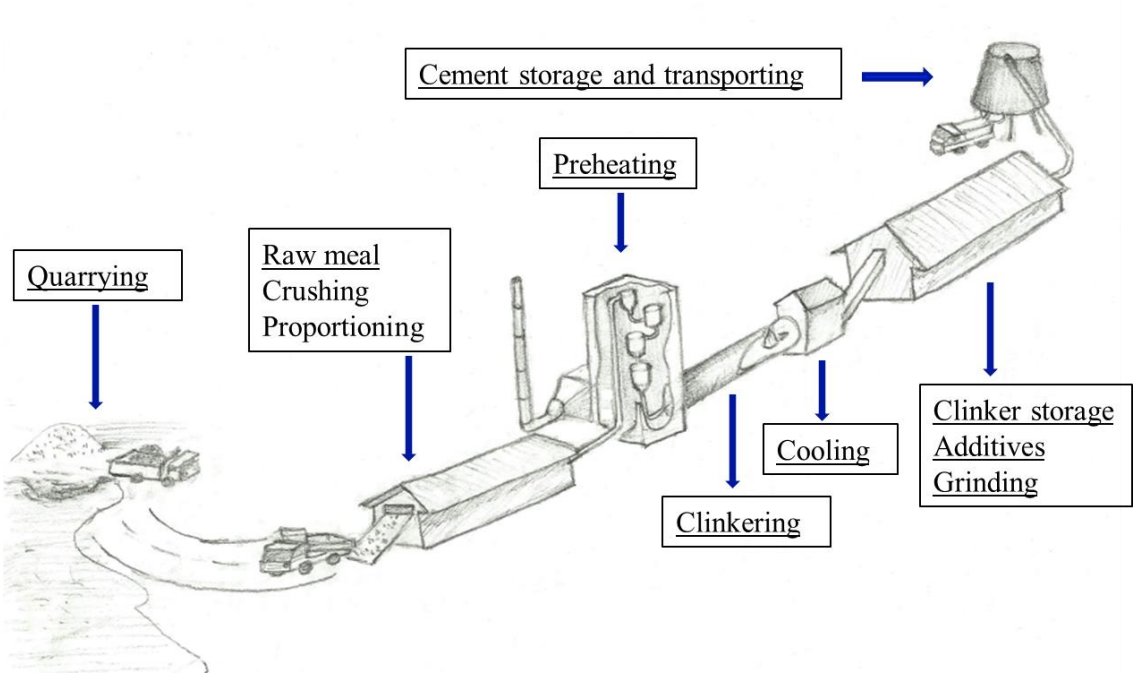

Figure 1.1: Simplified cement production process

(figure by Atia Ataie and used with permission)

Currently, SCMs, particularly industrial by-products, are used to partially replace portland cement in concrete. Fly ash, silica fume, and slag cement are examples of SCMs that are waste products from industrial processes. However, these materials are not available in large quantities at a low cost uniformly around the world. Natural SCMs such as volcanic ash, calcined clays, and agricultural residue ash (ARA) are gaining more attention for use as SCMs because of their low cost, availability, and excellent reactivity in concrete.

Every year, millions of tonnes of agricultural residues such as corn stover, wheat straw, and rice straw are produced worldwide [1.5]. Agricultural residue ash (ARA) such as corn stover ash (CSA), rice straw ash (RSA), and wheat straw ash (WSA) are potential resources for SCM production. Although pozzolanic properties of rice husk ash (RHA) are well established [1.6] [1.7], few studies have been performed on utilization of WS and RS for SCM production for concrete use [1.7] [1.8] [1.9] [1.10] [1.11]. Various pretreatments, including dilute hydrochloric acid, improve pozzolanic behavior of RHA by increasing the ash surface area and amorphous content [1.6]. Surface area and amorphous silica content of SCMs are important factors for determining potential reactivity of materials because they provide nucleation sites and reactive silica for calcium silicate hydrate (C-S-H) precipitation and production in cementitious systems [1.12]. Production of reactive agricultural residue ash is of great interest, particularly for developing countries where agricultural residues are widely available but other SCMs are not available at low cost.

Agricultural residues are potential renewable resources for biofuel production [1.13] [1.14] [1.15]. As lignocellulosic materials, corn stover, wheat straw, and rice straw are converted to liquid fuels by using either thermochemical or biochemical pathways [1.16] [1.17]. In the thermochemical route, lignocellulosic materials undergo either pyrolysis or gasification to produce syngas. Syngas is then upgraded to fuels such as ethanol and methanol [1.18] [1.19]. In the biochemical pathway, microorganisms convert lignocellulosic materials to fuels such as ethanol and methanol [1.18] [1.20]. During biochemical conversion, lignocellulosic materials undergo pretreatments, enzymatic hydrolysis, and fermentation [1.18]. Pretreatment methods such as dilute acid have been used to reduce the degree of cellulose polymerization and remove and breakdown hemicellulose and lignin structures in lignocellulosic materials [1.21]. The

primary purpose of pretreatments is to increase available surface area of the cellulose to hydrolytic enzymes, thus increasing bioethanol yield [1.18] [1.17] [1.16]. Enzymatic hydrolysis is used to breakdown cellulose and hemicellulose to glucose and other sugars. After enzymatic hydrolysis, sugars are fermented to ethanol.

Utilization of agricultural residues in concrete and biofuel industries may create future concerns about sufficient availability of agricultural residues. Biofuel byproducts are potential feedstock material for making SCMs for use in concrete. Byproducts of biofuel are biomass char and high lignin residue (HLR). Thermochemical conversion of biomass produces biomass char, and biochemical conversion of biomass produces HLR. Utilization of these byproducts for SCM production could create new revenue for the biofuel industry, leading to a more sustainable biofuel production and more sustainable and durable concrete.

1.2 Portland cement hydration:

Hydration of portland cement consists of multiple simultaneous and interdependent chemical reactions of its major phases. Notations and abbreviations used in cement chemistry are shown in Table 1.1.

Table 1.1: Common notations and abbreviations in cement chemistry

Oxide	Oxide abbreviation	Compound Name	Compound Formula	Compound notation
CaO	C	Ticalcium Silicate	$3CaO.SiO_2$	C_3S
SiO_2	S	Dicalcium Silicate	$2CaO.SiO_2$	C_2S
Al_2O_3	A	Tricalcium Aluminate	$3CaO.Al_2O_3$	C_3A
Fe_2O_3	F	Tetracalcium aluminoferrite	$4CaO.\ Al_2O_3.\ Fe_2O_3$	C_4AF
SO_3	$\hat{S}$	gypsum	$CaSO_4.2H_2O$	$C\hat{S}H_2$
H2O	H	Calcium Silicate Hydrate	$3CaO.SiO_2.3H_2O$	$C_3S_2H_3$

Hydration reactions of C_3S and C_2S are shown in Eq.1.1 and Eq.1.2, respectively. Both reactions produce calcium silicate hydrate (C-S-H) and calcium hydroxide (CH), but the quantity of CH

produced by C_2S is less when compared to C_3S. Eq.1.3 and Eq.1.4 give the hydration reaction of C_3A and C_4AF phases, respectively.

$$2C_3S + 6H \rightarrow C_3S_2H_3 + 3.(Ca(OH)_2) \qquad \text{Eq.1.1}$$

$$2C_2S + 4H \rightarrow C_3S_2H_3 + Ca(OH)_2 \qquad \text{Eq.1.2}$$

$$C_3A + 3C\bar{S}H_2 + 26H \rightarrow C_6A\bar{S}_3H_{32} \qquad \text{Eq.1.3}$$

$$C_4AF + 3C\bar{S}H_2 + 21H \rightarrow C_6(A,F)\bar{S}_3H_{32} + (F,A)H_3 \qquad \text{Eq.1.4}$$

Portland cement hydration can be divided into four stages, as indicated in Figure 1.2 [1.22] [23]. The first stage is called the dissolution period, followed by a slow reaction or induction period. The third period is the acceleration period, and the fourth period is deceleration. Upon direct contact with water, some tricalcium silicate (C_3S) rapidly dissolves in water. The dissolution reaction is shown in Eq.1.5 [1.22]. This reaction dissipates high amounts of heat, as indicated by stage 1 in Figure 1.2. As dissolution of C_3S continues, the solution saturation, with respect to Ca and Si ions, increases in a few minutes. As solution saturation approaches supersaturation, the reaction rate of C_3S decreases, as does the heat evolution [1.23]. This induction period of hydration is indicated as stage 2 in Figure 1.2. When the solution is supersaturated with respect to Ca and Si ions, calcium silicate hydrate ($3CaO.SiO_2.8H_2O$) nucleates and grows. This process decreases the concentrations of Ca and Si ions in the solution, and C_3S dissolves again at a higher rate. The higher rate of C_3S dissolution, nucleation and growth of C-S-H, and calcium hydroxide precipitation seen in the acceleration period as stage 3 in Figure 1.2 is also accompanied by a large heat release. The complete chemical reaction of tricalcium silicate with water is shown in Eq.1.1. Growth of C-S-H consumes water, reduces free space, and reduces cement grain access to water. As a result, the reaction slows down, as shown in the deceleration period in stage 4, Figure 1.2. Although the reaction rate of portland cement

becomes slow after 24 hours, hydration continues until all the portland cement is reacted or until the system is depleted of free water to react.

$$3CaO.SiO_2 + 3H_2O \rightarrow 3Ca^{2+} + H_2SiO_4^{2-} + 4(OH)^{1-} \qquad \text{Eq.1.5}$$

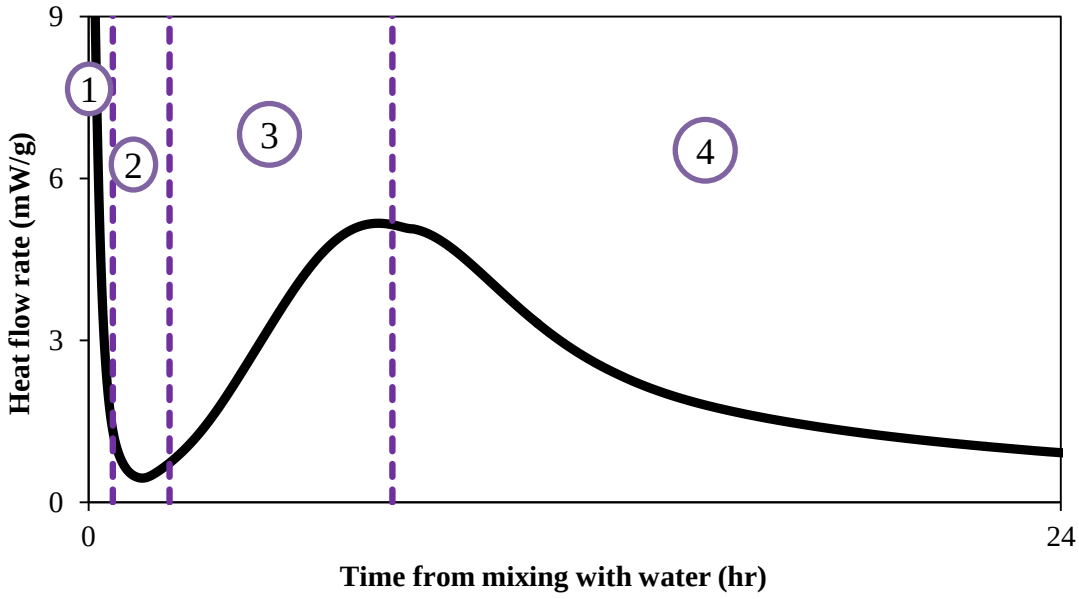

Figure 1.2: Portland cement hydration

1.3 Behavior of SCMs in cementitious systems:

Supplementary cementitious materials (SCMs) can be divided into two groups: pozzolanic and hydraulic. Pozzolanic SCMs, such as silica fume, react with calcium hydroxide in cementitious systems to produce calcium silica hydrate (C-S-H). Hydraulic SCMs, such as class C fly ash and blast furnace slag, react with water to form binding phases in addition to pozzolanic reaction [1.12]. The pozzolanic reaction is a reaction that occurs between a siliceous material and calcium hydroxide (CH) underwater to form C-S-H, as shown in Eq.1.6. As previously discussed, hydration silicate of phases of portland cement produces C-S-H and calcium hydroxide (CH). C-S-H is responsible for most of the compressive strength of concrete.

CH has a tendency to precipitate onto the aggregate surface in concrete, leading to a weak zone around the aggregate, called the interfacial transition zone (ITZ) [1.24] [1.25]. When SCMs are added to concrete, the silica compound in SCM reacts with CH to produce additional C-S-H. Reduction of CH in concrete improves the ITZ and increases C-S-H production in concrete. Over time, the pozzolanic reaction reduces porosity of concrete and size of the interfacial transition zone (ITZ) while increasing concrete strength [1.12] [1.26] [1.25] [1.27] [1.28] [1.29] [1.30]. Depending on the composition of SCMs, they can replace large percentages of portland cement used in conventional concrete. Utilization of SCMs in concrete materials reduces the cement content of concrete, reduces the carbon footprint of concrete materials, and improves the durability of concrete.

$$CH + S + H \rightarrow C - S - H \qquad \text{Eq.1.6}$$

The rate of pozzolanic reaction depends on the chemical and physical properties of SCMs, but the rate is much slower as compared to that of C_3S. Amorphous content and surface area are important factors affecting the pozzolanic reaction rate. ARAs can be highly reactive SCMs. ARAs can have high amorphous content and high surface area. The production process of ARAs, however, largely influences the composition and, hence, the pozzolanic reactivity of ARAs.

1.4 Scope of the research:

The goal of this research was to apply biofuel pretreatment methods to agricultural residues in order to produce highly reactive SCMs. Knowledge gained about the effects of biofuel pretreatments was used to examine the suitability of cellulosic ethanol byproducts for use as an SCM in concrete. Objectives of the research were accomplished by:

1- Studying the impact of distilled water and dilute acid pretreatments on pozzolanic properties of rice straw ash (RSA), wheat straw ash (WSA), and corn stover ash (CSA). Several burning conditions were used to prepare the ash samples. The impact of pretreatments on physical and chemical properties of ARA samples were also determined based on surface area, loss on ignition (LOI), and amorphous silica content of the ash samples. Reactivity of the ARAs was quantified using heat of hydration, calcium hydroxide consumption of cement paste samples containing ash samples, and mortar cube compressive strength. Twenty percent of the cement was replaced by ash when used, and results were compared to ash samples without pretreatments.
2- Studying the suitability of high lignin residue (HLR) for producing reactive SCMs. The influence of distilled water and dilute acid pretreatments on pozzolanic properties of CSA was also studied. HLR was a byproduct of bioethanol production from corn stover. Pozzolanic behavior of HLR ash was determined using methods mentioned previously. In addition, reactivity of HLR ash was compared to that of the CSA.
3- Exploring the impact of sodium hydroxide and dilute sulfuric acid pretreatments and enzymatic hydrolysis on properties of CSA, WSA, and RSA for concrete use. This was performed to study the impact of various bioethanol pretreatments on properties of bioethanol byproduct for SCM production.
4- Studying the influence of pretreatments on thermal degradation of agricultural residues.
5- Comparing pozzolanic behavior of pretreated ARA with that of silica fume.

1.5 Organization of dissertation:

Chapter two discusses details and findings as to the impact of pretreatments on pozzolanic properties and behavior of wheat straw ash and rice straw ash. Pozzolanic behavior

of high lignin residue ash and the impact of pretreatments on pozzolanic properties of corn stover ash are documented in the third chapter. Chapter four explores the impact of pretreatments and alkali and alkaline earth metals (AAEMs) on the thermal degradation of corn stover, wheat straw, and rice straw. The impact of enzymatic hydrolysis and sodium hydroxide and sulfuric acid pretreatments on corn stover, wheat straw, and rice straw is documented in chapter five. The influence of rice straw ash on the adsorption of air entraining agents in cementitious systems is discussed in chapter six. Chapter seven compares pozzolanic behavior of pretreated wheat straw ash and rice straw ash with that of silica fume. Although each chapter draws unique conclusions, generalized conclusions and recommendations for future research are explained in chapter eight. References are given in chapter nine.

Chapter 2 - Thermochemical Pretreatments for Agricultural Residue Ash Production for Concrete

Abstract:

Agricultural residue ash is known to be a very reactive source of supplementary cementitious material (SCM) for use in concrete. The influence of thermochemical pretreatments on the reactivity of agricultural residue ash (ARA) for use as an SCM was studied. It was shown that pretreatments are effective in partial removal of alkali metals and other impurities out of both wheat straw and rice straw leading to ARA with lower loss on ignition (LOI), higher internal surface area, and higher amorphous silica content than that of unpretreated ARA. It was shown that the ash alkali content correlated with the ash LOI and amorphous silica content. When used at a cement replacement rate of 20% by mass, pretreated ARA accelerated the hydration of cement paste samples while unpretreated ARA retarded the cement hydration. Pretreatments were found to increase ARA reactivity as measured by calcium hydroxide content reduction with time. ARA increased compressive strength of mortar samples by 25% when used as 20% replacement of cement in the samples. It was found that the CH content of paste samples and mortar compressive strength were correlated to the amorphous silica content of the ash.

2.1 Introduction:

The use of supplementary cementitious material (SCM) can reduce the energy and CO_2 intensity of concrete. Natural SCMs have received increasing interest because of their high reactivity, low cost, and availability in some regions where other SCMs are not available. Agricultural residue ash (ARA) such as rice husk ash (RHA) and sugarcane bagasse ash have been championed as SCMs that can greatly enhance strength and durability of concrete [2.1] [2.2] [2.3] [2.4] [2.5] [2.6]. Other agro-biomass such as wheat straw (WS) and rice straw (RS) could be a potential source for SCMs with similar pozzolanic reactivity to RHA. Pozzolanic reaction is a reaction between a siliceous material and calcium hydroxide (CH) under water to form a cementitious material, as shown in Eq.2.1.

$$CH + S + H \rightarrow CSH \qquad \text{Eq.2.1}$$

Note: Oxide notation is used throughout this paper, C = CaO, S = SiO_2, H=H_2O, A = Al_2O_3, F=Fe_2O_3.

The pozzolanic reaction kinetics is known to be affected by many factors such as ash mineralogy, surface area, and carbon content of the pozzolanic materials [2.7] [2.8].

Agro-biomass pretreatment processes can enhance ARA reactivity for use in concrete. Thermochemical pretreatment techniques, such as dilute acid, have been shown to improve pozzolanic reactivity by increasing surface area and amorphous silica content and decreasing carbon content of RHA [2.7] [2.9]. In the biofuel industry, thermochemical pretreatment of lignocellulosic biomass has proven to be very effective hydrolysis process for ethanol production [2.10] [2.11] [2.12]. The dilute acid pretreatments are effective in removal of some hemicellulose; breakdown, re-localization, and structure change of lignin; and defibration/decrystallization of cellulose of the biomass cell wall. Pretreatment of agro-biomass

has been shown to improve combustion properties of biomass for use as a fuel as a result of leaching impurities such as Na, K, Ca, and Mg [2.13]. These metals decrease the biomass melting temperature and promote the release of unwanted byproducts during combustion [2.13].

The pozzolanic properties of rice straw ash (RSA) and wheat straw ash (WSA) have been examined by only a few researchers. WSA that has not been pretreated has been found to be pozzolanically reactive when burned at 570^{o}C and 670^{o}C for 5 hours [2.14]. Al-Akhras and Abu-Alfoul [2.15] have reported that mechanical properties of autoclaved mortar specimens were improved with by WSA made by burning wheat straw at 650^{o}C for 20 hrs. RSA has been shown to improve mechanical properties of mortar and concrete specimens through a pozzolanic reaction [2.16]. One study showed that rice straw pretreated with hydrolysis could produce good quality ash for use in concrete; however no comparison with unpretreated rice straw ash was made to quantify the benefits of pretreatment [2.17]. The impact of thermochemical pretreatments on the RSA and WSA sensitivity to burning conditions and subsequent reactivity in a cementitious system has not been studied. Additionally, the mechanism by which pretreatments improve ARA pozzolanicity has not been fully established.

This paper documents the effects of thermochemical pretreatments on the physical properties, chemical properties, and reactivity of WSA and RSA in a cementitious system. Employing several pretreatments techniques and burning conditions, this study attempts to examine the mechanism(s) by which pretreatments enhance ARA reactivity. Distilled water (DW) and 0.1 N hydrochloric acid (HCl) were used to pretreat the biomass at 23^{o}C, 50^{o}C and 80^{o}C for several soaking durations followed by burning at 500^{o}C, 650^{o}C, 700^{o}C, and 800^{o}C. Loss on ignition (LOI), internal surface area, and amorphous silica content of ARA were measured for these ashes. Isothermal calorimetry, thermogravimetric analysis, electrical

conductivity measurements, and mortar compressive strength were used to quantify the ARA reactivity.

2.2 Materials:

An ASTM [2.18] Type I/II portland cement was used for this study with the cement properties shown in Table 2.1. Standard graded sand (ASTM 2006) was used for the mortar experiments. Wheat straw (WS) was purchased from Britt's farm in Manhattan, KS and Rice straw (RS) was obtained from Missouri Rice Research Farm, Glennonville, Missouri. Reagent grade HCl was obtained and diluted to 0.1 N for use in the study.

Table 2.1: ASTM C 150 Type I/II ordinary portland cement (OPC) Composition

Chemical Composition (wt%)	
SiO_2	21.85
Fe_2O_3	3.4
Al_2O_3	4.35
CaO	64.19
MgO	1.79
K_2O	0.52
Na_2O	0.17
SO_3	2.77
LOI	0.89
Blaine Surface area= 362 m^2/kg	

2.3 Experimental methods:

Hydrothermal and thermochemical pretreatment methods were performed on the WS and RS using distilled water (DW) and 0.1 N HCl. To pretreat the biomass, 250 g of biomass was immersed in 3100±100 mL of the solution in a 4000 mL glass jar. The sample was stored undisturbed at a constant temperature for the immersion period of interest. Three different

temperatures, 23°C, 50°C, and 80°C, were used to make ash for each pretreatment method which will be referred to as DW23°C, DW50°C, and DW80°C for the distilled water pretreatment at 23°C, 50°C, and 80°C and HCl23 °C, HCl50°C, and HCl80°C for the 0.1 N HCl pretreatment at 23°C, 50°C, and 80°C, respectively. AR samples were immersed for 0.5, 1, 2, 4, 8, and 24 hrs before burning. Leachate samples were collected from two separate containers of pretreated AR for each time and temperature. The Mg, Ca, K, and Na concentration was measured using atomic absorption spectroscopy (AAS) for each container. The Mg, Ca, K, and Na concentration was reported as the average concentration of the two containers. After pretreatment, the biomass was rinsed twice with distilled water and dried at 80°C for storage until burning. 200 g of biomass was burned in each ARA batch made. A stainless steel cage with two wire mesh shelves was used to hold the biomass during burning. A stainless steel pan was placed below the cage to catch any ash that fell through the mesh. A programmable electric muffle furnace was used to heat the samples to a predetermined temperature and hold time. Samples were heated to 500°C, 650°C, 700°C, or 800°C using 1, 2, or 3 hr soak times. Finally, the ash was ground for one hour at 85 revolutions per minute (rpm) in a laboratory ball mill.

Particle-size distribution and internal surface area of the ground ARA were determined using a laser diffractometer and BET nitrogen adsorption respectively. LOI of ARA was determined by measuring the mass loss after heating one gram of dry ARA (WSA or RSA) to 800°C for 3 hrs. LOI was calculated as the percentage mass loss during firing.

To measure the amorphous silica content of ARA, the ash impurities and soluble material content were measured [2.3]. The impurities content was measured by first boiling 0.5 g of ARA after the LOI test in 25 mL of 10% nitric acid. After boiling in acid the sample was filtered through a glass microfiber filter paper with 1.1 μm openings and rinsed with deionized water.

The sample was then dried at 90±10 ^{o}C and weighed. To measure the ash soluble material content, 3 g of ARA was boiled in 200 mL of 10% sodium hydroxide solution (2.5 N NaOH) for 5 minutes. After boiling, the sample was cooled to room temperature, filtered through a 1.1 µm glass microfiber filter paper, and washed with deionized water. The residue and filter paper was then heated to 800 ^{o}C for 3 hrs. The ash weight change after boiling in the sodium hydroxide and heating was recorded. The ARA amorphous silica content was then calculated using Eq.2.2:

$$Si_{am} = w_{sol} - LOI - w_{im} \qquad \text{Eq.2.2}$$

Where Si_{am} is the amorphous silica content of the ash (%), w_{sol} is the ash weight loss after boiling in sodium hydroxide and heating (%), LOI is the ash loss on ignition (%), and w_{im} is the weight of impurities (%).

The decrease in electrical conductivity of a calcium hydroxide solution mixed with SCMs has been used by other researchers as a simple reactivity index for pozzolanic behavior of SCMs [2.19] [2.20] [2.21] and was used in this study. One gram of ARA was mixed with 100 mL of saturated calcium hydroxide solution at 23±2 °C. The solution's electrical conductivity was then measured for 7 days.

For the cement paste experiments, ARA was used at a 20% replacement level by mass of cement when used. A water-cementitious materials ratio (w/cm) of 0.5 was used for all paste samples. The paste samples were mixed using a procedure previously used [2.22]. Distilled water was added to the cementitious material and mixed using a vertical laboratory mixer at 500 rpm for 90 seconds, followed by a 120 second rest period, and finally mixed at 2000 rpm for 120 seconds.

Isothermal calorimetry was used to study the reaction rate of ARA in a cementitious system. An eight-channel isothermal calorimeter was used in this study at 23°C. Paste samples

of approximately 30 g each were used. The calcium hydroxide (CH) content of cement paste samples was measured by thermogravimetric analysis to study the pozzolanic consumption of CH by ARA. Samples were wet cured starting at 24 hrs after casting at 23^{o}C. Cement paste hydration was stopped at 7, 28, and 90 days after mixing by means of solvent exchange with isopropanol. 3-5mm thick samples were cut and placed in isopropanol for 7 days. After 7 days in isopropanol, the samples were dried in a vacuum for at least 3 days. For thermogrametric analysis, samples were heated at 20°C/min up to 900^{o}C in a nitrogen environment.

Mortar cube compressive strength was measured according to ASTM C 109 [2.23] with a sand to cementitious material ratio of 2.75. A w/cm of 0.55 was used for all mortar samples because of the decreased workability of systems with ARA. ARA was used at a 20% replacement level by mass of cement when used. Mortar cube compressive strength was tested at 7 and 28 days with the results reported as the average of the compressive strength of three mortar cubes.

2.4 Results and discussion:

2.4.1 Pretreatments and alkali leaching

Pretreatments were very effective in altering the chemical and physical structure of the straw and removing K, Ca, and Mg. Figure 2.1 shows the leachate K concentrations for different pretreatments used for WS. The sodium concentrations were found to be much lower than K, and varied only slightly by pretreatment method. Figure 2.2 shows the calcium (Ca) and magnesium (Mg) leachate concentration for WS. HCl and higher temperatures increased the leaching rates of K, Ca, and Mg. A much larger difference between HCl and DW pretreatments was seen however with Ca and Mg removal from WS than K and Na. Similar trends were observed for RS.

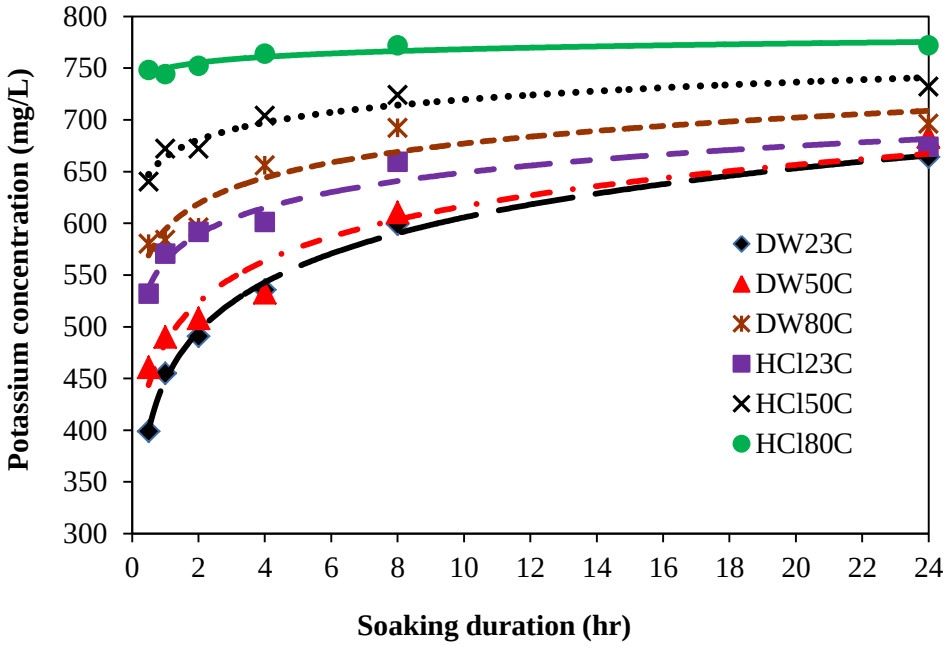

Figure 2.1: Potassium (K) concentration for wheat straw

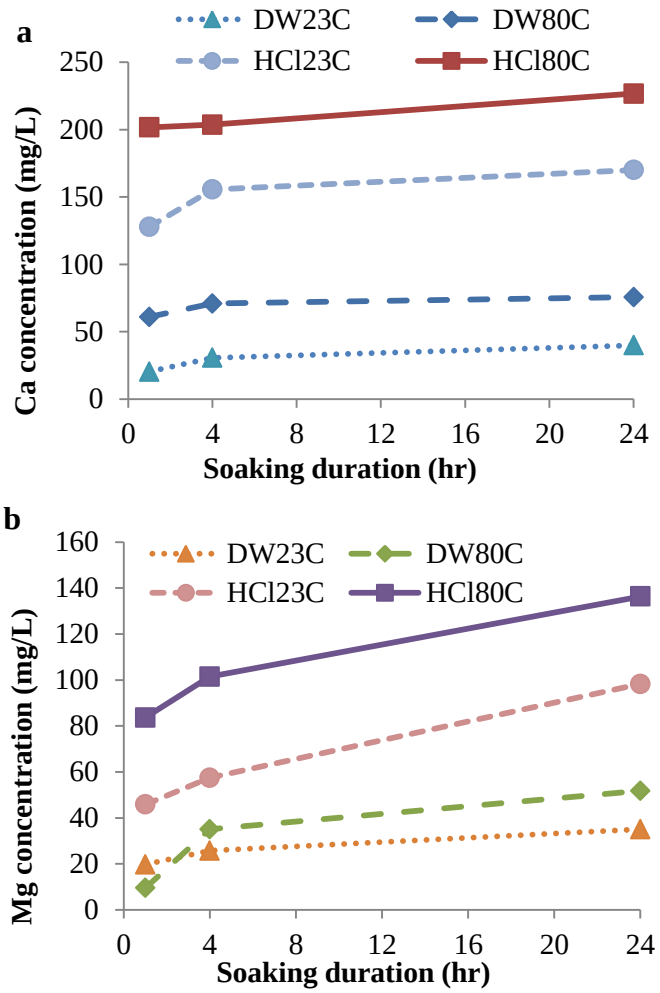

Figure 2.2: Ca (a) and (b) Mg concentration for wheat straw

The temperature sensitivity of K removal during pretreatments was quantified by calculating the dissolution activation energy. First, the leachate K concentration with time for a given pretreatment temperature was fit to Eq.2.3 [2.24]:

$$C(t) = C_{ult}\frac{K\cdot(t)}{1+K\cdot(t)} \qquad \text{Eq.2.3}$$

where *C(t)* is the potassium concentration as a function of soaking duration (ppm), t is the time passed after starting the pretreatment (days), C_{ult} is the ultimate potassium concentration assumed to be equal to the concentration measured at 24 hr of treatment (ppm), and K is the rate constant

of potassium dissolution. The Arrhenius plot was made by plotting the natural log of the rate constant K against the reciprocal of the pretreatment temperature in Kelvins. Figure 2.3 shows the Arrhenius plot for the rate constants calculated for the leachate K concentration for wheat straw. The activation energy was calculated as the slope of the fit line on the Arrhenius plot multiplied by the universal gas constant R (8.314 J/mol/K). The activation energy for leaching K with 0.1 N HCl was found to be 32.2 KJ/mol, versus 13.3 KJ/mol with DW pretreatments. This shows that the higher the acid concentration the more effectively heat can be used to remove K from the AR with high acid concentrations.

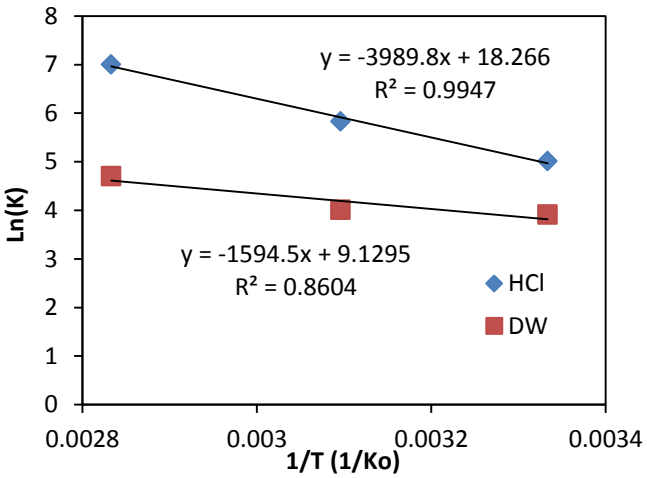

Figure 2.3: Arrhenius Plot for wheat straw

2.4.2 Surface area, LOI and amorphous silica content of ARA

Pretreatments were effective in reducing the carbon content in the ARA, increasing the internal surface area, and increasing the percentage of amorphous silica in the ash. Figure 2.4 shows the amorphous silica content of ARA. For a given burning temperature, pretreatments increased the amorphous silica content. Pretreated ARA burned at 500°C for 2 hrs had similar amorphous silica content as the one burned at 650°C for 1 hr. The unpretreated WSA had 21% crystalline silica and unpretreated RSA had 19% crystalline silica when burned at 650°C for 1

hour as calculated from the ash total silica content shown in Table 2.2 and the ash amorphous silica content shown in Figure 2.4. The ash pretreated with 0.1N HCl at 80°C showed little if any crystalline silica while the WSA pretreated with DW at 80°C had 8% crystalline silica. The increase in amorphous silica content of the pretreated ARA correlated with the removal of Ca, Mg, and K out of the biomass by pretreatments. Figure 2.5 shows the amorphous silica content of ARA versus the CaO, MgO, and K_2O content. The amorphous silica content of the ARA corresponded with a decrease in the CaO, MgO, and K_2O content, with the MgO showing a slightly better correlation. Figure 2.6 shows the LOI measured for WSA and RSA. The ARA LOI decreases as the burning temperature increases regardless of the pretreatment type. At a given burning temperature, pretreated ARA had a lower LOI than that of the unpretreated control ash. Figure 2.7 shows the metal impurity (Ca, Mg, and K) content of the ash for the WSA and RSA was also correlated to the ARA LOI. The RSA had a lower LOI than the corresponding WSA, possibly because of the lower alkali content of the RSA before pretreatment than the WSA. Even though distilled water pretreatments were not as effective as the more acidic pretreatments, when burned at 650°C for 1hr the WSA pretreated with DW23/24 still had 52% lower LOI and 15% higher amorphous silica than that of unpretreated WSA. RSA pretreated with DW23/24 had 55% lower LOI and 17% higher amorphous silica than that of unpretreated RSA.

Another important impact of the pretreatments is the decrease in temperature sensitivity of the biomass. Sensitivity reduction is vital for low cost ARA production in using simple kilns or large scale applications where it may be more difficult to control the temperature. The pretreatments were very effective in reducing the sensitivity to burning temperatures. The

HCl80/24 WSA burned at 800 ^{o}C had a higher amorphous SiO_2 content than that of the control burned at 500°C as shown in Figure 2.4.

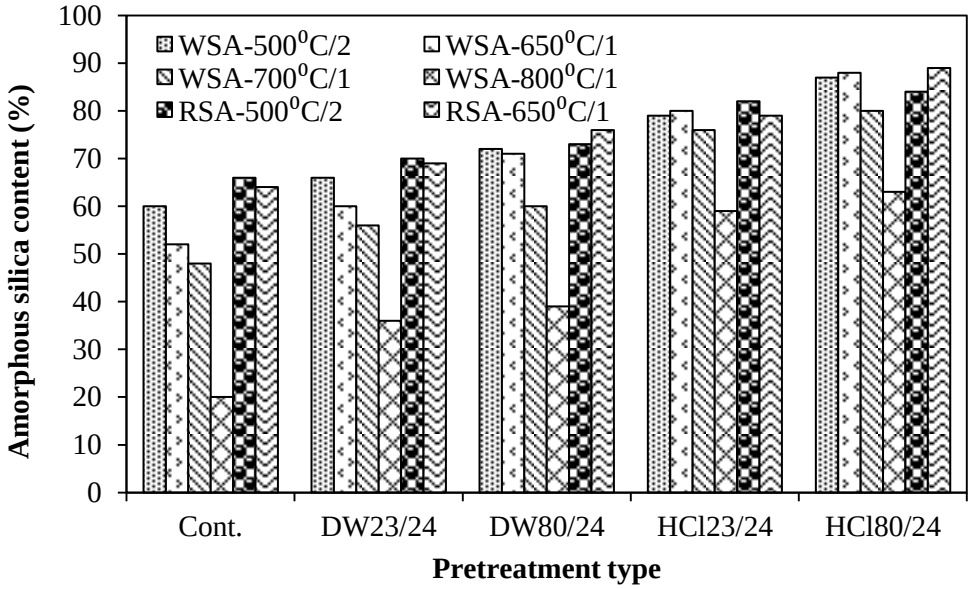

Figure 2.4: Amorphous silica content of pretreated and unpretreated ARA

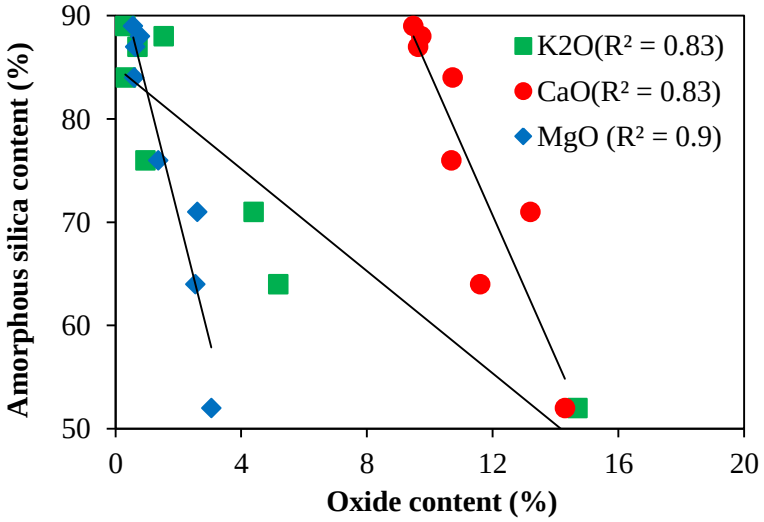

Figure 2.5: ARA amorphous silica vs. ARA (WSA and RSA) oxide content

Table 2.2: Oxide composition of selected ARA

Ash Type	SiO_2	Al_2O_3	Fe_2O_3	CaO	MgO	K_2O	Na_2O
WSA-Cont-650/1	66.3	0.26	1.12	14.3	3.05	14.7	0.15
WSA-DW80-650/1	78.8	0.12	1.05	13.2	2.61	4.4	0.12
WSA-HCl80-650/1	86.5	0.28	1.13	9.73	0.78	1.54	0.1
WSA-HCl80-500/2	87.9	0.05	1.07	9.63	0.63	0.7	0.08
RSA-Cont-650/1	79.1	0.34	0.82	11.6	2.54	5.18	0.5
RSA-DW80-650/1	85.4	0.45	0.92	10.69	1.36	0.96	0.26
RSA-HCl80-650/1	88.2	0.47	0.74	9.48	0.56	0.31	0.17
RSA-HCl80-500/2	85.7	1.4	1.02	10.73	0.6	0.34	0.23

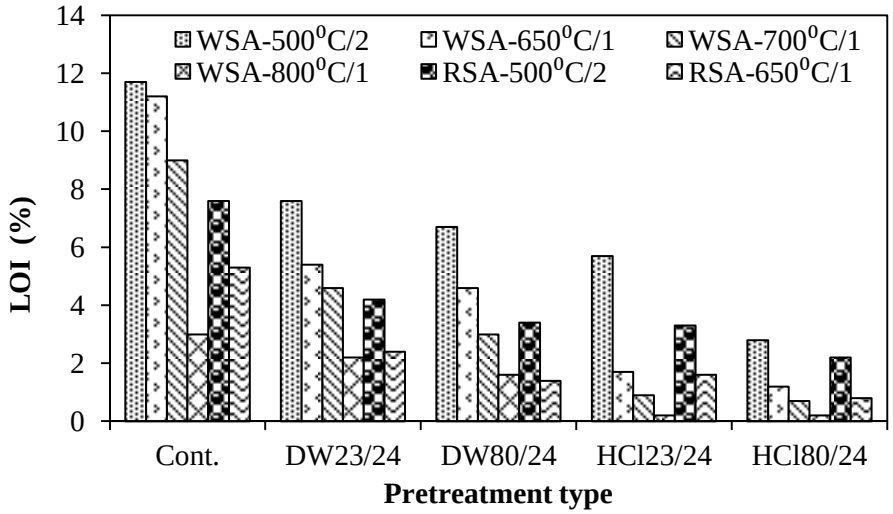

Figure 2.6: LOI of pretreated and unpretreated ARA

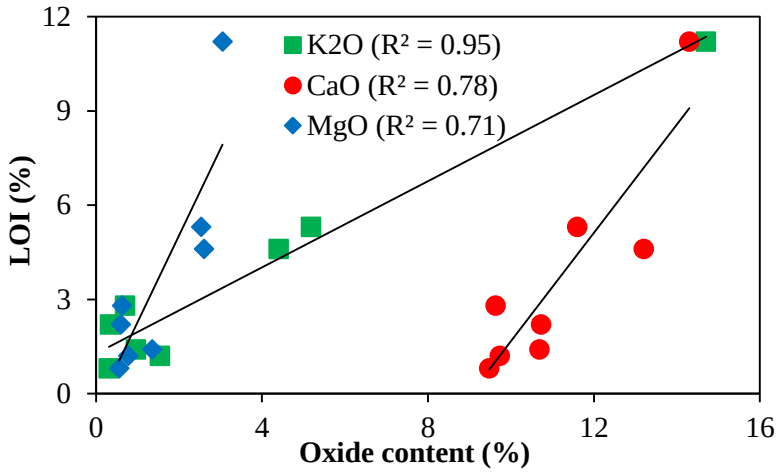

Figure 2.7: ARA LOI V vs. ash K_2O, CaO and MgO content

LOI and amorphous silica content of ARA was shown to be affected by the duration of burning. Table 2.3 shows the LOI and amorphous silica content for WSA pretreated with 0.1N HCl at 80°C for 24 hours and then burned at different temperatures and holding durations. There appears to be an optimum burning time for each temperature which appeared to coincide with the removal of most of the carbon. At 500°C, the optimum burning time was found to be between one and two hours whereas at 600°C it was found to be less than or equal to one hour. Burning periods longer than the optimum time did not appear to improve amorphous silica content or LOI.

Table 2.3: Effect of holding time on LOI and amorphous silica content

WSA type	Amorphous Silica (%)	LOI (%)
HCl80/24-500/1	72.70	17.58
HCl80/24-500/2	88.65	2.76
HCl80/24-500/3	88.7	2.62
HCl80/24-650/1	89.14	1.18
HCl80/24-650/2	88.99	1.1

Pretreatments changed the color of the ash, mainly because of the decrease in carbon content. Figure 2.8A shows WSA pretreated with 0.1N HCl at 80°C for 24 hrs, while Figure 2.8B shows control WSA samples ashed at four different temperatures. The WSA-HCL80/24 ash was much lighter in color than that of control WSA ashes regardless of the burning condition. Even though it had a low LOI, the WSA pretreated with HCl at 80°C for 24 hrs and burned at 800°C for one hr had a slightly darker color than the pretreated ashes made at lower temperatures (Figure 2.8A).

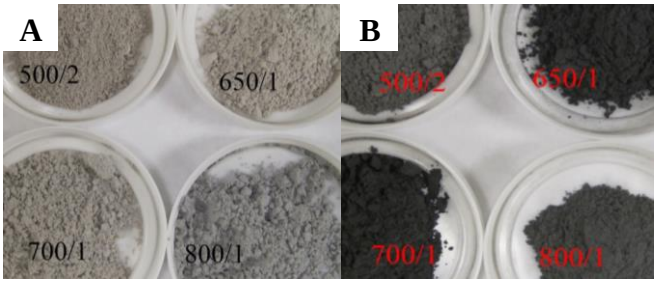

Figure 2.8: Color of wheat straw ash, a) HCl80/24 pretreated and b) unpretreated

Although the color of the ash is largely related to carbon content of the ash, impurities such as alkali metals can change the ash color. At higher temperatures these metals react with silicon (Si) to produce crystalline phases that may combined with carbon or contain iron giving the ash a darker color [2.25] [2.26]. It was also observed that washing the biomass after pretreatments is very important in removing alkalis from surface of biomass and reducing LOI of the resulted ash. This could be because when the straw was not washed after the pretreatment, potassium and other impurities in solution would precipitate on to the surface of the straw during drying. These precipitates could trap carbon during ashing, leading to higher ash LOI. Even though pretreatments remove metal impurities out of the biomass cell wall, it is beneficial to wash the biomass after pretreatment to limit the impurities that would precipitate on the biomass surface. For a given burning condition, pretreated but unwashed biomass resulted in ARA with

darker color and higher LOI compared to the ash obtained from pretreated and washed biomass. This could be attributed alkalis on the surface melting at lower temperature and trapping carbon.

Table 2.4 presents the ARA surface area determined by BET nitrogen adsorption while Figure 2.9 shows the particle-size distribution for some selected ARAs. For a given pretreatment, ashes burned at 500°C for 2 hrs had higher surface area than those burned at higher temperatures. This is probably because at higher temperatures melting of some material eliminating pores inside of the ash. The particle-size distribution was not significantly affected by pretreatments. Although the surface area of unpretreated RSA and WSA were similar, pretreated RSA had a larger surface area than that of pretreated WSA.

Table 2.4: BET data for WSA and RSA under different burning conditions

Ash type	BET surface area (m^2/g)
WSA-Cont-500/2	27.6
WSA-Cont-650/1	8.3
WSA-HCl80/24-500/2	168
WSA-HCl80/24-650/1	65
WSA-HCl80/24-700/1	39.7
RSA-Cont-500/2	16.9
RSA-Cont-650/1	9.6
RSA-HCl80/24-500/2	200
RSA-HCl80/24-650/1	134.5
RSA-DW80/24-650/1	58.94

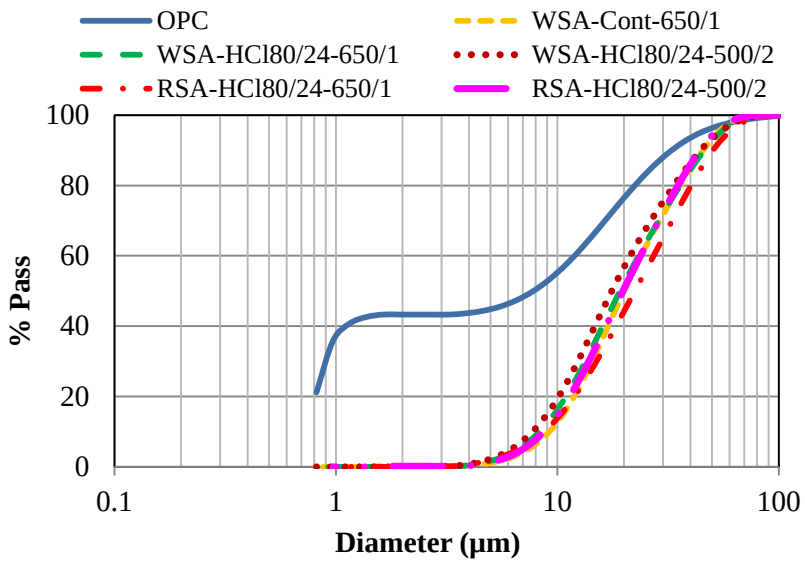

Figure 2.9: Particle size distribution of OPC and ARAs

2.4.3 Conductivity measurements

Figure 2.10 shows the normalized conductivity (the measured conductivity divided by the initial conductivity of the solution) data for WSA pretreated with 0.1N HCl at 23°C, 50°C, and 80°C and burned at 500°C for 2 hours and 650°C for 1 hour. The normalized conductivity for unpretreated WSA and WSA pretreated with DW and 0.1 N HCl is given in Figure 2.11. The pretreatment temperature did not significantly affect the measured conductivity change. WSA burned at 500^{o}C for 2 hrs shows a more rapid drop in conductivity than WSA burned at 650^{o}C for 1 hour indicating a higher reactivity consistent with the higher surface ash measured in the samples burned at 500°C. Very little difference was seen between different pretreatments in the conductivity experiments. Similar behavior was seen for RSA conductivity experiments. The initial increase in the electrical conductivity from the control sample is likely the result of dissolution of metal impurities such as Na, K, Ca, and Mg in the solution [2.19].

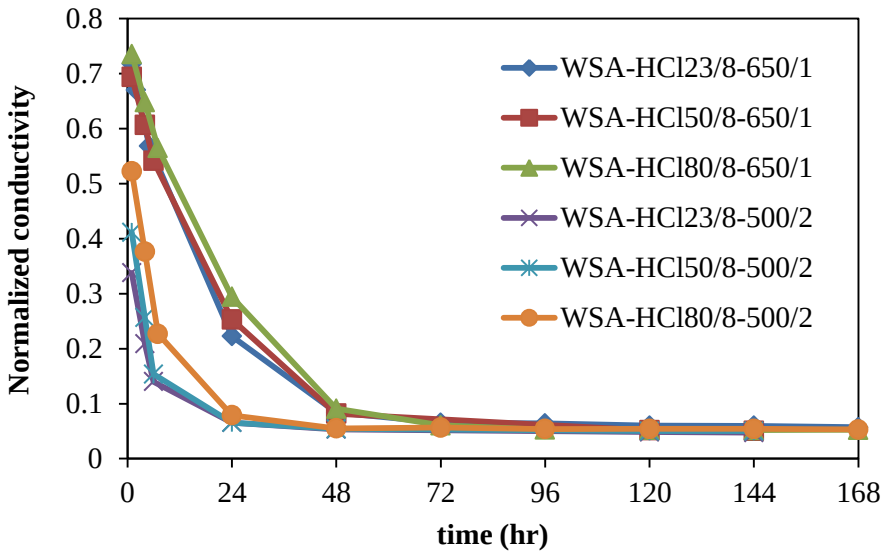

Figure 2.10: Electrical conductivity change of HCl pretreated wheat straw ash

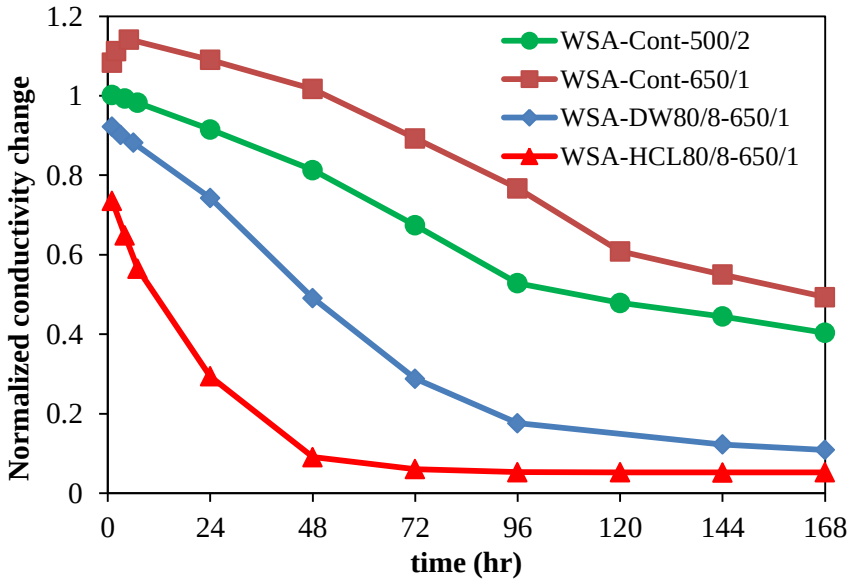

Figure 2.11: Electrical conductivity change wheat straw ash with different pretreatments

2.4.4 Isothermal Heat of Hydration

Figure 2.12 compares the heat of hydration for WSA burned at 650°C for 1 hour with and without thermochemical pretreatments. Large differences in hydration behavior were seen between the pretreated and control WSA. Figure 2.13 shows the total heat of hydration of cement paste samples containing WSA. The pretreated ashes show similar total heat of hydration during

the first 120 hours, indicating a similar degree of cement hydration at 120 hours. Figure 2.14 shows the heat flow rate for paste samples containing RSA. The hydration rate of pretreated ARA was accelerated compared to the control samples, whereas the samples with ARA that were not pretreated were retarded as seen in Figure 2.12 and Figure 2.14. The hydration acceleration is most likely caused by increased nucleation because of the very high ARA surface area [2.27] [2.28]. Also, the samples containing pretreated ARA (WSA and RSA) showed much more similar behavior to each other during the first 120 hours after mixing than the non-pretreated ARA.

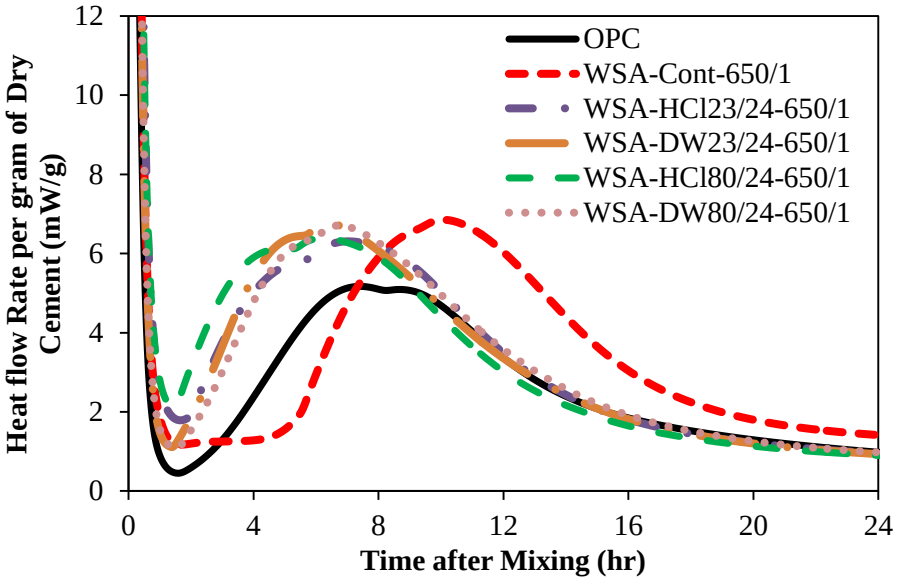

Figure 2.12: Heat flow rate of paste samples containing different wheat straw ash

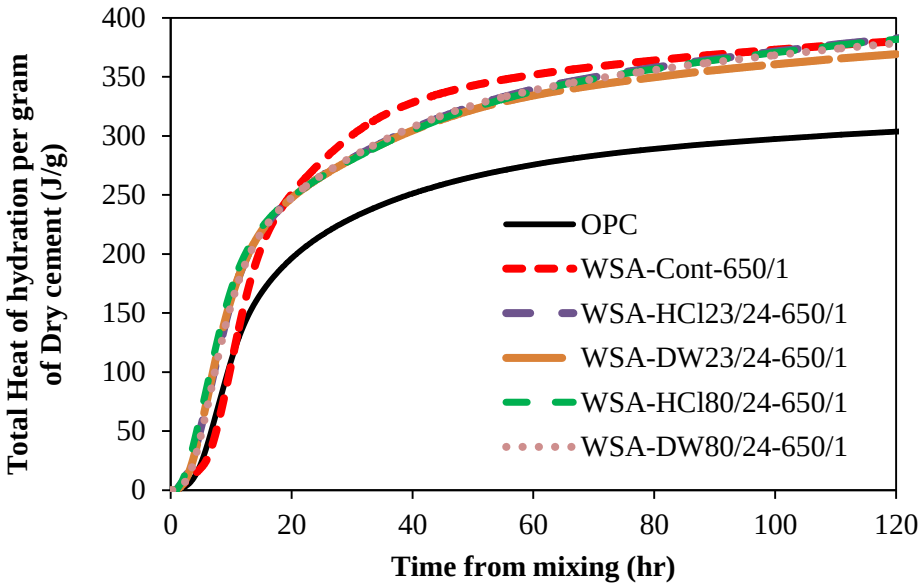

Figure 2.13: Total heat of hydration of paste samples containing different wheat straw ash

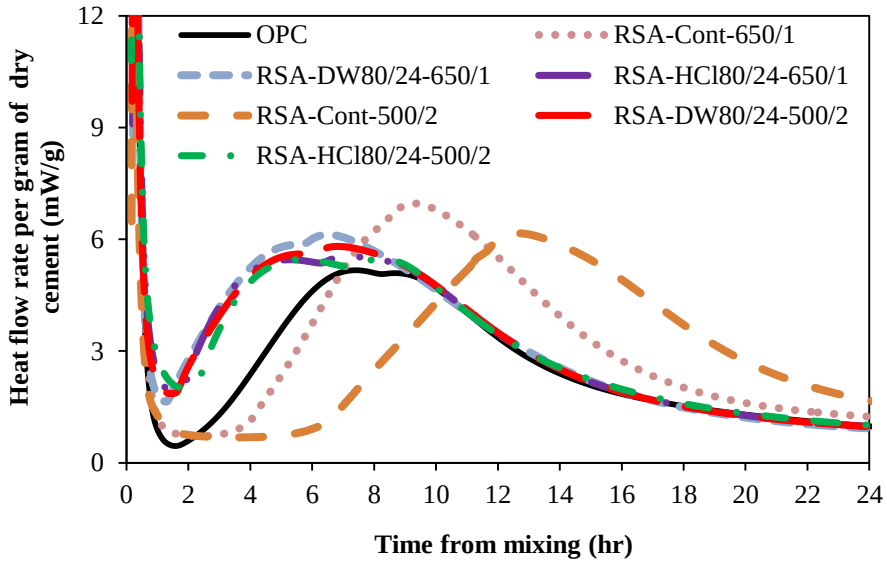

Figure 2.14: Heat evolution rate of paste samples with and without rice straw ash

2.4.5 Pozzolanic Reactivity

The decrease in CH content of cement paste samples containing ARA is a measure of the ARA pozzolanic reaction. The CH content for cement paste samples with and without ARA was measured using TGA at 7, 28, and 90 days of hydration as shown in Figure 2.15 and 16 for WSA

and RSA, respectively. For a given pretreatment type and age, samples containing ARA (WSA or RSA) burned at 500^{o}C for 2 hr had a lower CH content than those burned at higher temperatures. This can be attributed to the higher surface area of ARA burned at 500^{o}C for 2 hr. At a given burning condition, samples containing ARA pretreated with 0.1N HCl at 80^{o}C for 24 hrs had a lower CH content than any other pretreatment type. At a given age, samples containing WSA at burned at 500°C showed lower CH content than those containing RSA burned at 500°C.

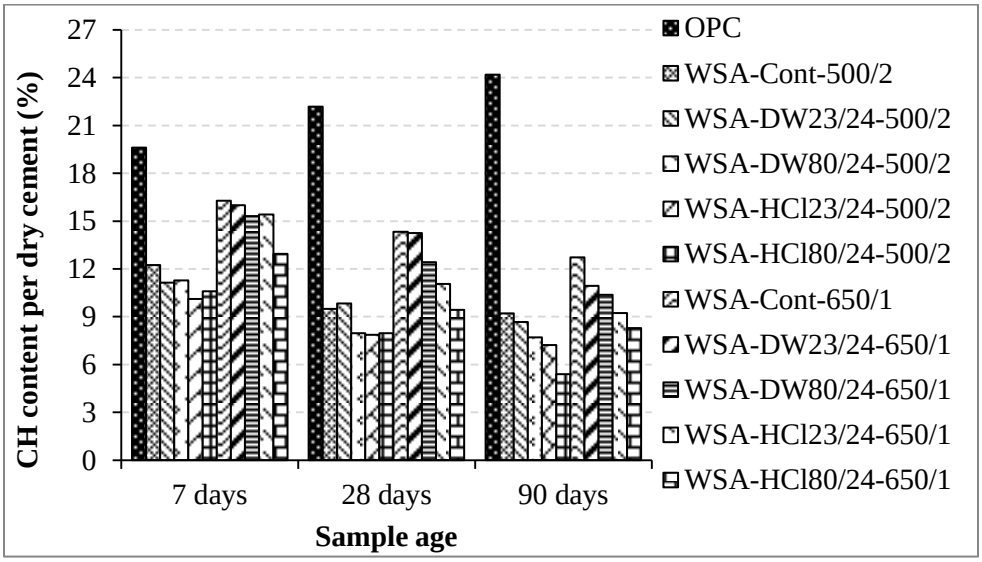

Figure 2.15: CH content of cement paste containing wheat straw ash

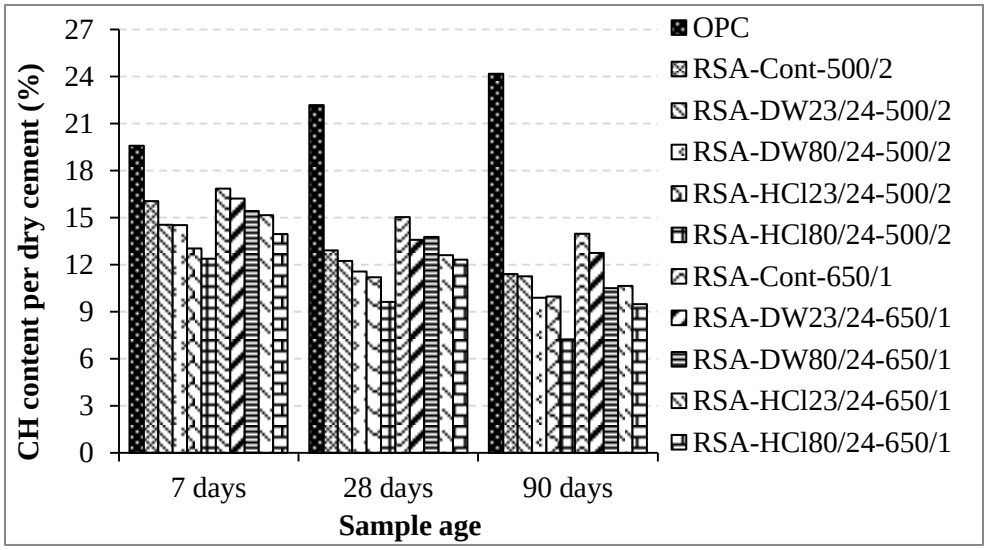

Figure 2.16: CH content of cement paste containing rice straw ash

Figure 2.17 shows the compressive strength development for mortar with and without 20% cement replaced by ARA. The WSA and RSA pretreated with HCl at 80°C for 24 hours showed the highest compressive strength development, with a 25% increase in strength over the ordinary portland cement (OPC) mixture at 28 days of age. The increased strength seen with pretreated ashes confirms the increased pozzolanic reaction seen with the reduction of CH content with time in samples containing the pretreated ARA.

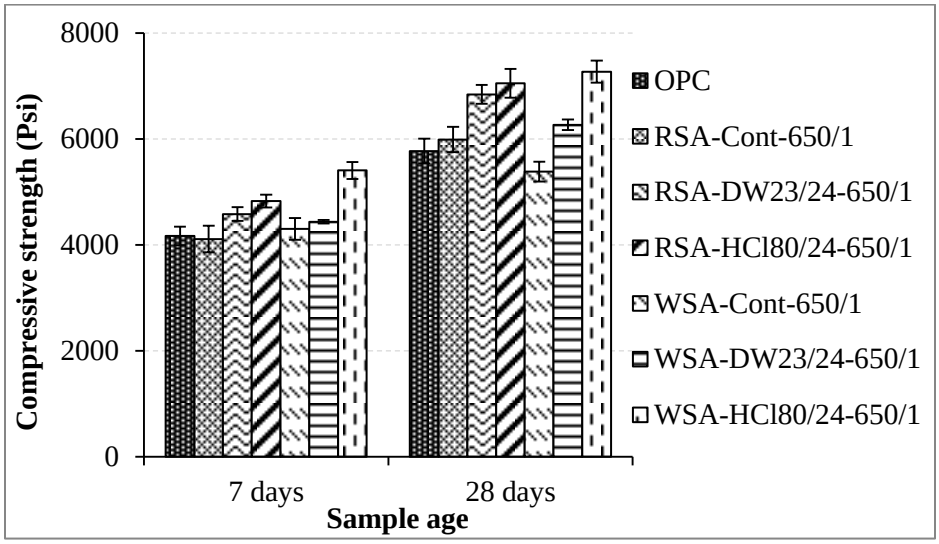

Figure 2.17: Mortar cube compressive strength data

A comparison of the ARA material characteristic improvement from the pretreatments (amorphous silica and surface area) and CH content at 90 days is shown in Figure 2.18. The increase in amorphous silica content of ARA and surface area correlated with a decrease in the CH content of paste samples containing ARA and increases compressive strength of mortar samples containing ARA. The isothermal calorimetry results did not show a reduced hydration development with the use of ARA indicating that the decrease in CH content seen with the ARA is likely from the pozzolanic reaction and not a lower cement degree of hydration. Additionally the OPC mixture showed an increase in CH content while the mixtures with ARA showed a decrease in CH between 7 and 28 days.

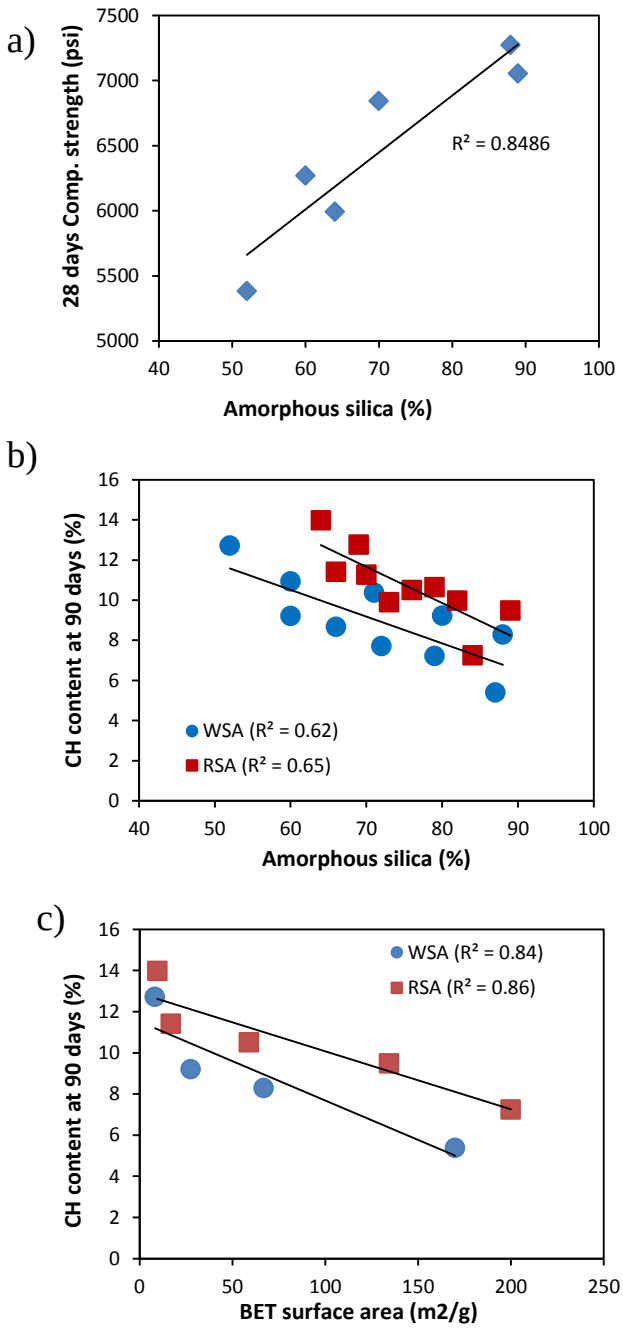

Figure 2.18: Relation between material characteristics and performance a) amorphous silica content vs. 28 days mortar cub strength, b) amorphous silica content vs. CH content of paste after 90 days c) Surface area of ash vs. CH content of paste after 90 days

2.5 Conclusions:

The material physical and pozzolanic properties of wheat straw ash (WSA) and rice straw ash (RSA) were studied. From this study, the following conclusions can be made:

1- Pretreatments are effective in partial removal of Ca, K, and Mg out of the biomass. The activation energy for K leaching was higher for dilute acid pretreatment than distilled water pretreatment. This shows that heating samples during pretreatment even more effective for the more acidic pretreatments.

2- Pretreatments increased the amorphous silica content and surface area and decreased the LOI of ARA at a given burning temperature. It was shown that amorphous silica content inversely correlated with the Ca, K, and Mg content of the ash while LOI of ARA is directly correlated with the Ca, K, and Mg content of the ash. Alkalis seemed to encase or combine with carbon during burning. Pretreatments reduced the sensitivity of the ash to the burning temperature, showing less of a decrease in amorphous silica content than the non-pretreated ash at 700°C and 800°C.

3- Pretreatments improved the system hydration kinetics. Non-pretreated ARA retarded the cement hydration, whereas pretreated WSA and RSA accelerated the cement hydration. The acceleration may be from increased nucleation from the increased material surface area.

4- Cement paste sample containing ARA burned at 500°C for 2 hrs contained lower CH than those samples containing ARA burned at 650°C for 1 hr. This was attributed to the higher surface area of the ash burned at 500°C for 2 hrs. It was shown that CH content of the paste after 90 days of hydration was inversely correlated with amorphous silica content and surface area of the ash used in the paste. Samples containing WSA showed

lower CH content at 90 days than the RSA with similar surface area and amorphous silica content.

5- When used as 20% replacement of cement in mortar samples, pretreated ARA increased compressive strength of mortar samples at 28 days by 25% compared to the OPC sample. Mortar samples containing pretreated ARA showed a 32% increase in 28 day compressive strength compared to samples containing unpretreated ARA. It was also shown that mortar compressive strength correlated well with the ash amorphous silica content.

2.6 Acknowledgements:

Financial support for this project was provided by the National Science Foundation (CMMI-103093). The authors thank Dr. Donn Beighley for providing the rice straw. The help of Dr. Kenneth J. Klabunde for providing access to the BET Nitrogen equipment is appreciated. The help of Monarch Cement Company in chemical analysis of samples is greatly acknowledged. Valuable advice from Dr. Maria Juenger throughout this paper is greatly appreciated. Antoine Borden's assistance with the pretreatment experiments is gratefully acknowledged.

Chapter 3 - Use of Bioethanol Byproduct for Supplementary Cementitious Material Production

Abstract:

Corn stover has the potential for use as a supplementary cementitious material (SCM) for concrete. The impact of distilled water and dilute acid pretreatments and post-treatments on the pozzolanic reactivity of corn stover ash (CSA) was studied. Additionally, the potential use of a bioethanol byproduct called high lignin residue (HLR) for SCM production was examined. Pretreated CSA and high lignin residue ash (HLRA) increased the early reactivity of cement paste when used as 20% replacement of cement in the system whereas unpretreated CSA was found to severely suppress the hydration reaction. The highest compressive strength was obtained from samples containing HLRA.

3.1 Introduction:

Greenhouse gas emissions from fossil fuel burning have created increasing interest in the use of biomass for renewable energy production. Thermochemical and biochemical conversion techniques have been used to convert biomass, including agricultural residues, to biofuel [3.1] [3.2]. Combustion, gasification, and pyrolysis are widespread thermochemical conversion techniques for converting biomass into electricity and bio-oil. Biochemical conversion of biomass involves hydrolysis of biomass into its constituent sugar followed by sugar fermentation to bioethanol [3.2] [3.3]. Besides biofuel production, biomass has been used to produce supplementary cementitious materials (SCMs) to reduce the carbon footprint of concrete [3.4] [3.5] [3.6] [3.7].

Utilization of biomass for either biofuel or SCM production has posed certain challenges. The presence of alkali and alkaline earth metals (AAEMs) in the biomass can adversely affect the quality of the bio-oil and cause slagging and fouling during combustion [3.8] [3.9]. It has been shown that removal of AAEMs out of the biomass prior to pyrolysis by the use of pretreatments improves the yield and the quality of the bio-oil during pyrolysis, and reduces ash slagging and fouling during combustion [3.9] [3.10] [3.11]. Biomass pretreatments are commonly performed by soaking the biomass in acidic or basic solutions [3.12]. It has also been shown that pretreatments, particularly dilute acid, improve the reactivity of agricultural residue ash (ARA) such as rice husk ash in cementitious systems by increasing the amorphous silica content and surface area of the ash [3.5] [3.6] [3.13].

In the biochemical conversion, the biomass undergoes three basic processes: pretreatment, enzymatic hydrolysis, and fermentation [3.2] [3.3]. Pretreatments improve the biomass ethanol yield by increasing the accessibility of cellulose for enzymatic hydrolysis [3.14].

Enzymatic hydrolysis (saccharification) is performed on the pretreated biomass to convert the cellulose and hemicellulose to C5 and C6 sugars. After the enzymatic hydrolysis, the sugar rich liquid phase is seperated from the solid residue, refered to as high lignin residue (HLR) in this paper. The liquid phase is then fermented to ethanol. Simultaneous saccharification and fermentaion (SSF) processes are also common where the solid residue isn't removed until after the enzymatic hydrolysis and fermentaion [3.15] [3.16]. HLR is currently burned in boilers or landfilled. Figure 3.1 depicts the production process of bioethanol. Increasing worldwide interest in the production of ethanol from biomass, particularly corn stover, could boost the quantity of HLR available for SCM production.

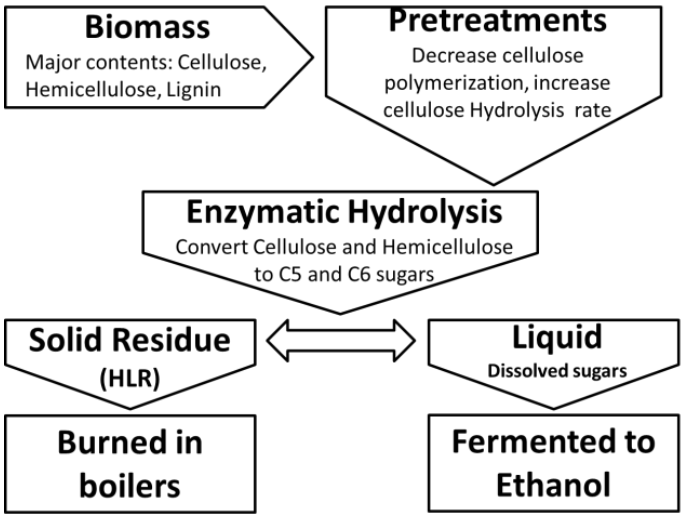

Figure 3.1: Bioethanol production process

The major constituents of HLR are lignin, cellulose, and other inorgranic constituents such as silica. Because HLR contains a high quantity of silica in a weakly polymerized organic structure, it could be a potential resouce for highly reactive SCMs production. If this can be shown, the cost of lignocellulosic ethanol production and the cost of SCMs produced from biomass can be substantially reduced. Additionally, if it can be shown that HLR burned at higher

temperatures could result in a highly reactive ash, the HLR can be burned in biolers to produce energy and at the same time the resulting ash can be used as reactive SCM in concrete at no cost.

This is the first study on the reactivity of high lignin residue ash (HLRA) in cementitious systems. Also, the impact of distilled water and dilute acide pretreatments on the reactivity of corn stover ash (CSA) using different burning conditions was investigated. Pretreated and unpretreated corn stover and HLR were burned at controlled temperatures of 500°C and 650°C for several different oven residence times. Ash characterizations, heat of hydration, and compressive strength data were used to compare the pozzolanic behavior of pretreated and unpretreated CSA with that of HLRA.

3.2 Materials and methods:

3.2.1 Materials:

An ASTM C 150 [3.17] Type I/II portland cement was used for this study with the cement properties shown in Table 3.1. Standard graded sand [3.18] was used for the mortar experiments. Corn stover was purchased from a local farm in Manhattan, KS. The high lignin residue (HLR) material used was the solid residue taken after an SSF process using corn stover as the feedstock material and was supplied by the National Renewable Energy Laboratory at Golden, CO. The HLR material contained 30% cellulose and 70% lignin on dry mass. Reagent grade hydrochloric (HCl) and sulfuric acid were obtained and diluted to 0.1 N for use in the study. Phosphorus pentoxide (P_2O_5) and potassium hydroxide (KOH) used were ACS grade.

Table 3.1: Chemical compositions of cement and corn stover ash

Sample ID	SiO_2	Al_2O_3	Fe_2O_3	CaO	MgO	P_2O_5	Na_2O	K_2O	LOI	BET (m2/gr)
CSA-HCL80-4-500/2	76.54	1.59	0.79	4.05	1	3.31	0.58	3.93	6.09	64
CSA-HCL80-4-650/1	77.94	1.5	2.17	3.86	1.12	3.34	0.7	4.41	3.82	14.3
CSA-DW80-4-650/1	47.37	1.67	2.65	14.5	3.29	6.06	0.57	10.56	10.64	10.6
CSA-Cont-650/1	28.42	0.89	0.56	7.83	3.3	6.78	0.42	25.41	22.78	8.5
HLRA-650/1	81.34	3.46	1.42	3.21	0.48	0.54	1.87	1.84	1.8	67
Portland Cement	21.8	4.35	3.4	64.2	1.79	--	0.17	0.52	0.89	--

3.2.2 Experimental Methods:

3.2.2.1 Treatments:

Hydrothermal pretreatment methods were performed on chopped corn stover (CS) using distilled water (DW), 0.1N HCl, and 0.1N Sulfuric acid. To pretreat the biomass, 250 g of biomass was immersed in 3100±100 mL of the solution in a 4000 mL glass jar. The sample was stored undisturbed at a constant temperature of either 23^{o}C or 80^{o}C for a given immersion period. After immersion, samples of leachate were collected for further analysis. After pretreatments, the biomass was rinsed either twice or four times, each time with 2500 mL of distilled water and dried at 80^{o}C in an oven.

Post-treatment for corn stover ash (CSA) was performed by soaking the 20 gr of ash in 100 gr of distilled water and stirring the slurry for one hour at 23^{o}C. After stirring, the slurry was filtered and the solid residue (post-treated ash) was dried at 80^{o}C in an oven. Leachate samples were collected for further analysis. Leachate Concentrations of magnesium (Mg), calcium (Ca), potassium (K), sodium (Na), and phosphorus (P) were determined using inductively coupled plasma mass spectrometry (ICP-MS).

3.2.2.2 Ash production:

A programmable electric muffle furnace was used to heat the biomass samples to a predetermined temperature and hold time. To prepare corn stover ash (CSA), 200 g of dried corn stover was burned in each batch made. A stainless steel cage with two wire mesh shelves was used to hold the biomass during burning. A stainless steel pan was placed below the cage to catch any ash that fell through the mesh. High lignin residue ash (HLRA) was prepared by placing 100 gr of HLR on the stainless steel pan and heating in the furnace. Samples were heated to 500^{o}C for two hours (500/2) or 650^{o}C for one hour (650/1). Finally, the ash was ground for one hour at 85 revolutions per minute (rpm) in a laboratory ball mill. The naming convention for ash samples is as follows: type of ash-pretreatment-washing times-burning temperature/holding time. For example, the name of corn stover ash pretreated with 0.1 N HCl at 80°C that was washed 4 times after pretreatments and burned at 500^{o}C for 2 hrs would be CSA-HCl80-4-500/2. CSA-650/1-Post and CSA-500/2-Post are post-treated CSA-Cont-650/1 and CSA-Cont-500/2 samples, respectively. (OPC+650/1-leachate) and (OPC+500/2-leachate) are paste samples in which the leachate from the post-treatment of CSA-Cont-650/1 and CSA-Cont-500/2 samples was used as mixing water, respectively.

3.2.2.3 Biomass ash characterizations:

Particle-size distribution and surface area of the ground biomass ash (CSA and HLRA) were determined using a laser diffractometer and BET nitrogen adsorption. ARA loss on ignition (LOI) was determined by measuring the mass loss after heating one gram of dry biomass ash (CSA and HLRA) to 900^{o}C for 3 hrs. LOI was calculated as the percentage mass loss during firing. To determine crystalline phases of the ash samples, x-ray diffraction (XRD) analysis was performed (Cu Kα radiation with λ=1.5046Å). A step size of 0.02°/2s and a scan range of 5°–70°

2θ was used. The chemical composition of ash samples were determined using x-ray fluorescence (XRF).

3.2.2.4 Biomass ash pozzolanic reactivity determination:

For cement paste experiments, 20% of the cement was replaced by CSA when used. A water-cementitious materials ratio (w/cm) of 0.5 was used for all paste samples. Distilled water was added to the cementitious material and mixed using a vertical laboratory mixer at 500 rpm for 90 seconds, followed by a 120 second rest period, and finally mixed at 2000 rpm for 120 seconds [3.19].

For determining heat of hydration of cement pates, an eight-channel isothermal calorimeter was used in this study. Approximately 30 g of cement paste was used and the calorimeter was run at 23°C for one week. The calcium hydroxide (CH) content of cement paste samples was obtained using thermogravimetric analysis to study the pozzolanic consumption of CH by biomass ash. Paste samples were cast in polystyrene vials. Samples were wet cured starting at 24 hrs after casting at 23^{o}C. Cement paste hydration was stopped at 7, 28, and 91 days of hydration by means of solvent exchange with isopropanol. Approximately 2 mm thick slices were cut and placed in isopropanol for 7 days. After 7 days in isopropanol, the samples were dried in a vacuum for at least 3 days. Free water content was obtained as the difference between the weight of samples before soaking in isopropanol and after drying. 25 to 30 mg of dried paste was heated at 20°C/min to 900^{o}C in a nitrogen environment using a thermogravimetric analyzer (TGA). The CH content of paste samples was obtained using thermogravimetric analysis.

Mortar cube compressive strength was measured according to ASTM C109 [3.20] with a sand to cementitious material ratio of 2.75. A w/cm of 0.55 was used for all mortar samples because of the decreased workability of systems with pretreated CSA samples. CSA was used at

a 20% replacement level by mass of cement when used. Mortar cube compressive strength was tested at 7, 28, and 91 days with the results reported as the average of the compressive strength of three mortar cubes.

3.3 Results and discussion:

3.3.1 Biomass ash characteristics:

The major influence of pretreatments seen is the removal of metal impurities out of the biomass. Table 3.2 shows the amount of metal impurities removed by the pretreatments out of the corn stover. The data shows that all of the pretreatments removed similar amounts of potassium (K). However, distilled water pretreatments did not remove as much Ca, Mg, and P as the dilute acid pretreatments.

Table 3.2: Metal impurities concentrations measured in corn stover leachate

Pretreatment	Leachate Concentration (mg/g biomass)				
	Na	K	Ca	Mg	P
HCl23°C	0.05	22.06	3.57	1.56	1.95
HCl80°C	0.67	25.99	5.48	1.91	2.34
DW23°C	0.04	19.12	1.19	0.99	1.34
DW80°C	0.24	24.13	1.40	1.31	1.44
Sul.80°C	0.41	26.62	5.03	1.95	2.33

The effect of removing the impurities was reflected in the physical and chemical properties of the CSA. Pretreatments decreased the crystallinity of the ash. Figure 3.2 shows the XRD results of pretreated and unpretreated corn stover ash burned at 650°C for one hour. Unpretreated corn stover ash (CSA-Cont-650/1) had higher crystalline content compared to the pretreated samples (CSA-HCl80-2-650/1 and CSA-HCl80-4-650/1).

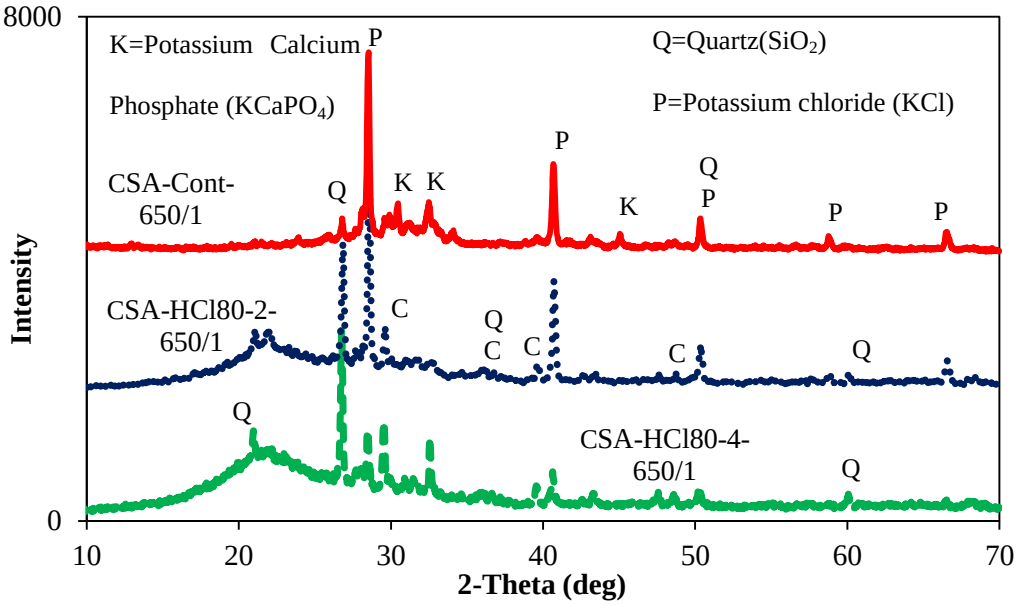

Figure 3.2: XRD result for corn stover ash burned at 650°C for 1 hr.

The major crystalline phases in the unpretreated ash were sylvite (potassium chloride) and $KCaPO_4$. Although pretreatments removed most of the potassium out of the biomass, pretreated ash still contained some potassium chloride as can be seen in CSA-HCl80-2-650/1 sample. However, CSA-HCl80-4-650/1 showed low intensity XRD peaks for potassium chloride and larger amorphous hump than that of CSA-HCl80-2-650/1. Pretreated and unpretreated ash samples contained crystalline quartz. HCl80 pretreated CSA burned at 500°C for 2 hrs showed similar XRD patterns to that of 650°C for 1 hr, as shown in Figure 3.3. Corn stover ash pretreated with distilled water (DW80) showed different XRD patterns than the ash pretreated by HCl80 as shown in Figure 3.4. The major crystalline phases in the DW80 pretreated samples were calcite and quartz. HCl80 pretreated corn stover ash had a larger amorphous hump than the DW80 pretreated sample, suggesting that the former had a higher amorphous content. Furthermore, CSA pretreated with sulfuric acid (Sul80) did not show sylvite phase, as illustrated in Figure 3.5. Besides quartz, potassium sulfate was the second major crystalline phase in the dilute sulfuric acid pretreated CSA (CSA-Sul80-4-500/2). Although HLRA contained some

quartz, neither potassium chloride nor calcite phases were found in the samples, as can be seen in Figure 3.5.

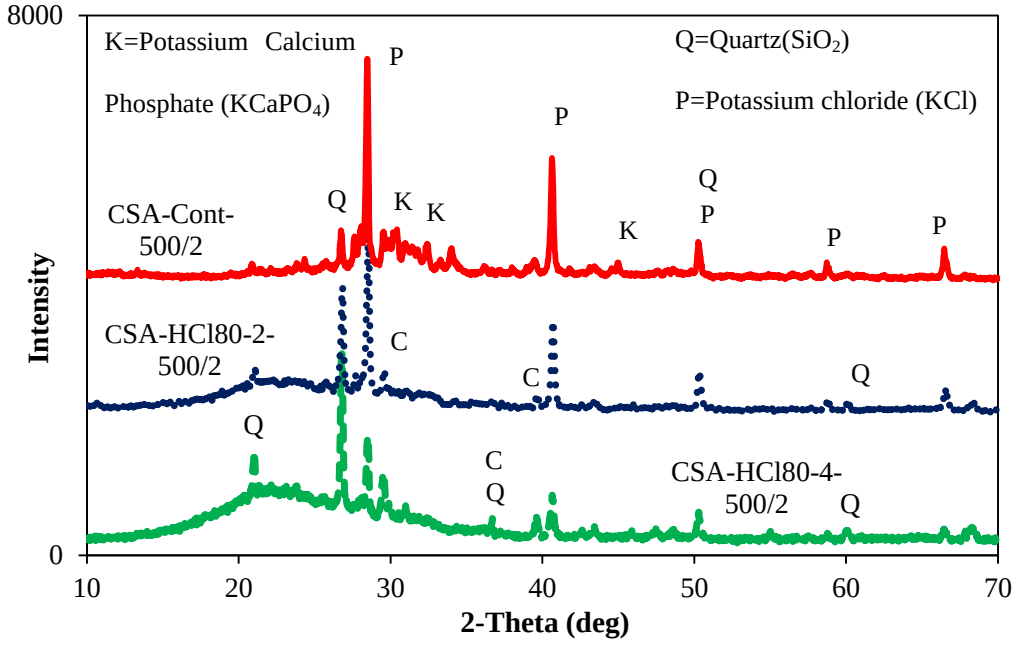

Figure 3.3: XRD result for corn stover ash burned at 500°C for 2 hr

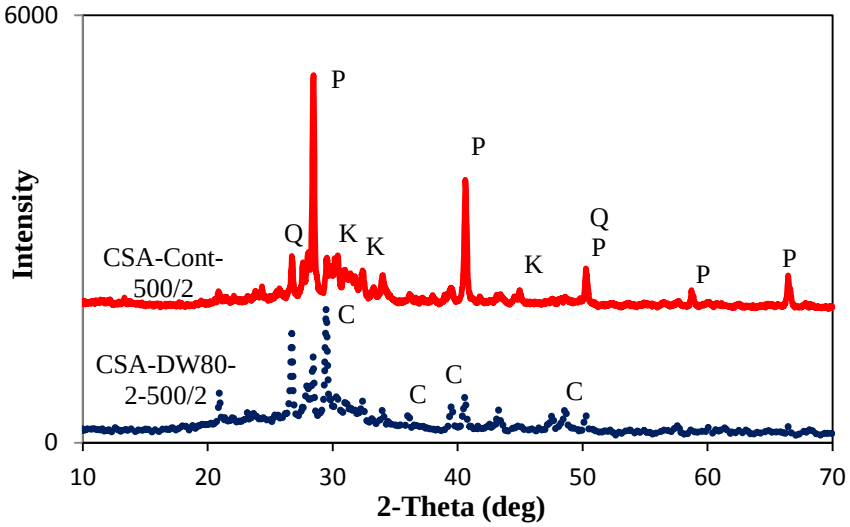

Figure 3.4: XRD pattern for CSA pretreated with DW80

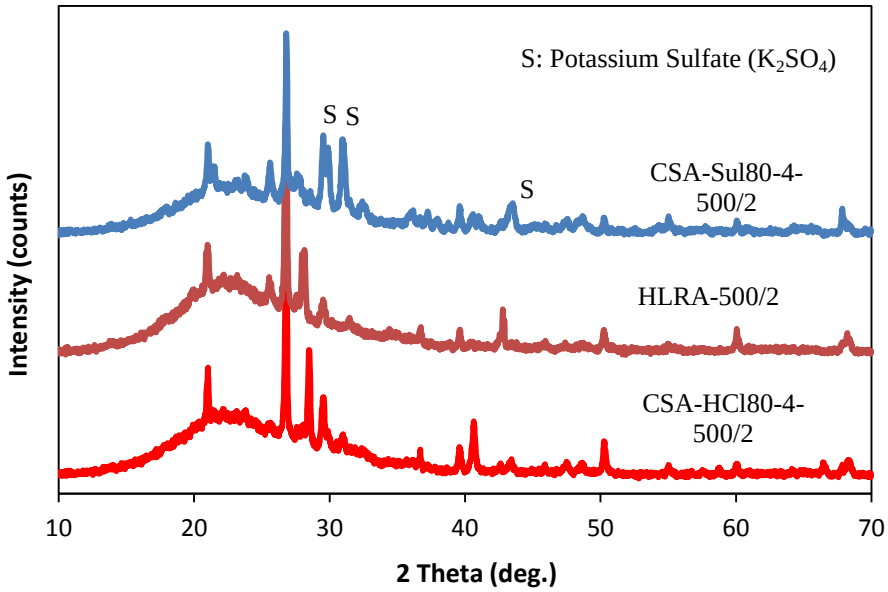

Figure 3.5: XRD pattern for HLRA and dilute acid pretreated CSA

The presence of crystalline potassium chloride phases in unpretreated and HCl pretreated corn stover ash samples suggests that the potassium in the biomass reacts with chlorine during the burning to form potassium chloride (KCl). The absence of KCl in the ash sample pretreated with Sul80 could be because the pretreatment removed the chlorine out of the biomass and the acid did not provide an additional supply of Cl like the HCl did. Instead, potassium sulfate was formed in Sul80 pretreated samples. Potassium removal from the biomass leads to a decrease in biomass ash crystallinity because the potassium easily reacts with other anions during ashing [3.21]. Moreover, the existence of high amounts of calcite in the DW80 pretreated CSA could be because DW80 removed less calcium out of the biomass compared to Sul80 and HCl80 pretreatments because acids can dissolve many calcium bearing phases that could be found in the stover.

Besides the change in biomass ash crystalline content, pretreatments also changed the chemical composition of the biomass ash. Pretreatments increased the silica content of the biomass ash by reducing the carbon content (LOI) and other metal oxide impurities in the ash, as

shown in Table 3.1. HLRA had higher silica content compared to the other CSA samples. Pretreatments increased the ash specific surface area. Pretreatments, particularly dilute acid, dramatically reduced the LOI of the biomass ash as illustrated in Table 3.3. Additionally, the LOI was reduced by increasing the number of rinsing times during pretreatments. This could be because of removal of metal impurities, particularly potassium, from the biomass surface during rinsing. The lowest LOI was obtained for HLRA followed by the ash pretreated with dilute sulfuric acid (Sul80). The higher surface area and lower LOI of HLRA compared to dilute acid pretreated CSA could be attributed to the removal of cellulose out of the biomass and to the structural change of lignin by enzymatic hydrolysis and also to the lower metal impurities, particularly potassium, content of HLR compared to that of dilute acid pretreated corn stover. Removal of cellulose and structural change of lignin could cause the lignin and the remaining organic compounds in the HLR to better burn off leading to lower LOI and higher surface area for HLRA.

Table 3.3: Loss on ignition (LOI) of biomass ash

Treatment type	Burning condition	
	500/2	650/1
CSA-Cont	24.6	22.7
CSA-DW80-2	13.6	12.3
CSA-DW80-4	13.1	8.6
CSA-HCl80-2	10	8.6
CSA-HCl80-4	6	3.8
CSA-Sul80-4	4.7	2.6
HLRA	2.3	1.8

Note: Data are given in percent of initial weight

Although the particle size distribution was slightly changed by DW80 and HCl80 pretreatments, HLRA showed an overall smaller particle size distribution than other CSA as shown in Figure 3.6.

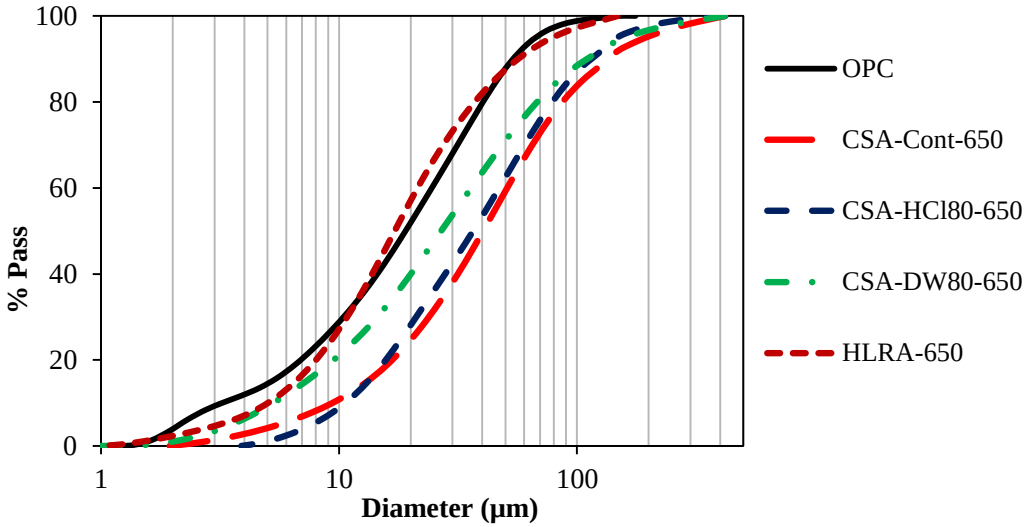

Figure 3.6: Particle sized distribution of cement and biomass ash

3.3.2 Biomass ash pozzolanic reactivity:

3.3.2.1 Heat of hydration

Pretreatments and post-treatments dramatically increase CSA early heat of hydration. Unpretreated CSA suppressed cement hydration whereas CSA pretreated by either distilled water or dilute acid improved the early hydration, as shown in Figure 3.7a. Additionally, the pretreatment temperature seemed to have little impact on the early hydration behavior, as shown in Figure 3.7b.

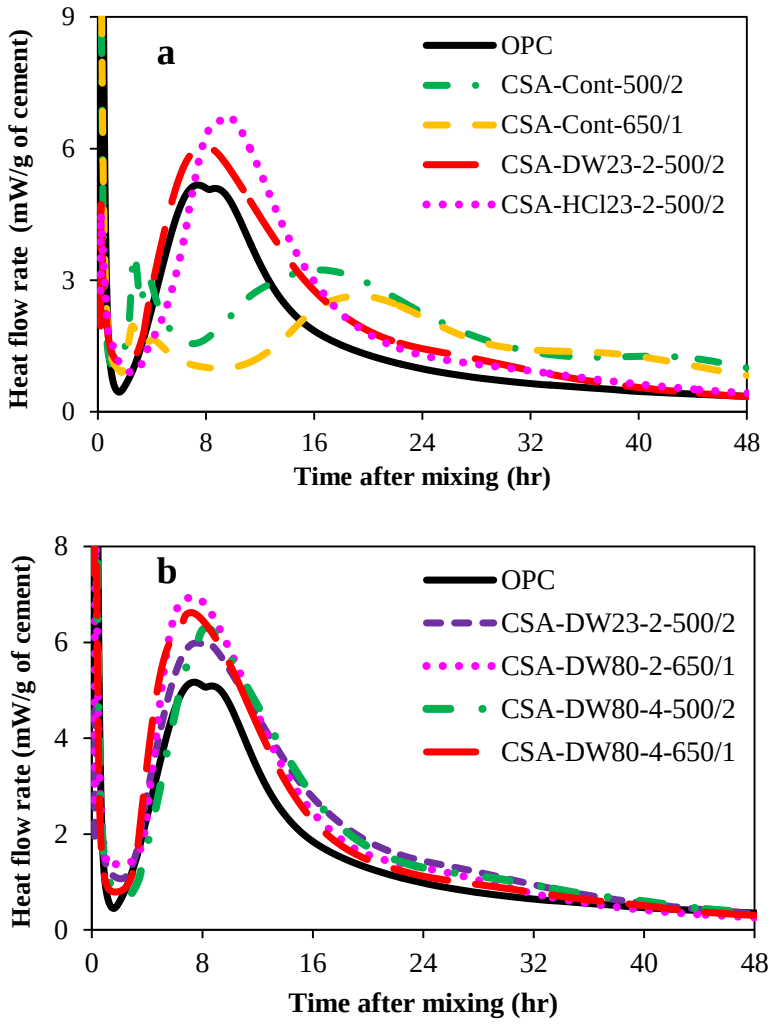

Figure 3.7: Heat of hydration of pretreated and unpretreated (Cont.) CSA

Although samples containing CSA pretreated with dilute acid showed shorter induction periods than those containing CSA pretreated with distilled water (DW), the total heat of hydration during the first 24 hrs is similar for all paste samples containing pretreated CSA, as illustrated in Figure 3.8a. However, after 24 hrs of hydration, samples containing CSA pretreated with dilute acid, either HCl or sulfuric acid, showed a higher heat of hydration than those containing CSA pretreated with DW, see Figure 3.8b.

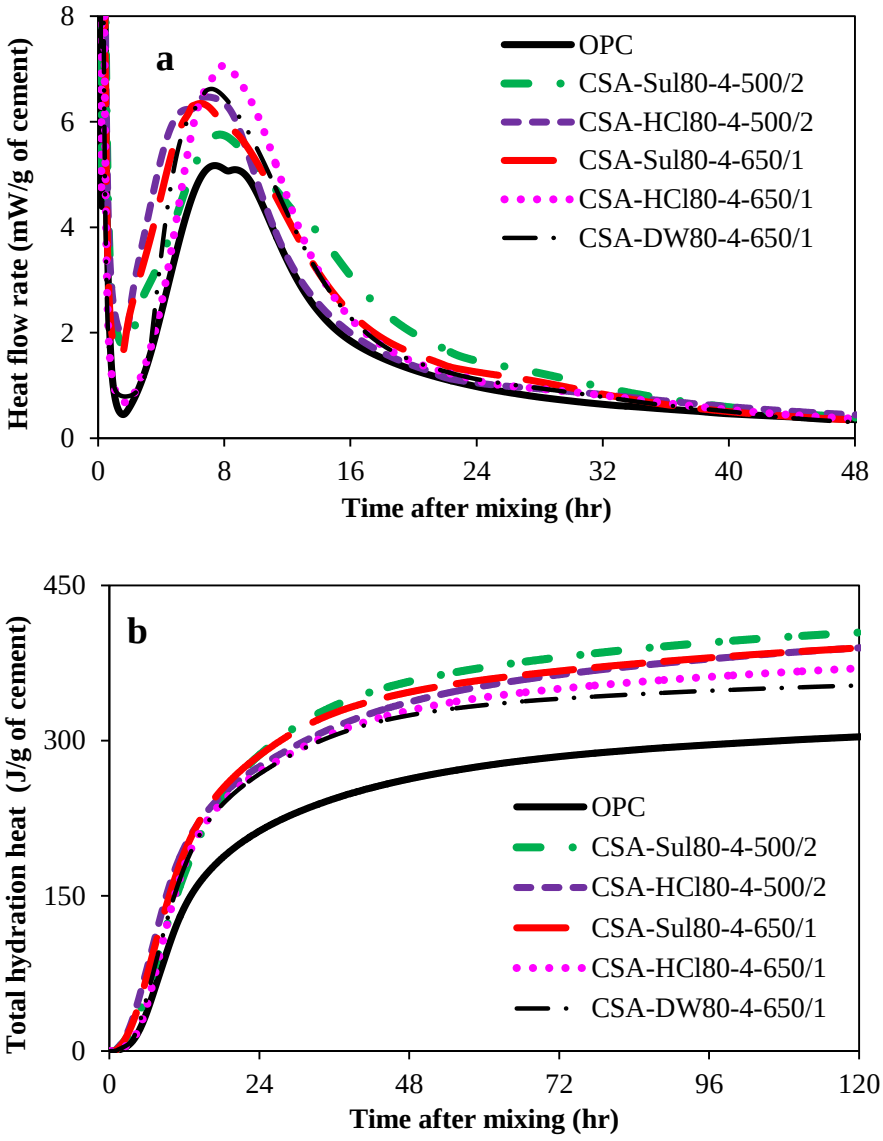

Figure 3.8: Heat of hydration of dilute acid pretreated CSA

While paste samples containing HLRA showed a shorter dormant period than samples containing dilute acid pretreated CSA, the total heat of hydration of both samples was similar, as shown in Figure 3.9. The total heat of hydration of paste samples containing pretreated CSA or HLRA at one day was almost the same as the total heat of hydration of OPC samples at 5 days of hydration. Although the unpretreated CSA retarded the hydration reaction, the total heat of hydration of paste samples containing unpretreated CSA, either CSA-Cont-650/1 or CSA-Cont-500/2, was higher than OPC samples. Paste samples containing CSA-Cont-500/2 showed similar

total heat of hydration at five days as those containing pretreated CSA as it can be seen from Figure 3.9b.

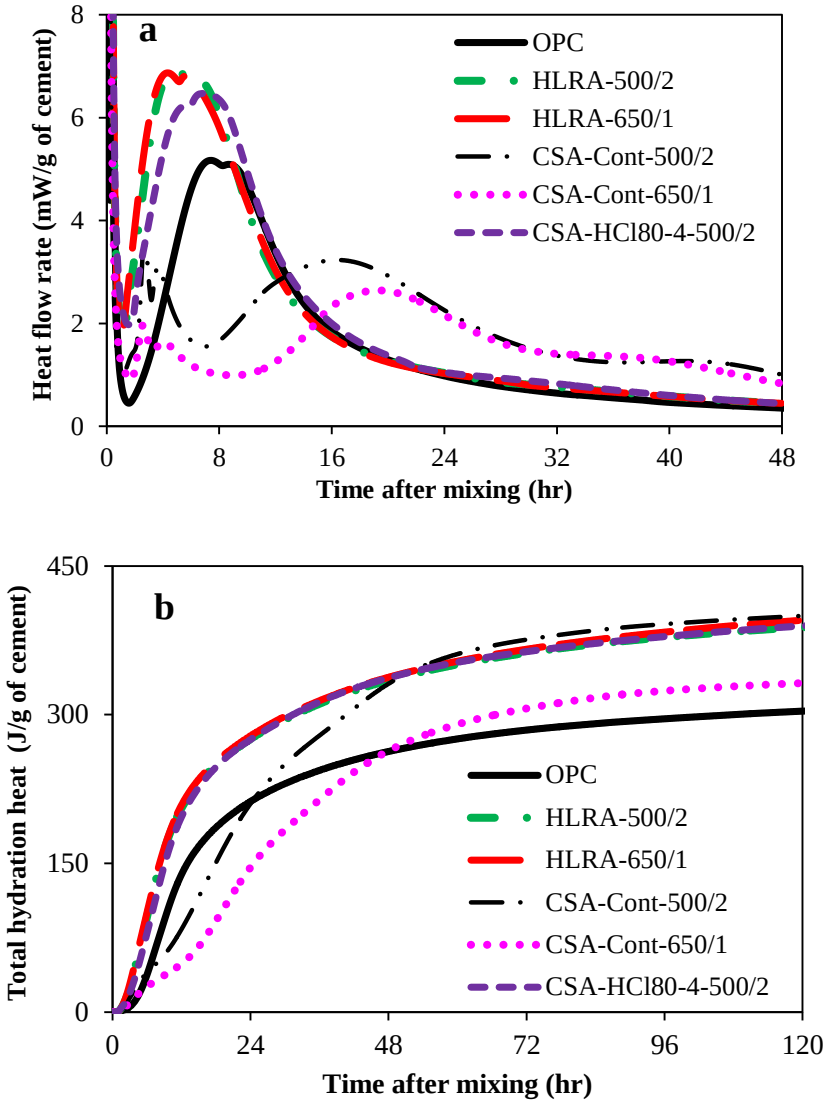

Figure 3.9: Heat of hydration of HLRA

Post-treatments were effective in eliminating the excessive retardation seen with CSA, as shown in Figure 3.10. Noticeably, the heat of hydration of (OPC+500/2-leachate) sample was similar to the paste sample containing CSA-500/2-Post. However, (OPC+650/1-leachate) sample showed suppressed hydration similar to the paste sample containing CSA-Cont-650/1. There could be several factors influencing the hydration behavior of CSA. Pretreatments removed some

phosphorous out of the biomass, reduced the LOI and crystallinity of the biomass ash and increased the silica content and surface area of the ash. Amongst these factors, the phosphorus (P) removal and the increase in specific surface area could play a major role in enhancing the early reaction of pretreated CSA. An increase in the ash surface area increases the number of nucleation sites for precipitation of calcium-silicate-hydrate (CSH) which could increase the early heat of hydration [3.22].

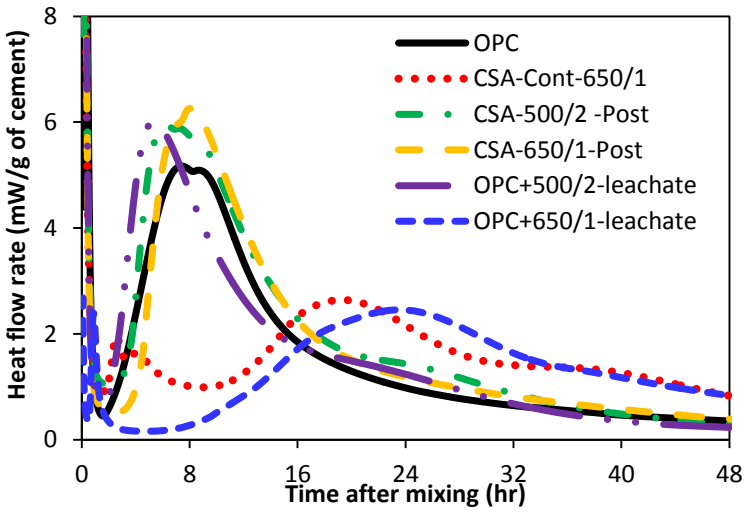

Figure 3.10: Heat of hydration of post-treated CSA

The impact of phosphorus and potassium on cement hydration was studied by adding 0.5 wt% (weight percent of dry cement) of phosphorus pentoxide or potassium hydroxide to cement paste, respectively. Phosphorus retarded the cement hydration similar to that seen in the unpretreated CSA, whereas added potassium had only minimal impact on early hydration behavior as shown in Figure 3.11. While the unpretreated CSA ashed at 650°C showed similar hydration to the mixture with added phosphorous, there seems to be other factors affecting the hydration of the CSA containing cement paste samples. The leachate from the CSA ashed at 500°C showed a low phosphorous content as shown in Table 3.4, and no retardation; however the corresponding post-treated CSA also showed no retardation. It is possible that the form of

phosphorus found in the CSA-Cont-500/2 leaches more at high pH values seen in pore solutions, but not in the post treatment leachate. Since some of the phosphorous was removed by post-treatment, the amount of phosphorus released into the paste from CSA-500/2-Post might not be enough to cause retardation. While it is possible that the high level of phosphorous in the leachate from CSA-Cont-650/1 could be the reason behind the hydration suppression in OPC+650/1-leachate sample, clearly the cause is more complex.

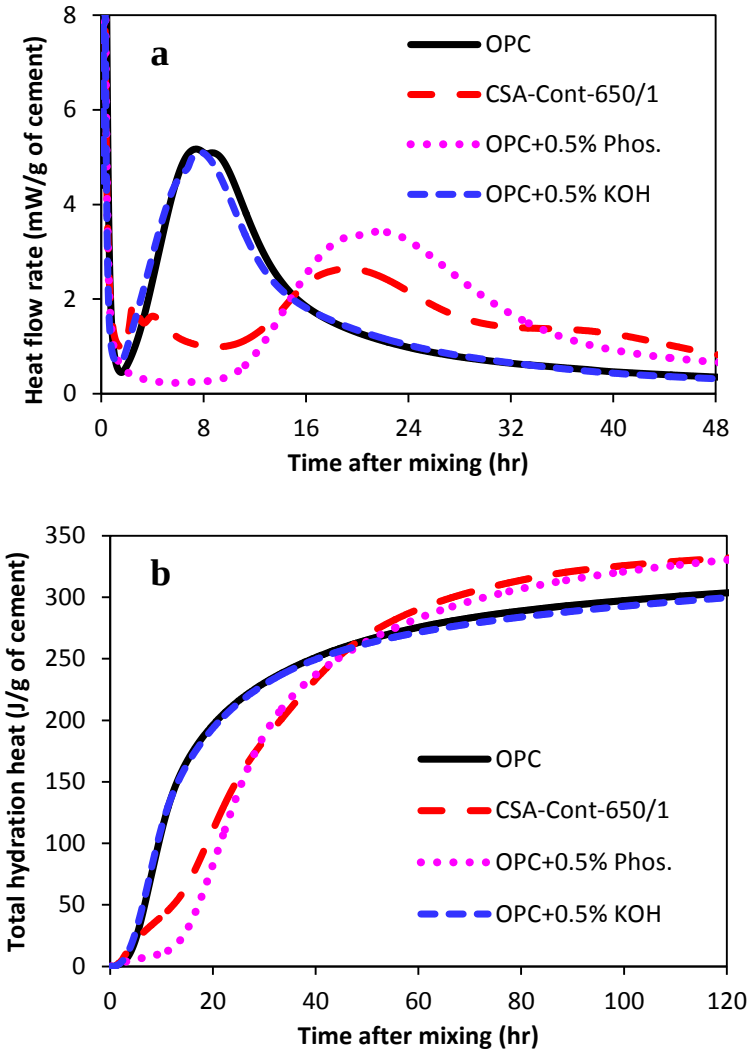

Figure 3.11: Cement hydration under phosphorus and KOH

3.3.2.2 Calcium hydroxide consumption and mortar compressive strength:

The calcium hydroxide (CH) content of cement paste samples containing CSA was less than that of OPC samples, as shown in Figure 3.12. The CH content of OPC paste samples increased with time. The CH content of samples containing unpretreated CSA (CSA-cont-500/2 and CSA-Cont-650/1) remained constant or increased between 7 and 91 days of hydration. Samples containing DW80 pretreated ash (CSA-DW80-4-650/1 and CSA-DW80-4-500/2) did not show a reduction in the CH content over time. This could be because these ashes had a lower reactivity and the CH consumption was balanced by the continued cement reaction and CH production. For more reactive ashes, such as dilute acid pretreated ones and HLRA, the CH consumption rate was higher than the CH production rate, lowering the CH content after 7 days. It was seen that samples containing CSA burned at 500°C for 2 hours (500/2) had lower CH content that those containing CSA burned at 650°C for 1 hour (650/1). This could be attributed to the higher surface area of samples burned at 500/2. Samples containing HLRA-500/2 showed the lowest CH content at 28 and 91 days of age.

Table 3.4: Post-treatment leachate concentrations

Sample ID	Post-preatment leachate concentrations (mg/g of ash)				
	P	Na	Ca	K	Mg
CSA-Cont-500/2	0.46	0.23	0.09	57.24	0.03
CSA-Cont-650/1	4.50	0.33	0.09	58.73	0.04

The small increase in compressive strength from 7 to 91 days in the samples made with the unpretreated CSA ash (CSA-Cont-650/1), as shown in Figure 3.13, suggests that the addition of unpretreated ash limited the cement reaction. Post-treatment improved the compressive strength by 46% at 7 days and by 67% at 28 days compared to the unpretreated (control) ash,

however the post-treated ash compressive strength was still only 91% and 87% of the OPC sample at 7 days and 28 days, respectively.

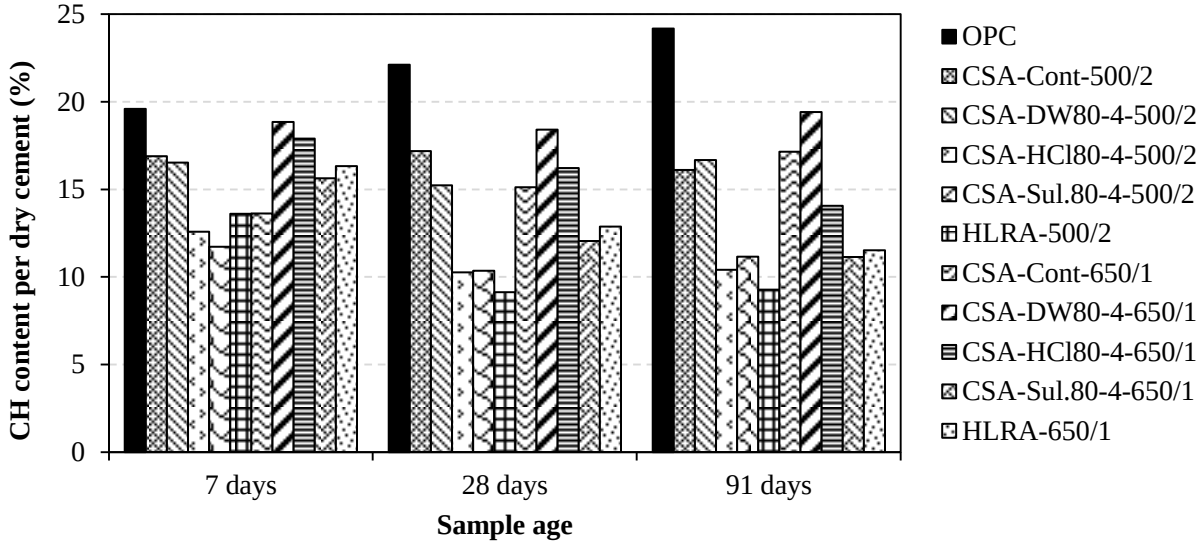

Figure 3.12: CH content of cement paste samples

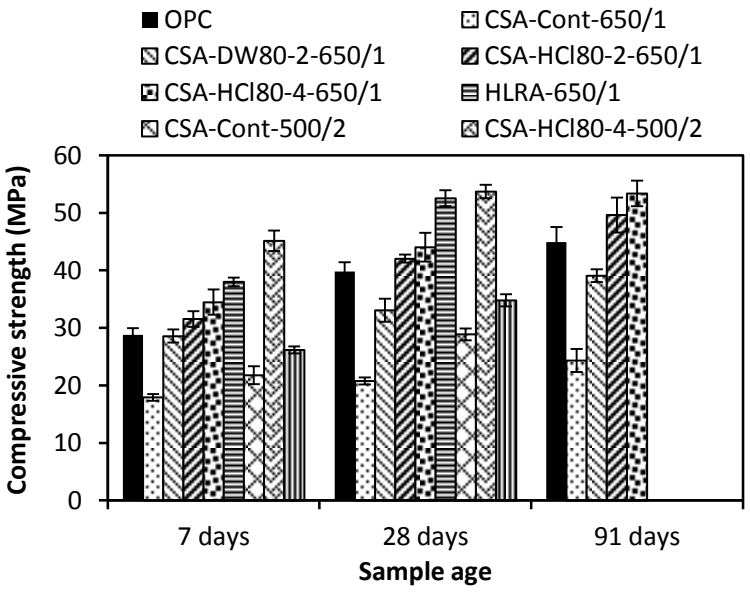

Figure 3.13: Mortar cubes compressive strength

Mortar samples containing CSA-HCl80-2-650/1 and CSA-HCl80-4-650/1 showed higher strength than those without CSA (OPC samples). It was also seen that the number of times

rinsing the sample after soaking had a negligible effect on the compressive strength since both CSA-HCl80-2-650/1 and CSA-HCl80-4-650/1 had similar compressive strength. Among mortar samples containing biomass ash burned at 650°C, the highest mortar compressive strength was obtained from samples containing HLRA-650/1. Use of 20% HLRA-650/1 increased the 28 days compressive strength by 32% compared to OPC samples. However, mortar samples containing CSA-HCl80-4-500/2 showed 22% higher compressive strength than those containing CSA-HCl80-4-650/1 at 28 days. This could be associated with the high surface area of the ash burned at 500/2.

3.4 Conclusions

The pozzolanic properties of high lignin residue ash (HLRA) and the impact of pretreatments on the pozzolanicity of corn stover ash (CSA) were studied. The findings of this study can be summarized as follows:

1. It was found that pretreatments improve the pozzolanic properties of CSA by removing AAEMs out of the biomass. It was shown that the existence of potassium and calcium in the biomass cause the formation of crystalline phases in the ash.
2. Pretreatments, particularly dilute acid, reduced the crystallinity of the corn stover ash, increased surface area, and reduced LOI of the ash. At a given burning condition, it was shown that HLRA had the highest surface area and the lowest LOI.
3. Unpretreated CSA suppressed the hydration reaction when mixed in cement paste. Also, the mortar samples containing 20% unpretreated CSA, namely CSA-Cont-650/1 and CSA-Cont-500/2, as cement replacement showed lower compressive strength than control (OPC) mortar samples. It is possible that phosphorus can be leached from the unpretreated CSA into the pore solution retarding hydration.

4. Post-treatments with distilled water at room temperature improved the hydration reaction by removing AAEMs and phosphorus out of the CSA. More phosphorus was removed in the post-treatment from the CSA-Cont-650/1 compared to CSA-Cont-500/2.
5. When used as 20% cement replacement level, dilute acid pretreated CSA increased the mortar compressive strength significantly. It was found that burning at lower temperatures increased the ash reactivity, even at temperatures lower than that typically needed to melt the silica.
6. HLRA was shown to have excellent pozzolanic reactivity, even higher than those pretreated by dilute acid. This is because of higher amorphous silica content, higher surface area, and lower LOI of the HLRA compared to other CSA samples. The improved pozzolanic performance of HLRA could be attributed to the impacts of enzymatic hydrolysis on the biomass chemical and physical properties. This could be mainly because of the organic material depolymerization.

3.5 Acknowledgements:

Financial support for this project was provided by the National Science Foundation (CMMI-103093). The author thanks NREL for the supply of HLR materials. The help of Dr. Kenneth J. Klabunde for providing access to the BET Nitrogen equipment is appreciated. The help of Central Plains Cement LLC in chemical analysis of samples is greatly acknowledged. Antoine Borden's assistance with the pretreatment experiments is gratefully acknowledged.

Chapter 4 - The impact of pretreatments and inorganic metals on thermal decomposition of agricultural residues

Abstract:

Impacts of pretreatments and alkali and alkaline earth metals (AAEMs) on thermal degradation of biomass and biomass ash properties for potential use as a supplementary cementitious material in concrete were investigated. Results showed that the influence of pretreatments on the biomass thermal degradation was largely manifested in the removal of potassium out of the biomass. The presence of potassium in the biomass increased the char percentage at temperatures higher than 380°C. Pretreatments were effective at removing potassium from biomass and dramatically reducing the char percentage at temperatures higher than 380°C. The best burning temperature for biomass ash production was 500°C because, at this temperature, thermal degradation of biomass was completed under pure combustion. Removing AAEMs, particularly potassium, not only increased the bio-oil yield but improved the quality of char as a potential candidate for supplementary cementitious materials for concrete application.

4.1 Introduction:

Awareness of construction carbon footprints has created an increasing worldwide interest in the use of supplementary cementitious materials (SCMs) as partial replacement for portland cement in concrete. Agricultural residues, such as wheat straw, rice straw, and corn stover, are potential resources for SCMs. These agro-residues are burned at controlled temperature conditions and the ashes can be used for partial replacement of cement in concrete [4.1] [4.2] [4.3]. Depending on agro-residue types and composition, agricultural residue ash (ARA) such as wheat straw ash (WSA), rice straw ash (RSA), and corn stover ash (CSA) could have negative impacts on cement hydration [4.3]. Distilled water or dilute acid pretreatments of agro-residues can improve reactivity of ARA in cementitious systems [4.1] [4.3]. It has been postulated that the removal of alkali and alkaline earth metals (AAEMs), such as potassium, calcium, and magnesium, out of the biomass by pretreatments is the reason for improved reactivity of ARA in cementitious systems [4.3]. Ash from pretreated agro-residues has lower crystallinity and carbon content compared to ash from unpretreated agro-residues [4.1] [4.3]. In addition, ARA prepared at lower temperatues has higher surface area and lower crystallinity, an important factor for ARA reactivity in concrete [4.3]. ARA obtained at lower temperatures has higher carbon content, however, which can be detrimental for concrete containing air entraining chemical admixtures. Furthermore, crystallization of the ash reduces its reactivity in cementitiou systems. Ashing at the lowest possible burning temperature at which agr-residues decompose completely should produce high quality ash for use in concrete.

Besides the adverse impact on ash quality for concrete use, the presence of AAEMs in agro-residues can adversely affect the quality of bio-oil [4.4]. The use of pretreatments to remove AAEMs from the biomass prior to pyrolysis improves the yield and quality of the bio-oil [4.4] [4.5]. Pyrolysis, the most common thermochemical conversion method, is the process in which the biomass is combusted in an oxygen-free environment. During pyrolysis, the biomass is converted to three main phases of char (solids), tar or bio-oil (liquid), and gas (syngas). Several researchers have studied the impact of AAEMs on the thermal decomposition of agro-residues and their major constituents, hemicellulose, cellulose, and lignin [4.6] [4.7] [4.8]. Research shows that the presence of potassium in biomass catalyzes thermal decomposition of biomass and increases char content during pyrolysis [4.4] [4.6]. Nowakowski and Jones (2008) studied the impact of potassium on pyrolytic behavior of the major constituents in biomass, namely cellulose, hemicellulose, and lignin. They showed that potassium has a catalytic effect on cellulose and lignin and increases the char yield. However, potassium did not have a significant impact on thermal degradation of hemicellulose.

Biomass char is not currently used in concrete as SCM because its composition and crystallinity have negative impacts on cementitious systems. For many kilns used to produce supplementary cementitious materials (SCMs), oxygen deficiencies would give conditions in-between that seen for pyrolysis and combustion. This is especially true for rudimentary kilns that could be used for producing ash for low-cost housing. Studying pyrolysis and combustion of biomass will lead to a better understanding of thermal degradation of biomass in oxygen-limited environments. The impact of pretreatments and

AAEMs on both pyrolysis and combustion of biomass at different temperatures is very important for developing technologies for biofuel production and for utilization of biomass char in concrete materials.

Thus, this study investigated the impact of pretreatments and AAEMs on the thermal degradation of wheat straw, rice straw, and corn stover during pyrolysis and combustion. Distilled water, dilute hydrochloric acid, and hot water pretreatments were used. A better fundamental understanding of the thermal decomposition process is provided for development of better ashing processes for making SCMs and using biomass char for concrete.

4.2 Materials and methods:

4.2.1 Materials:

Wheat straw (WS) and corn stover (CS) were purchased from a local farm in Manhattan, Kan., and rice straw (RS) was obtained from Missouri Rice Research Farm, Glennonville, Missouri. Hydrochloric acid (HCl), potassium chloride (KCl), potassium acetate (CH_3COOK), and magnesium chloride ($MgCl_26H_2O$) used were ACS grade. Analytical grade magnesium acetate [$(CH_3COO)_2$ Mg $4H_2O$] and high purity grade calcium acetate ($C_4H_6O_4Ca0.5H_2O$) were also used.

4.2.2 Methods:

4.2.2.1 Pretreatments:

In this study, hydrothermal pretreatments with distilled water were performed at four temperatures, 23°C, 80°C, 120°C, and 200°C and are referred to as DW23, DW80,

DW120, and DW200, respectively. For DW23 and DW80 pretreatments, 250 g of chopped biomass was immersed in 3100±100 mL of distilled water (DW) in a 4000 mL glass jar for 24 hours at 23°C and 80°C, respectively. For DW120, 250 g of chopped biomass and 3100±100 mL of distilled water (DW) were placed in an autoclave at 120°C for 30 min. The DW200 pretreatment was performed in a high pressure reactor (Parr 4843). Forty g of biomass and 480 mL of distilled water were placed inside the reactor and heated at 200°C for 10 minutes. After 10 minutes of treatment, pressure was gradually released. In the dilute acid pretreatment, the biomass was pretreated in the same manner as the DW23 and DW80 pretreatments, except that 0.1N HCl was used instead of distilled water at 23°C (HCl23) and 80°C (HCl80). Leachate samples were collected after each pretreatment and analyzed using atomic absorption spectroscopy (AAS). The wheat straw and rice straw were rinsed twice and the corn stover was rinsed four times with distilled water to remove surface elements and dried at 80°C.

Pretreated samples were impregnated by metal acetates and metal chlorides to better understand the role that various metal impurities play on the biomass thermal decomposition. This will also help understand the role that feedstock variability plays in ash quality. To study the influence of potassium, calcium, and magnesium on biomass thermal degradation, 0.5 g of pretreated and unpretreated biomass was soaked in 20 ml of 1 wt% potassium chloride (KCl), potassium acetate (CH_3COOK), calcium acetate ($C_4H_6O_4Ca0.5H_2O$), magnesium chloride ($MgCl_26H_2O$), and magnesium acetate [$(CH_3COO)_2Mg\ 4H_2O$] solutions at room temperature for 24 hrs. The biomass was then filtered through a 25µm filter paper and dried at 80°C for further analysis.

4.2.2.2 Thermal degradation characterization:

The biomass was ground into pieces approximately 2 mm in length before TGA testing. The thermal degradation behavior of biomass was studied by heating 15 to 20 mg of biomass in a TGA (TGA Q50 series) at a rate of 20°C /min up to 800°C in both nitrogen enriched and air-enriched atmospheres. The balance gas flow rate used was 40 mL/min and the furnace gas flow rate was 60 mL/min.

4.2.2.3 Biomass ash production and characterization:

A programmable electric muffle furnace was used to heat biomass samples at 500^{o}C for 2 hr of hold time. To prepare the ash, 200 g of dried biomass was burned in each batch made. A stainless steel cage with two wire mesh shelves was used to hold the biomass during burning. A stainless steel pan was placed below the cage to catch any ash that fell through the mesh. Finally, the ash was ground for one hour at 85 revolutions per minute (rpm) in a laboratory ball mill. Loss on ignition (LOI) of the ash was determined by measuring mass loss after heating one gram of dry biomass ash (CSA, WSA or RSA) to 900°C for three hours. LOI was calculated as the percentage mass loss during firing. Surface area of the biomass ash samples was determined using BET nitrogen adsorption. The naming convention for ash samples is as follows: type of ash-pretreatment-burning temperature/holding time. For example, the name of corn stover ash pretreated with 0.1 N HCl at 80°C and burned at 500°C for 2 hrs would be CSA-HCl80-500/2.

4.3 Results and Discussion:

4.3.1 Influence of pretreatments on AAEM removal:

AAEMs concentrations for wheat straw, rice straw, and corn stover leachate for different pretreatments are shown in Table 4.1. At a given temperature, the dilute acid pretreatment was more effective in removing calcium (Ca) and magnesium (Mg) out of the biomass than distilled water pretreatment. Moreover, for a given pretreatment, the increase in temperature increased AAEMs removal. It is worth noting that corn stover contained higher amounts of AAEMs than wheat straw and rice straw. Removal of AAEMs, particularly potassium, from the biomass is important for improving biomass ash quality for concrete application as well as reducing corrosion of biofuel reactors and kilns [4.3] [4.4].

Table 4.1: Biomass leachate inorganic concentrations

	Temp.	Potassium(K) mg/L		Calcium (Ca) mg/L		Magnesium(Mg) mg/L	
		DW	HCl	DW	HCl	DW	HCl
Wheat Straw	23°C	665	673	40	170	35	98
	80°C	690	772	76	226	51	136
	200°C	868		70		51.2	
Rice Straw	23°C	936.8	1084	5.44	124	68	93
	80°C	962	1144	16	214	54	90
	200°C	1227		20		138	
Corn Stover	23°C	1500	1730	115	235	72	108
	80°C	1875	2176	118	333	81	122
	200°C	2280		120		72	

4.3.2 The impact of pretreatments on carbon content and surface area of biomass ash:

Table 4.2 shows carbon content, in terms of LOI and BET surface area, of pretreated and unpretreated CSA, WSA, and RSA. Pretreatments dramatically reduced the LOI and increased the surface area of the ash. HCl80 pretreated ash had 75% less unburned carbon than unpretreated ash. The high LOI of unpretreated corn stover ash (CSA-Cont-500/2) could be attributed to the high potassium content of corn stover. Figure 4.1 shows the correlation between MgO, K_2O, and CaO content of biomass ash and LOI. A linear relationship between K_2O of the ash and its LOI, suggests a relationship between potassium and thermal decomposition. The relationship between MgO of the ash and its LOI also appeared to be linear, whereas the CaO content of the ash did not correlate well with LOI of the ash. Surface area of the RSA pretreated with HCl80 sample (RSA-HCl80-500/2) was more than 20 times higher than the unpretreated RSA sample (RSA-Cont-500/2). Likewise, surface area of WSA-HCl80-500/2 was six times higher than WSA-Cont-500/2. Relationships between AAEMs content and ash carbon content led to additional experiments to further understand how these elements affect biomass thermal decomposition.

Table 4.2: Surface area and LOI of biomass ash

Ash Type	Unburned Carbon		BET surface area (m^2/g)
	LOI (%)	S.D	
WSA-Cont-500/2	11.5	0.65	27.6
WSA-DW23-500/2	7.6	0.45	---
WSA-DW80-500/2	6.9	0.35	---
WSA-HCl23-500/2	6	0.25	---
WSA-HCl80-500/2	2.9	0.46	168
RSA-Cont-500/2	7.5	0.55	9.6
RSA-DW23-500/2	4.6	0.50	---
RSA-DW80-500/2	3.5	0.35	---
RSA-HCl23-500/2	3.5	0.40	---
RSA-HCl80-500/2	2.2	0.31	200
CSA-Cont-500/2	25.1	0.60	11.3
CSA-DW80-500/2	13.2	0.45	---
CSA-HCl80-500/2	6.1	0.40	64

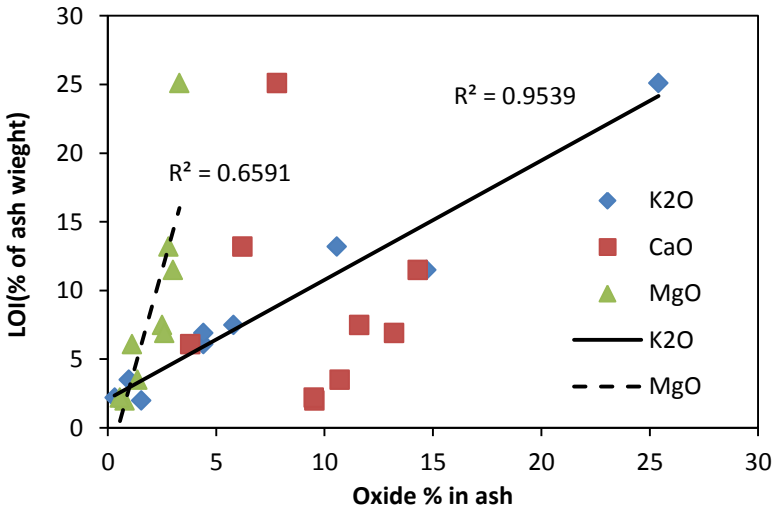

Figure 4.1: Correlation between LOI and k_2O, CaO, and MgO content of ash

4.3.3 The impact of pretreatments on biomass pyrolysis:

Figure 4.2a shows differential thermogravimetric (DTG) results for thermal decomposition of unpretreated (RS-Cont), DW80 pretreated (RS-DW80), dilute acid pretreated (RS-HCl80), and DW200 pretreated (RS-DW200) rice straw samples during pyrolysis. A shallow mass loss peak seen for unpretreated rice straw at approximately 210°C could be associated with decomposition of minor compounds present in the straw. The mass loss peak for unpretreated rice straw that occurs at 330°C could be attributed to decomposition of hemicellulose and cellulose. RS-DW80 showed distinct mass loss peaks (DTG peaks) at 310°C and 360°C. These peaks can be attributed to decomposition of hemicellulose and cellulose, respectively [4.6] [4.9]. Both RS-HCl80 and RS-DW200 samples revealed a large DTG peak which primarily represents the decomposition of cellulose. However, the mass loss peak for RS-DW200 occurred at a slightly higher temperature (380°C) and magnitude compared to the DTG peak for RS-HCl80, possibly because of the existence of hemicellulose in RS-HCl80, higher content of cellulose in the DW200 sample, and structural change of cellulose in DW200 sample. The coexistence of hemicellulose with cellulose can reduce the mass loss rate of cellulose [4.10]. Although all samples had lignin, DTG plots did not show a separate mass loss peak for lignin. Previous research shows that the presence of hemicellulose decreases the mass loss rate of lignin [4.10]. It is worth noting that the hemicellulose mass loss peak is almost absent in the DW200 pretreated samples, suggesting that DW200 removed most of the hemicellulose [4.11]. HCl80 pretreatment also seems to remove some of the hemicellulose out of the biomass. The absence of a third distinguishable mass loss rate peak normally associated

with lignin (RS-Cont and RS-DW80) could result from a decrease in the rate of mass loss by hemicellulose and overlap of the lignin DTG peak with that of the cellulose. Thermal degradation behavior of samples pretreated with distilled water at 23°C (DW23) and dilute acid at 23°C (HCl23) was similar to that of samples pretreated with distilled water at 80^{o}C (DW80), possibly because these three pretreatments did not remove hemicellulose but leached most of the potassium out of the biomass. As shown in Figure 4.2b, wheat straw showed similar thermal degradation behavior as rice straw. Corn stover also showed a similar trend, as illustrated in Figure 4.2c.

4.3.4 The impact of AAEMs on biomass pyrolysis:

Changes in the thermal decomposition behavior of biomass constituent materials by pretreatments could be attributed to the removal of AAEMs from the biomass. To investigate the impact of different AAEMs on thermal degradation, pretreated biomass and unpretreated biomass were impregnated by metal chlorides and metal acetates. Figure 4.3 shows the influence of KCl and Potassium acetate (K-acetate) impregnation on the thermal degradation of unpretreated and DW80 pretreated wheat straw samples. For both DW80 pretreated and unpretreated samples, KCl impregnated samples (WS-DW80-KCl and WS-Cont-KCl) revealed distinct mass loss peaks for hemicellulose and cellulose. Furthermore, KCl impregnation catalyzed the thermal degradation of both cellulose and hemicellulose. However, potassium acetate impregnation did not significantly change the thermal behavior of the unpretreated sample, likely because the unpretreated sample already contained a large amount of potassium.

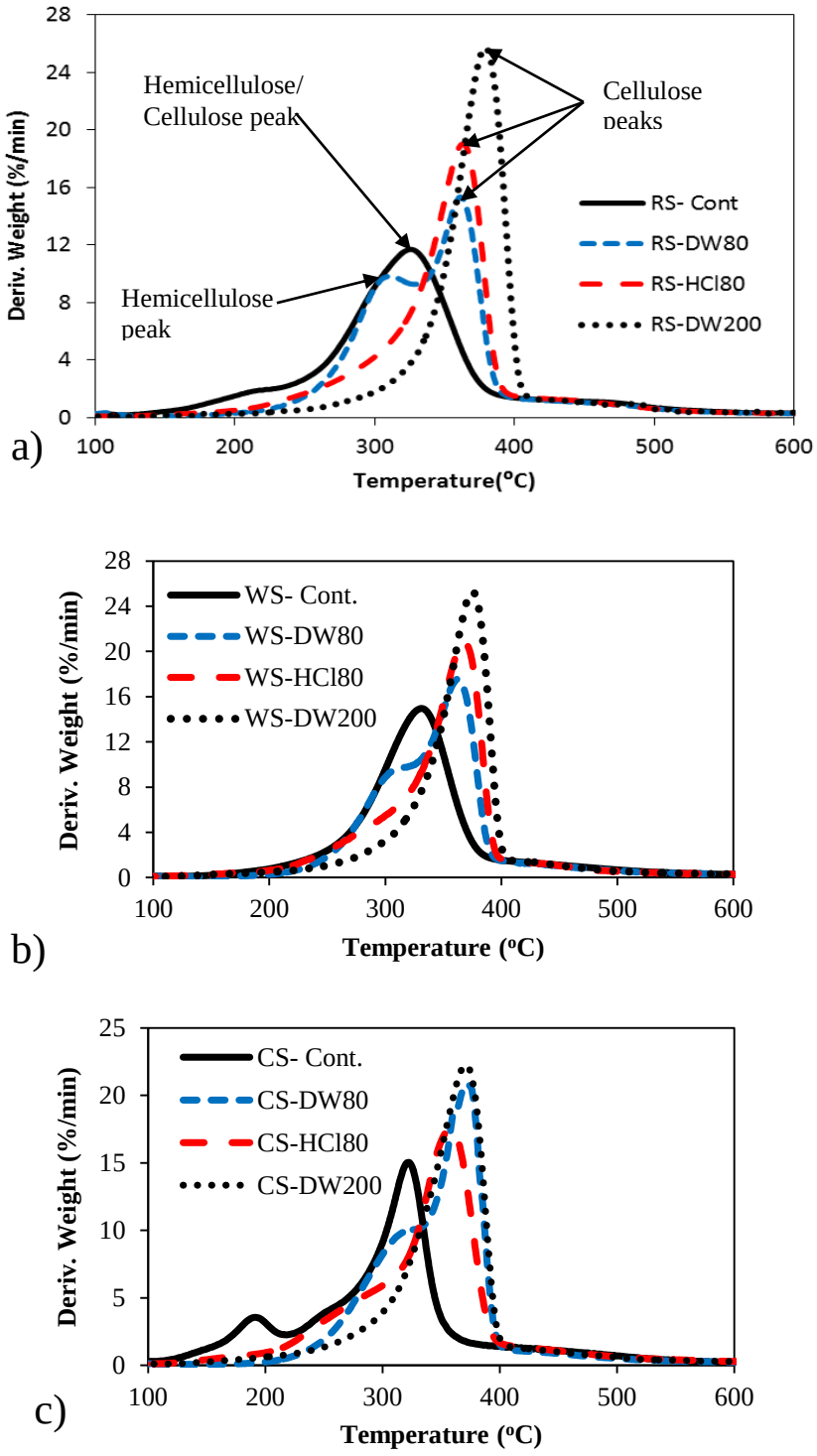

Figure 4.2: DTG plots of pretreated and unpretreated (a) Rice straw and (b) wheat straw and (c) corn stover

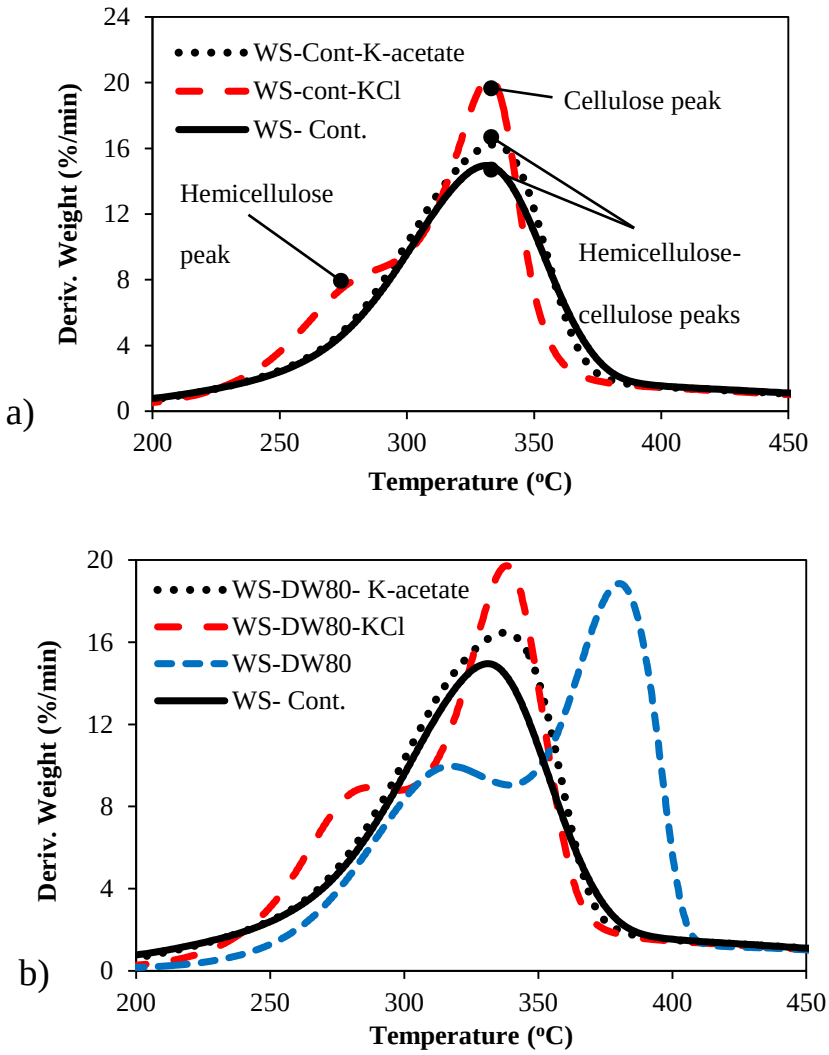

Figure 4.3: DTG graphs for Potassium acetate and KCl impregnated (a) unpretreated, and (b) pretreated wheat straw

When the DW80 pretreated sample was impregnated with potassium acetate (WS-DW80-Potassium acetate), maximum weight loss rate of hemicellulose and cellulose occurred at lower temperatures, as shown in Figure 4.3b. Differences between the potassium acetate and KCl impregnation show that potassium catalyzes the thermal degradation of cellulose only, whereas chlorides appear to catalyze the thermal degradation of hemicellulose and cellulose. The samples impregnated with Potassium acetate showed

that the cellulose maximum mass loss rate temperature shifted to a lower temperature, making the hemicellulose and cellulose mass loss rate peaks overlap.

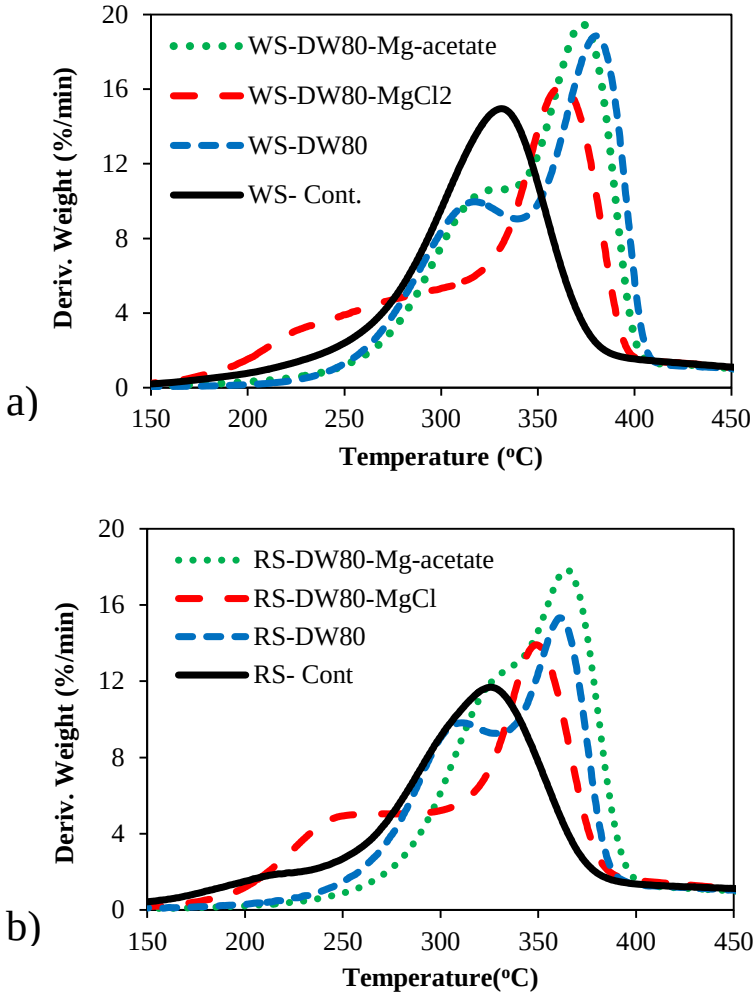

Figure 4.4: DTG graphs for (a) Mg impregnated wheat straw, and (b) Mg impregnated rice straw

$MgCl_2$ impregnation of the DW80 pretreated sample slightly reduced the temperature at which the cellulose maximum mass loss rate occurs and completely changed the thermal degradation of hemicellulose, as shown in Figure 4.4a and Figure 4.4b. Impregnation with Mg-acetate only slightly changed the thermal behavior of

the sample. Comparison of KCl impregnation with $MgCl_2$ impregnation reveals that the influence of chlorine on biomass thermal degradation depends on the cation that accompanies it. DTG plots of $MgCl_2$ impregnated samples showed a mass loss peak occurring from 200°C to 300 °C, whereas DTG curves for KCl impregnated samples showed mass loss peak for hemicellulose from 250°C to 300°C, see Figure 4.4b and Figure 4.5. Ca-acetate impregnation of pretreated wheat straw did not significantly change the thermal degradation behavior, as seen in Figure 4.6. Clearly, the type of cation is important. Similar behavior was seen for corn stover and rice straw samples.

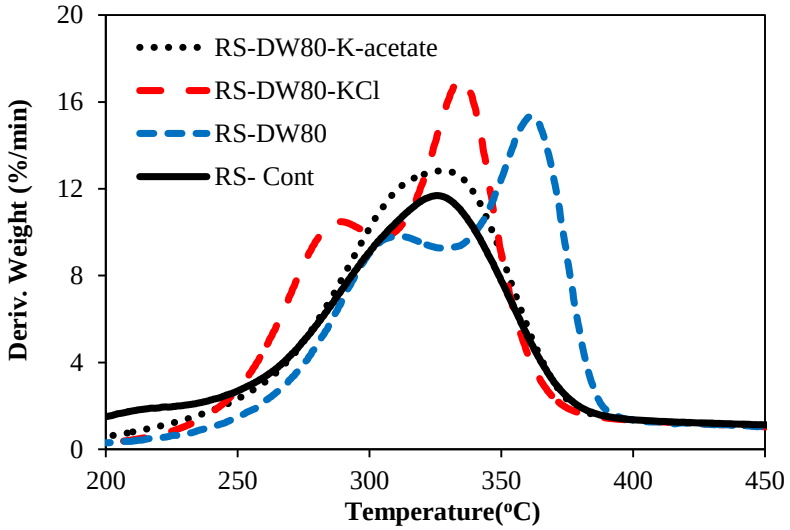

Figure 4.5: DTG graphs for Potassium acetate and KCl impregnated-pretreated rice straw

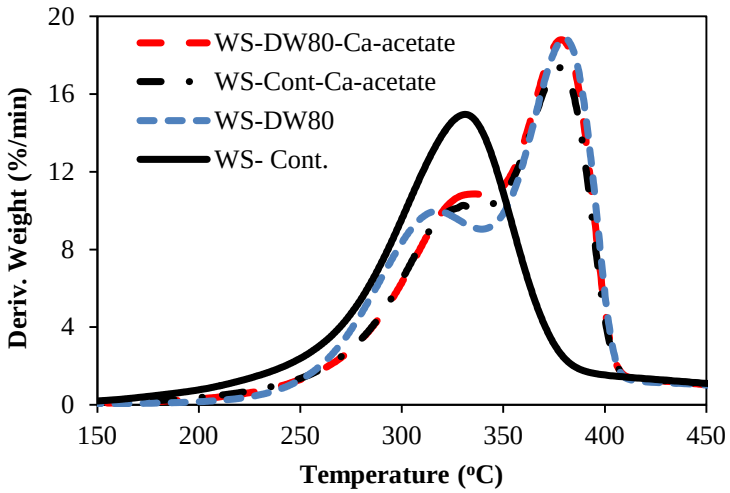

Figure 4.6: DTG graphs for Ca impregnated wheat straw

Biomass impregnation with metal acetates better simulated the actual pyrolytic behavior of biomass compared to metal chlorides because Potassium acetate impregnation of DW80 pretreated biomass samples showed similar pyrolytic degradation to that of unpretreated biomass, as seen in Figure 4.3. Thus, in order to study the impact of AAEMs on the pyrolytic behavior of biomass and its product distribution, metal acetate, rather than metal chlorides, should be used as impregnation media.

The impact of K, Mg, and Ca on weight loss during biomass pyrolysis is shown in Figure 4.7. As shown, unpretreated samples (control samples) and potassium impregnated DW80 samples have higher mass loss at temperatures lower than 380°C compared to pretreated and Mg and Ca impregnated samples. However, at temperatures higher than 380°C, the weight loss is higher for pretreated and Mg and Ca impregnated samples compared to potassium impregnated and unpretreated samples. Comparison of WS-DW80 sample with WS-DW80-Potassium acetate sample revealed that, at 330°C, WS-DW80 had 14% less weight loss whereas, at 700^{o}C, it had 6% more weight loss. A similar trend was

also observed for rice straw and corn stover samples. The positive impact of potassium is that, at temperatures lower than 380°C, it acts as a catalyst or flux agent and promotes thermal decomposition. The negative impact of potassium is that, at temperatures higher than 380°C, it suppresses decomposition, increasing the amount of carbon remaining in the char. The increase in char content could be attributed to the deposition of potassium as potassium chloride (KCl) on the surface of organic compounds, possibly leading to carbon entrapment during decomposition [4.8] [4.12] [4.13]. Removing elements, such as potassium, that can be harmful for pyrolysis equipment and char reactivity in concrete not only increases the bio oil yield but improves the quality of char as a potential candidate for SCMs. Thus, pretreatments have twofold benefits: increasing bio-oil yield and improving char quality for concrete applications.

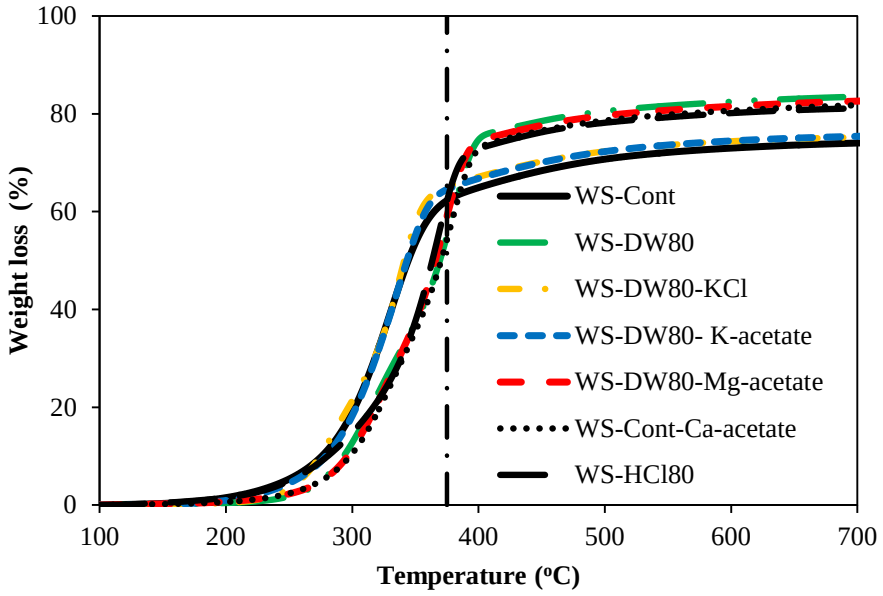

Figure 4.7: The impact of K, Mg, and Ca on char percentage of biomass

4.3.5 The impact of pretreatments on biomass combustion:

Thermogravimetric (TG) and differential thermogravimetric (DTG) curves for wheat straw and rice straw combustion are shown in Figure 4.9 and Figure 4.9, respectively. Similar to pyrolysis, pretreatments increased the maximum mass loss rate as well as the temperature at which the maximum mass loss occurs. Although unpretreated samples showed higher weight loss at temperatures lower than 330°C as compared to pretreated samples, the weight loss for all pretreated and unpretreated samples was similar at temperatures higher than 500°C. A similar trend was also seen for corn stover. The combustion (abundant oxygen availability) of rice straw, wheat straw, and corn stover completes at around 500°C. At this or higher temperatures, resulting ash should have little to no unburned carbon, regardless of pretreatments. This means that if the biomass had undergone pure combustion in the muffle furnace when ashes were made, the LOI of all ashes would have been close to zero because the biomass was burned at 500°C. On the other hand, if the condition in the muffle furnace was similar to pure pyrolysis, the LOI would have been similar to the char percentage minus the ash content. However, the LOI of biomass ashes were lower than the char percentages. For instance, the LOI of WSA-DW80-500/2 was 6.9%, whereas the char % of WS-DW80 sample at this temperature was 22 (including 5% ash). Therefore, it can be said that the condition in the muffle furnace had been in between pure pyrolysis and pure combustion. Because of this, pretreatments significantly reduced the LOI of biomass ash, as seen in Table 4.2. The increase in surface area of pretreated biomass ash could also indicate that the biomass had undergone partial pyrolysis. Because at temperature higher than 380°C during pyrolysis, potassium present in

unpretreated biomass does not allow the organic compound burn off completely and thus decreasing the surface area, as shown in Figure 4.7.

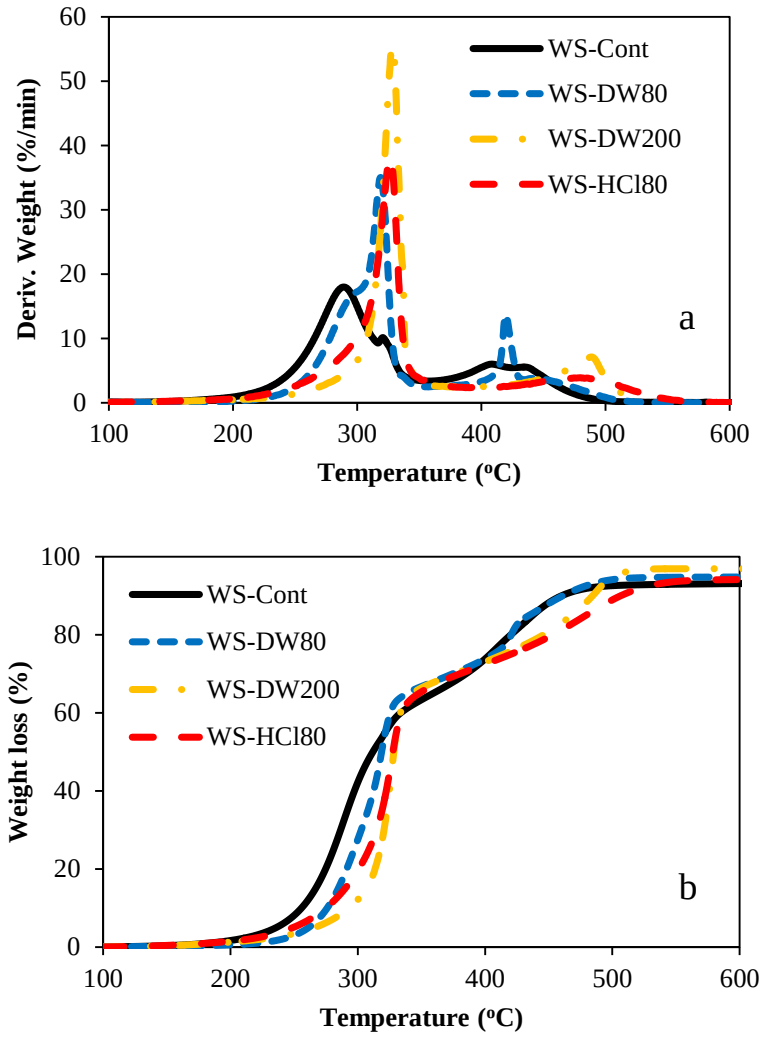

Figure 4.8: (a) DTG and (b) TG plots for wheat straw combustion

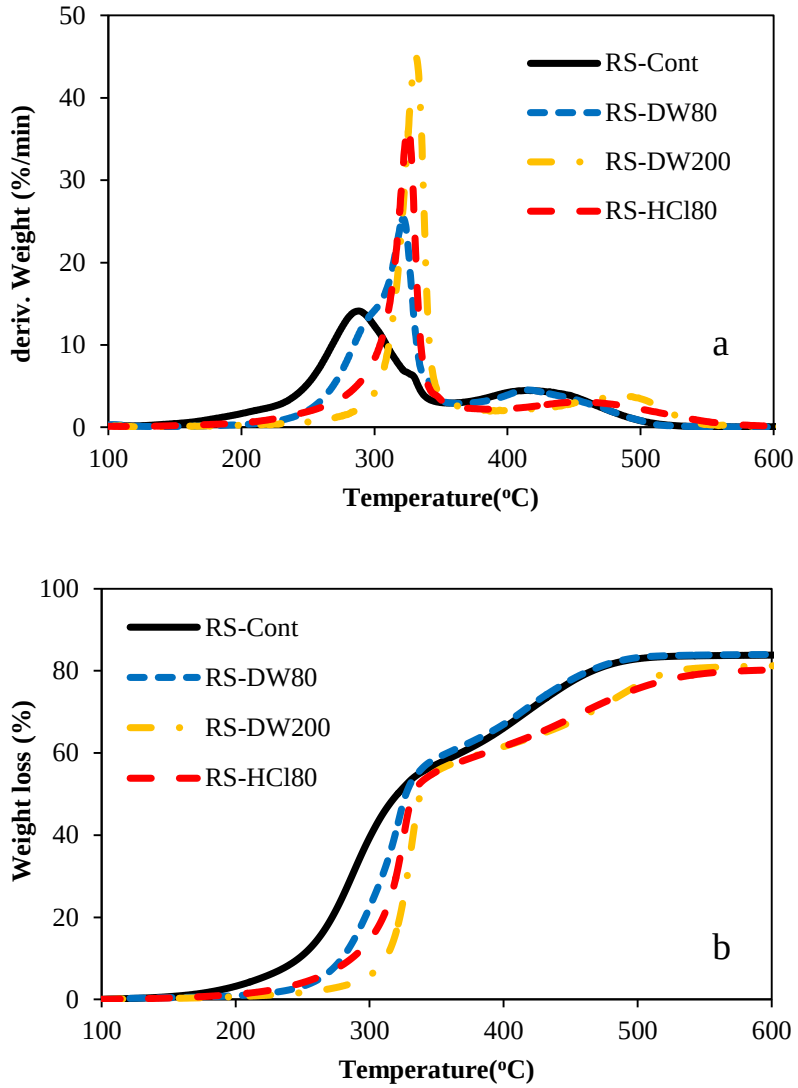

Figure 4.9: (a) DTG and (b) TG plots for rice straw combustion

4.3.6 Immediate char combustion:

Biomass char cannot be used in concrete partly because of its high carbon content. Another alternative for producing reactive ash from biomass char could be oxygen insertion into the pyrolysis reactor immediately at the end of the pyrolysis process without increasing the temperature. Figure 4.10 shows the thermal decomposition of corn stover and wheat straw where air was introduced in the furnace immediately at the end of

pyrolysis. Pyrolysis was performed up to 500°C (500-pyr) or 700°C (700-pyr) when nitrogen gas was switched to air. After switching gases, temperature was kept constant at either 500°C or 700°C.

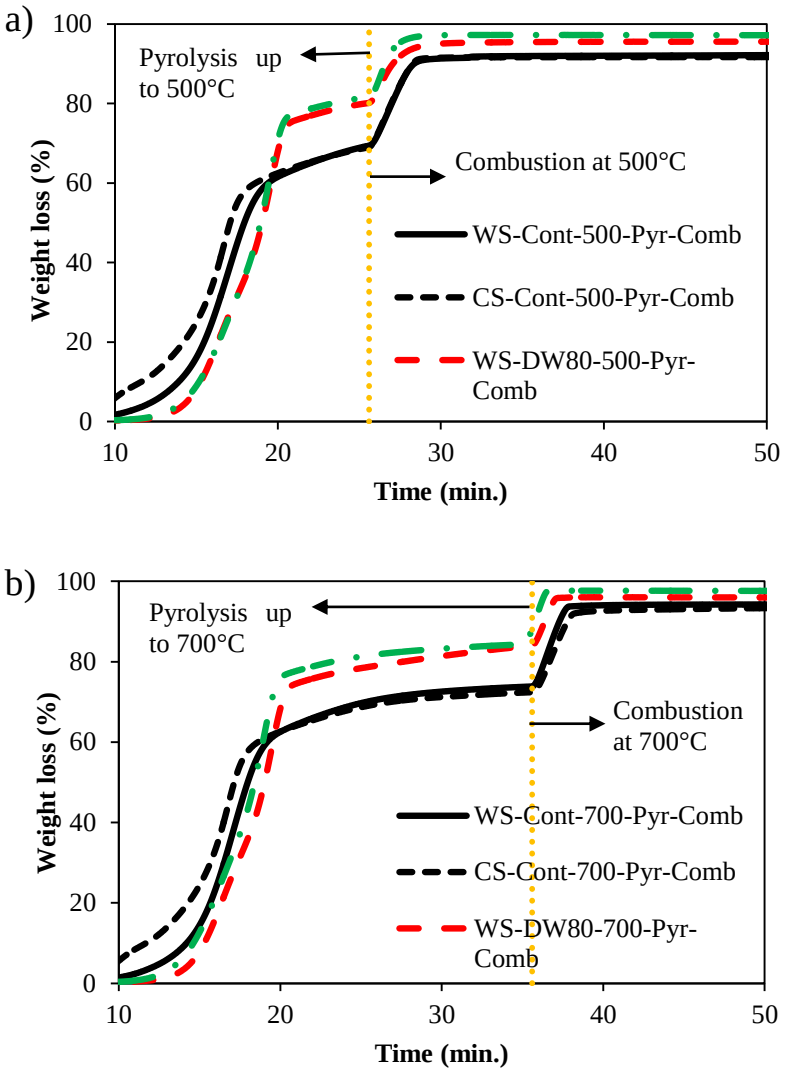

Figure 4.10: Wheat straw and corn stover pyrolysis followed by combustion, a) pyrolysis up to 500°C; b) pyrolysis up to 700°

Pyrolysis temperature and pretreatments did not affect the char decomposition because, for a given sample, the final weight loss was almost the same at both pyrolysis temperatures. Figure 4.10 shows that, although temperatures higher than 380°C yield a

greater amount of char for unpretreated samples (WS-Cont, and CS-Cont) compared to pretreated samples (WS-DW80 and CS-DW80), final weight loss is similar for pretreated and unpretreated samples. It is worth noting that the char completely decomposed in a very short time, approximately two minutes, after oxygen was introduced into the furnace. This is an important observation for developing technologies for simultaneous pyrolysis and reactive ash production for concrete use. Regardless of pretreatments, the char can be combusted to produce ash with low carbon content. However, pretreatments help remove other constituents, such as potassium, from the biomass char that cause crystallization of the char and reduce its reactivity in concrete.

4.4 Conclusions:

During pyrolysis of wheat straw, rice straw, and corn stover, the presence of potassium in the biomass slightly decreased the char percentage at temperatures lower than 380°C, whereas the char percentage increased at temperatures higher than 380°C. Pretreatments dramatically reduced the char percentage at temperatures higher than 380°C. Although pretreatments removed some Mg and Ca out of the biomass, the impact of pretreatments on thermal degradation of biomass during pyrolysis was largely pronounced by the removal of potassium from the biomass. The carbon content of biomass ash, which was prepared in an electrical muffle furnace with limited oxygen, was well correlated with the ash potassium content. The high char yield of unpretreated biomass and the high carbon content of unpretreated biomass ash were shown to be because of the presence of potassium in the biomass that can entrap carbon during pyrolysis. Removal of potassium out of the biomass via pretreatments reduces the LOI and increases the surface area of the

biomass ash when the biomass is ashed even in oxygen-limited environments. Thus, removing AAEMs, particularly potassium that can be harmful for pyrolysis equipment and char reactivity in concrete not only increases bio-oil yield but improves the quality of char as a potential candidate for SCMs.

4.5 Acknowledgements:

This study was funded by the National Science Foundation award #: CMMI-103093. The authors are grateful to Dr. Donn Beighley for providing the rice straw. Antoine Borden's assistance with pretreatment experiments is gratefully acknowledged.

Chapter 5 - Impact of Pretreatments and Enzymatic Hydrolysis on Agricultural Residue Ash Suitability for Concrete

Abstract:

Agricultural residues such as corn stover, wheat straw, and rice straw are emerging as potential renewable resources for biofuel production. Byproducts from biofuel production have potential for use as supplementary cementitious materials (SCMs) in concrete after ashing. This study investigated effects of the lignocellulosic ethanol production process on the potential use of the byproduct as an SCM. Sodium hydroxide (2%) and dilute sulfuric acid (1%) pretreatments at 121°C and enzymatic hydrolysis were conducted on corn stover, wheat straw, and rice straw. Results showed that biomass pretreatment with sodium hydroxide is not an effective method for increasing reactivity of biomass ash in concrete. Sodium hydroxide pretreatment removed large amounts of silicon from the biomass, but was not effective in removing phosphorous and other metal impurities out of the biomass. Additionally, NaOH pretreatment did not remove all crystalline phases out of the biomass. Sulfuric acid pretreatment was found to be an effective pretreatment method for producing reactive biomass ash because sulfuric acid removed most of the crystalline phases out of the biomass. When NaOH pretreatments were used, enzymatic hydrolysis could positively affect reactivity of ash because enzymatic hydrolysis leached some of the inorganic elements that were not leached during NaOH pretreatment. Therefore, when evaluating bioethanol byproduct for concrete

applications, sulfuric acid is a better pretreatment than NaOH because, if sulfuric acid pretreatment is used, the bioethanol byproduct would be a potential candidate for producing reactive SCMs.

5.1 Introduction:

Awareness of global warming and anticipated depletion of fossil fuel deposits have increased interest in biofuel production, especially lignocellolusic bioethanol [5.1] [5.2] [5.3]. As lignocellulosic materials, agricultural residues such as corn stover, rice straw, and wheat straw are potential renewable resources for biofuel production [5.4] [5.5] [5.6] [5.7]. Lignocellulosic materials are converted to fuels using either thermochemical or biochemical pathways [5.2] [5.3]. In the thermochemical route, lignocellulosic materials undergo pyrolysis or gasification to produce syngas, which is then upgraded to various types of fuels, such as ethanol and methanol [5.2] [5.8]. For the biochemical approach, microorganisms convert lignocellulosic materials to fuels, such as ethanol and methanol [5.2] [5.9]. During biochemical conversion, lignocellulosic materials undergo three main processes: pretreatment, enzymatic hydrolysis, and fermentation [5.2] [5.3].

Pretreatment methods have been used to reduce the degree of polymerization of cellulose and remove and breakdown hemicellulose and lignin structures in lignocellulosic materials [5.10]. The primary purpose of pretreatments is to increase available surface area of the cellulose to hydrolytic enzymes, thus increasing bioethanol yield [5.2] [5.3] [5.10]. Among the characteristics of efficient pretreatments include: (1) increased digestibility of cellulose in enzymatic hydrolysis, (2) limited formation of harmful compounds by reducing sugar and lignin degradation, and (3) low energy demand and cost requirements [5.2]. Pretreatments are grouped in three main categories of physical, chemical, and biological [5.10]. In the physical pretreatment methods, such as size reduction, steam explosion, and liquid hot water, no chemicals or organisms are used in the process.

Chemical pretreatments use acids or alkalis to remove hemicellulose and/or lignin from biomass and increase cellulose accessibility to enzymes. In biochemical pretreatments, microorganisms such as soft-rot fungi and bacteria alter lignocellulosic biomass structure and composition to enhance enzymatic digestibility of the biomass [5.10]. Enzymatic hydrolysis is used to breakdown cellulose and hemicellulose to glucose and other sugars, such as xylose. Sugars are fermented to ethanol after enzymatic hydrolysis.

Biochemical conversion leaves behind high lignin residue (HLR) materials that can be used to produce supplementary cementitious materials (SCMs) for concrete use. Silica from agricultural residues could be potentially reactive in concrete after ashing. Pretreatments such as dilute acid enhance properties of agricultural residue (ARA) for ashing and use in concrete [5.11] [5.12]. Effects of the enzymatic hydrolysis on potential use of byproducts for SCMs production have not been studied yet.

High lignin residue is commonly used in boilers for energy generation [5.1]. Burning HLR in boilers produces high lignin residue ash (HLRA) that can be rich in silica and calcium. It was shown in chapter three that HLRA can be used as a SCM in concrete to reduce cement content as well as improve concrete quality. However, use of HLRA in concrete depends on its physical and chemical properties. Physical and chemical properties of HLRA depend on the burning conditions and composition of HLR. Since various pretreatments have different impacts on lignocellulosic materials [5.2] [5.3] [5.10], HLR properties and, consequently properties of HLRA, can be influenced by pretreatments.

This study aims to investigate the impact of pretreatments and enzymatic hydrolysis on the physical properties of agricultural residue ash (ARA). Dilute sulfuric

acid and sodium hydroxide, the two most commonly used chemical pretreatments, and three types of agricultural residues, namely corn stover, rice straw, and wheat straw, were used in this study. Effectiveness of pretreatments and enzymatic hydrolysis on ARA properties for concrete use was determined based on the removal of crystalline phases and inorganic compounds from the biomass by pretreatments and enzymatic hydrolysis.

5.2 Materials and methods:

5.2.1 Materials:

Corn stover (CS) and wheat straw (WS) were purchased from a local farm. Rice straw (RS) was obtained from Missouri Rice Research Farm, Glennonville, Missouri. The biomass (CS, WS, and RS) was ground to 5-10 mm using a hammer mill and then dried in an oven at 80°C. An aqueous solution of cellulase from Trichoderma reesei (ATCC 26921) was used for enzymatic hydrolysis. ACS grade sodium hydroxide, sodium acetate, acetic acid, and sulfuric acid were used. 2% NaOH and 1% sulfuric acid were used for pretreatments. Sodium acetate and acetic acid were used to prepare a 50 mM of buffer solution for enzymatic hydrolysis.

5.2.2 Methods:

5.2.2.1 Chemical Pretreatment:

Several studies have performed sodium hydroxide pretreatments at 1% to 4% concentrations and sulfuric acid pretreatments at concentrations of 0.5% to 1.5% for bioethanol production [5.7] [5.13] [5.14] [5.15]. In this study, 2% sodium hydroxide and 1% sulfuric acid pretreatments were utilized. To pretreat the biomass, 40 g of biomass (CS,

WS, or RS) was placed in a 1000 ml straight-sided wide-mouth glass container. 400 ml of either 2% sodium hydroxide or 1% sulfuric acid solution was then added to the container, placed in an autoclave, and heated at 121°C for 30 minutes. The containers were cooled to room temperature, after which the biomass was filtered through a #100 sieve (150 µm). The filtrate was collected for elemental analysis, and the filtered biomass was washed three times. Two liters (2L) of tap water were used for each washing, followed by rinsing with 2L of distilled water. Finally, the biomass was dried at 80°C. The pretreatment process is shown in Figure 5.1.

5.2.2.2 Enzymatic hydrolysis of pretreated biomass:

Ten grams of pretreated biomass was placed in a 250 ml Erlenmeyer flask, and 150 ml of 50 mM sodium acetate buffer solution (pH=5) was then added to the flask [5.4] [5.13]. 300 µl of the cellulase enzymes solution was then added to the solution, which is equivalent to 25 filter paper unite (FPU) per gram of pretreated biomass [5.13]. FPU is defined as the amount of enzyme that releases 1 µmol of glucose during hydrolysis [5.16] [5.17]. An incubator shaker was used to shake the flasks at 150 rpm for 48 hrs at 50°C. The biomass was then filtered with a #70 sieve, and the leachate was collected for elemental analysis. Finally, the biomass was washed three times each with 2L of tap water and once with 2L of distilled water and dried at 80°C.

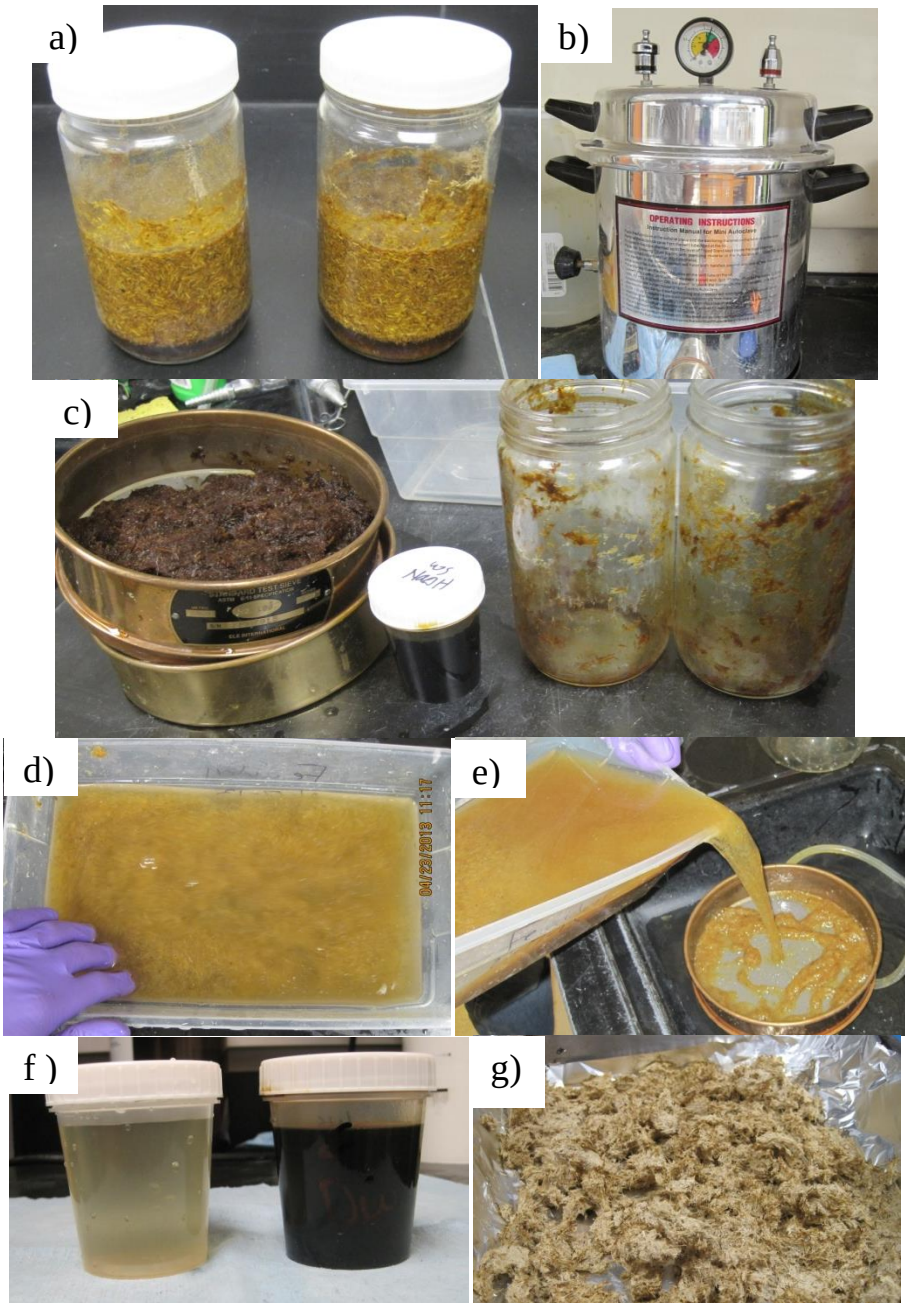

Figure 5.1: Pretreatment process.: a) Biomass in pretreatment solution in glass jars, b) Autoclave used to heat glass jars to 121°C, c) Biomass filtered through #100 sieve after pretreatment, d) Pretreated biomass is washed, e) Pretreated biomass is sieved after washing, f) Filtrate collected after pretreatment (dark color) and after last washing, g) Dried pretreated biomass

5.2.2.3 Elemental analysis:

Filtrates after pretreatments and enzymatic hydrolysis were collected for elemental analysis. Silicon (Si), calcium (Ca), magnesium (mg), potassium (K), and phosphorous (P) concentrations of the filtrate were measured using inductively coupled plasma mass spectrometry (ICP-MS).

5.2.2.4 Ashing and XRD measurements:

To prepare biomass ash, 50 gr of biomass was placed on a stainless steel pan and burned in an electrical muffle furnace at 600°C for one hour. The biomass was burned at three different stages: before pretreatments (control ash samples), after pretreatments but before enzymatic hydrolysis (pretreated ash samples), and after enzymatic hydrolysis (hydrolyzed ash samples). Five types of ash were prepared for each type of biomass. For corn stover, the five types of ash included unpretreated ash (CSA-Cont), NaOH pretreated ash (CSA-NaOH), sulfuric acid pretreated ash (CSA-Sulf), ash prepared after NaOH pretreatment and enzymatic hydrolysis (CSA-NaOH-Hyd), and ash prepared after sulfuric acid pretreatment and enzymatic hydrolysis (CSA-Sulf-Hyd). A similar naming convention was used for WSA and RSA.

To determine crystalline phases of ash samples, x-ray diffraction (XRD) analysis was performed (Cu Kα radiation with λ=1.5046Å). A step size of 0.02° 2θ and a step time of four sec were used. A scan range of 5°–70° 2θ was considered.

Thermal degradation of biomass at each stage of treatments was obtained by heating 8-10 mg of biomass in a thermogravimetric analyzer (TGA) in a compressed air

environment. The biomass was heated to 700°C at a heating rate of 10°C/min. The ash percentage of biomass was calculated as weight percentage at 700°C.

5.3 Result and discussion:

5.3.1 Effect of pretreatments on the inorganic elements leaching:

Table 5.1 shows the concentration of inorganic elements in the filtrate after pretreatments measured with ICP-MS. Removal of these inorganic elements varied by pretreatment type. The 2% sodium hydroxide pretreatment (NaOH) removed higher amounts of silicon compared to 1% sulfuric acid pretreatment (Sulf). However, the sulfuric acid pretreatment removed higher amounts of calcium, magnesium, and phosphorous. Both pretreatment types removed similar amounts of potassium from the biomass.

Inorganics were also leached from the pretreated biomass during enzymatic hydrolysis, as shown in Table 5.2. Enzymatic hydrolysis removed higher amounts of phosphorous, calcium, and magnesium from NaOH pretreated samples (CS-NaOH, WS-NaOH, and RS-NaOH) than those pretreated with sulfuric acid (CS-Sulf, WS- Sulf, and RS- Sulf). Enzymatic hydrolysis removed higher CA, Mg, and P out of NaOH pretreated samples as compared to sulfuric acid pretreated samples because the sulfuric acid pretreatment removed most of Ca, Mg, and P out of the biomass, whereas NaOH pretreatment removed only small amounts of these elements.

Table 5.1: Filtrate from pretreatments

Sample ID	Silicon (Si) (ppm)		Phosphorous (P) (ppm)		Calcium (Ca) (ppm)		Potassium (K) (ppm)		Magnesium (Mg) (ppm)	
	Avg.	St.D.	Avg.	St.D.	Avg.	St.D.	Avg.	St.D.	Avg.	St.D.
CS-NaOH	214.6	43.6	17.3	4.4	7.9	5.7	756.3	141.7	3.3	2.7
CS-Sulf	16.5	1.6	190.6	2.7	354.8	3.5	1216.2	13.3	125.8	2.3
WS-NaOH	155.0	97.8	4.0	3.9	2.3	2.0	121.7	112.4	0.8	0.9
WS-Sulf	47.9	4.6	168.2	3.1	151.4	3.8	852.6	4.4	58.0	0.9
RS-NaOH	1579.2	48.3	69.3	1.1	3.7	0.5	722.4	20.8	1.7	0.1
RS-Sulf	80.1	7.6	144.9	1.4	193.2	0.6	858.1	3.8	161.4	2.9

Avg.= Average; St.D.= Standard deviation

Table 5.2: Filtrate from enzymatic hydrolysis

Sample ID	Silicon (Si) (ppm)		Phosphorous (P) (ppm)		Calcium (Ca) (ppm)		Potassium (K) (ppm)		Magnesium (Mg) (ppm)	
	Avg.	St.D.	Avg.	St.D.	Avg.	St.D.	Avg.	St.D.	Avg.	St.D.
CS-NaOH	109.2	4.6	39.6	1.2	205.4	2.0	17.6	0.9	141.4	2.0
CS-Sulf	56.0	1.2	4.6	0.3	26.4	2.1	6.2	0.8	7.4	0.5
WS-NaOH	115.5	1.5	38.8	1.0	210.0	3.7	14.1	0.7	107.6	1.8
WS-Sulf	100.1	0.7	6.6	0.1	15.7	2.2	3.7	0.3	3.9	0.8
RS-NaOH	145.4	4.0	19.3	0.2	277.3	4.7	15.0	0.9	234.9	7.4
RS-Sulf	115.3	5.7	8.9	0.3	21.7	2.5	4.6	0.9	2.9	0.6

Plants need silicon, calcium, phosphorous, and magnesium sources for optimum growth. These elements are precipitated in the form of silica, calcium carbonate, calcium oxalate, calcium phosphate, and magnesium oxalate in plant cell walls [5.18] [5.19] [5.20].

Solubility of these crystalline phases is pH dependent. Solubility of silica is constant up to a pH of 9 and then dramatically increases at higher pH values [5.21] [5.22] [5.23]. However, solubility of calcium carbonate, calcium phosphate, calcium oxalate, and magnesium oxalate increases with an increase in solution pH [5.24] [5.25] [5.26] [5.27]. The pH of 2% sodium hydroxide solution used for pretreatment was 12.5, and the pH of 1% sulfuric acid pretreatment was 2.75. Therefore, the removal of low amounts of Ca, P, and Mg but high amounts of Si from the biomass by NaOH pretreatment could be attributed to high pH of the NaOH pretreatment. Additionally, solubility of higher amounts of silicon from rice straw as compared to wheat straw and corn stover could be attributed to the amorphous nature of silica in rice straw [5.23].

Incorporating biomass ash containing phosphorous suppresses cement hydration in concrete and reduces the compressive strength of concrete, as was discussed in Chapter Three. Additionally, potassium in the biomass reduces the surface area of the biomass ash, as discussed in Chapters Two and Three. Reduction in biomass ash surface area decreases ash pozzolanic reactivity in cementitious systems [5.12]. Therefore, phosphorous and potassium removal from the biomass is beneficial to the reactivity of biomass ash in concrete. Therefore, biomass ash pretreated with NaOH could cause retardation in cementitious systems, as NaOH pretreatment did not remove phosphorous out of the biomass.

5.3.2 Biomass thermal degradation:

Thermal degradation of corn stover, wheat straw, and rice straw at different stages of treatment is shown in Figure 5.2 through Figure 5.4. The weight loss of unpretreated

biomass at temperatures between 100°C and 330°C is higher than that of pretreated biomass, possibly because of potassium removal from biomass by pretreatments. Potassium catalyzes the thermal degradation of biomass and increases the thermal degradation rate [5.28], as discussed in Chapter Four. In addition, because pretreatments partially remove hemicellulose out of the biomass [5.10], higher weight loss of unpretreated biomass could be attributed to thermal decomposition of hemicellulose [5.29]. Pretreated biomass and enzymatic hydrolyzed biomass showed similar thermal degradation, but the difference between thermal degradation of samples pretreated with sulfuric acid and those pretreated with NaOH was that former samples had higher ash content (weight percent at 700°C). Table 5.3 shows ash content of biomass at different stages. Enzymatic hydrolysis further reduced ash content of the biomass pretreated by NaOH. Reduction in ash content by NaOH pretreatment could be attributed to the removal of silicon from the biomass by NaOH pretreatment, as shown in Table 5.1. Additionally, it has been shown that NaOH pretreatments are effective in removing lignin out of the biomass, whereas sulfuric acid pretreatments are effective in removing hemicellulose out of the biomass [5.2] [5.10]. Decreased ash content of biomass by NaOH pretreatment could also be explained by lignin removal that could be associated with more leaching of inorganic compounds or elements. Therefore, using sulfuric acid for bioethanol production produces a byproduct with a high ash percentage, whereas using NaOH pretreatments leaches out high amount of the silica and decreases ash content of the bioethanol byproduct.

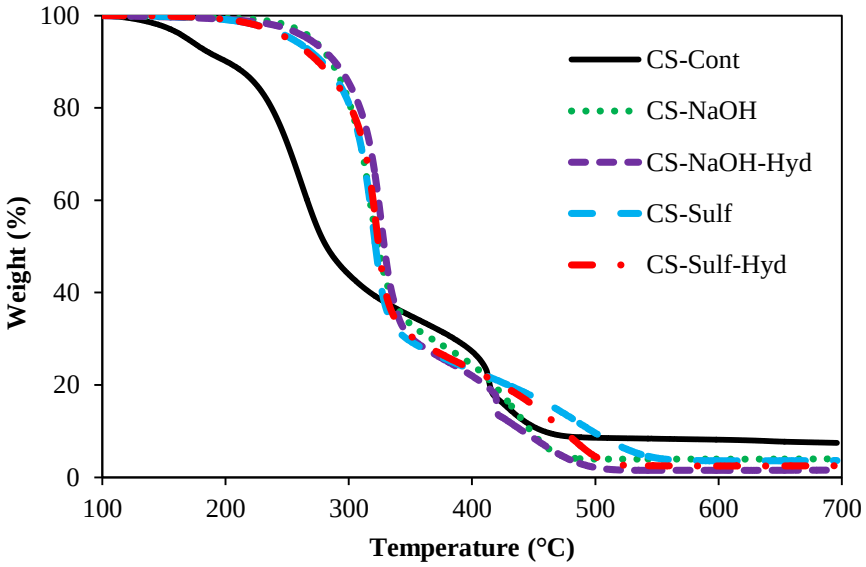

Figure 5.2: Thermal degradation of corn stover

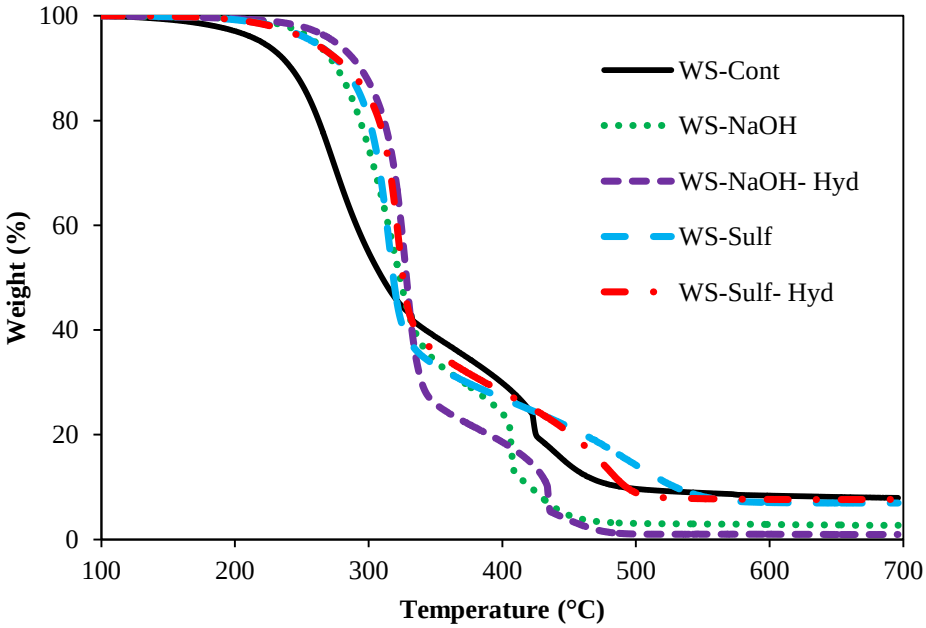

Figure 5.3: Thermal degradation of wheat straw

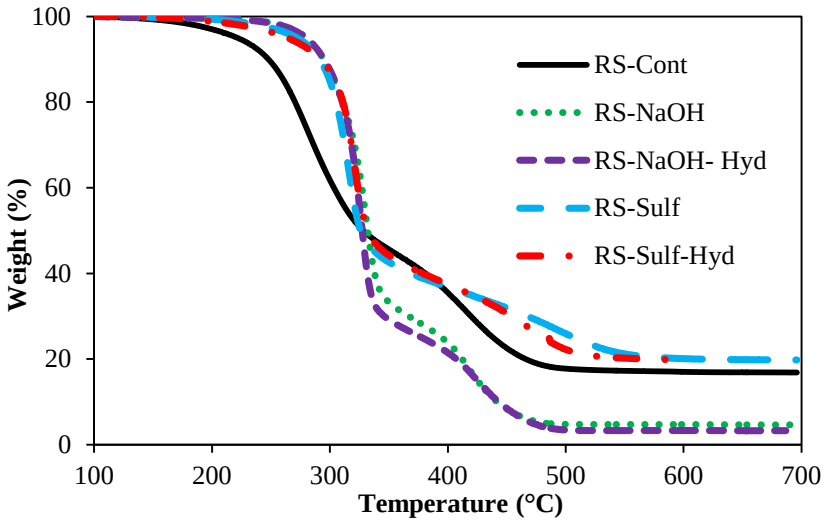

Figure 5.4: Thermal degradation of rice straw

Table 5.3: Ash content of the biomass

Sample ID:	Ash (%)
CS-Cont	7.5
CS-NaOH	4.0
CS-NaOH-Hyd	1.6
CS-Sulf	3.6
CS-Sulf-Hyd	2.5
WS-Cont	7.9
WS-NaOH	2.7
WS-NaOH-Hyd	0.9
WS-Sulf	6.9
WS-Sulf-Hyd	7.6
RS-Cont	16.9
RS-NaOH	4.6
RS-NaOH-Hyd	3.3
RS-Sulf	19.8
RS-Sulf-Hyd	19.6

5.3.3 Biomass ash XRD characterization:

Unpretreated biomass ash samples, CSA-Cont, WSA-Cont, and RSA-Cont, contained crystalline phases that are non-reactive in concrete. NaOH pretreatment removed potassium chloride (KCl) from corn stover ash (CSA), as seen in Figure 5.5. However, CSA pretreated with NaOH contained crystalline phases of calcium phosphate. Sulfuric acid pretreatment removed all crystalline phases from the biomass, resulting in amorphous

corn stover ash. Enzymatic hydrolysis did not significantly change corn stover ash crystallinity, as pretreated ash samples and ash samples after enzymatic hydrolysis had similar XRD pattern for a given pretreatment type. Similar results were shown for wheat straw samples, as illustrated in Figure 5.6. NaOH pretreatment was seen also to increase crystallinity of wheat straw ash; however, sulfuric acid pretreatment removed almost all crystalline phases from wheat straw prior to burning. Similarly, NaOH pretreatment increased crystallinity of RSA, whereas sulfuric acid pretreated RSA had no crystalline phases, as illustrated in Figure 5.7.

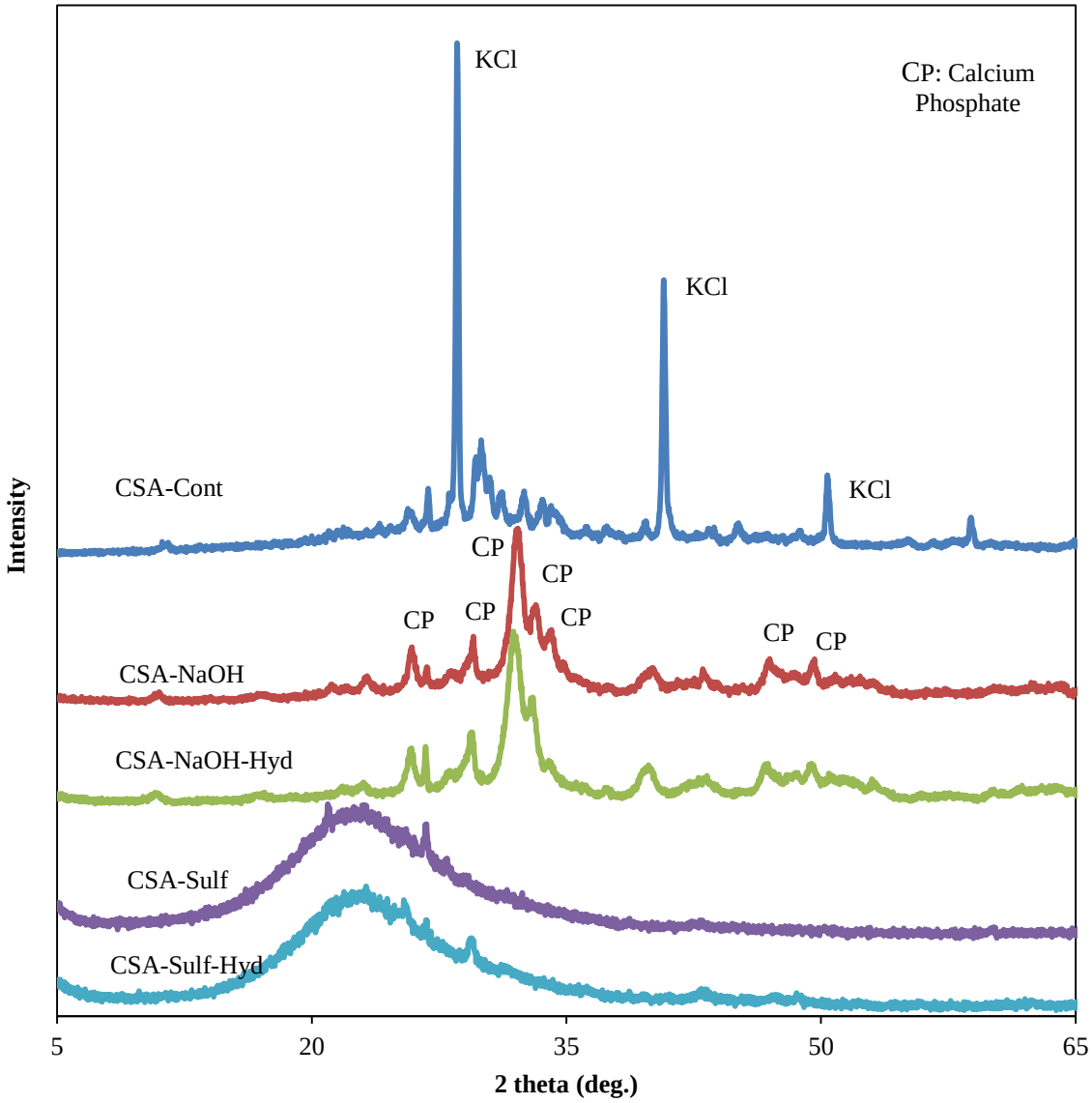

Figure 5.5: XRD pattern of corn stover ash at different stages

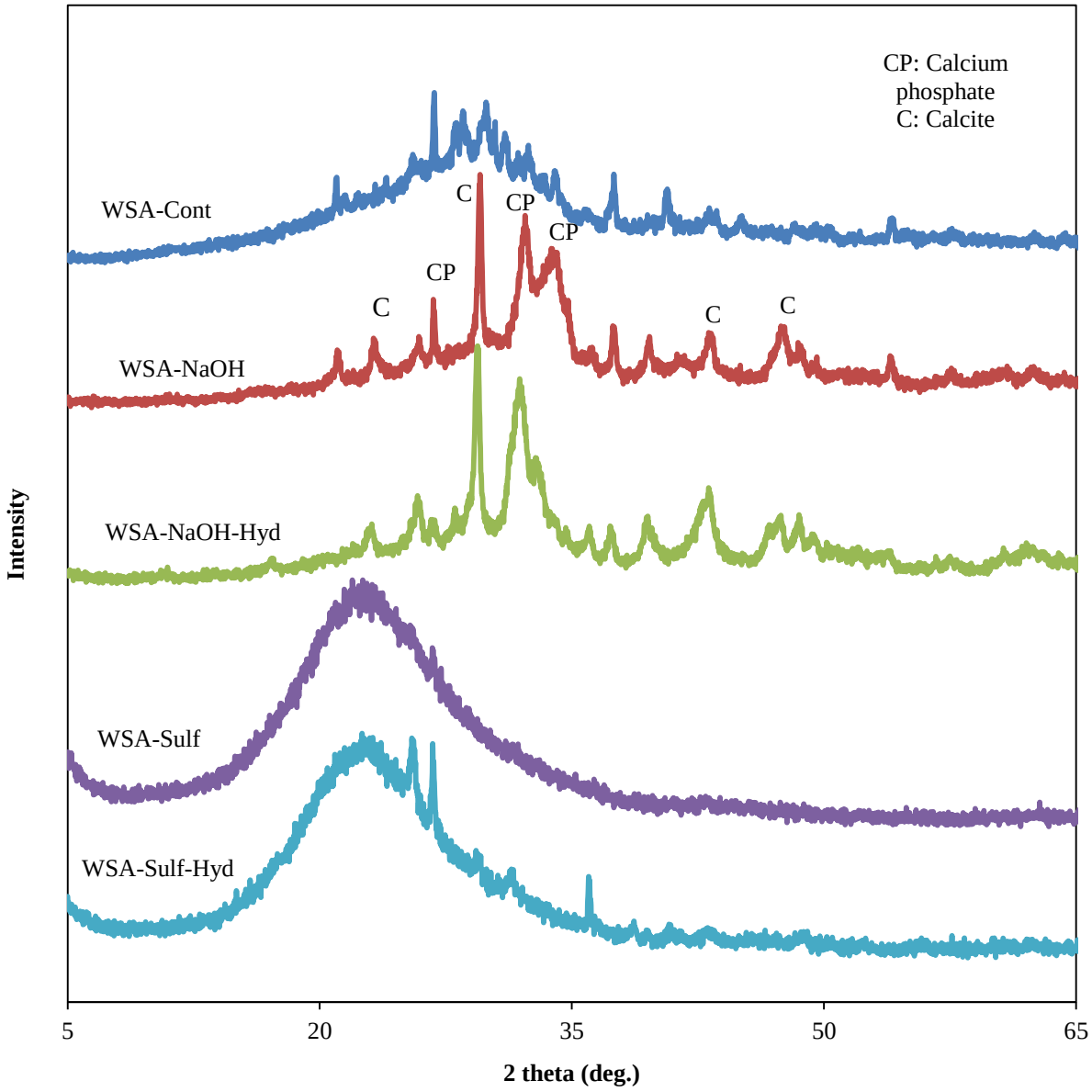

Figure 5.6: XRD pattern of wheat straw ash at different stages

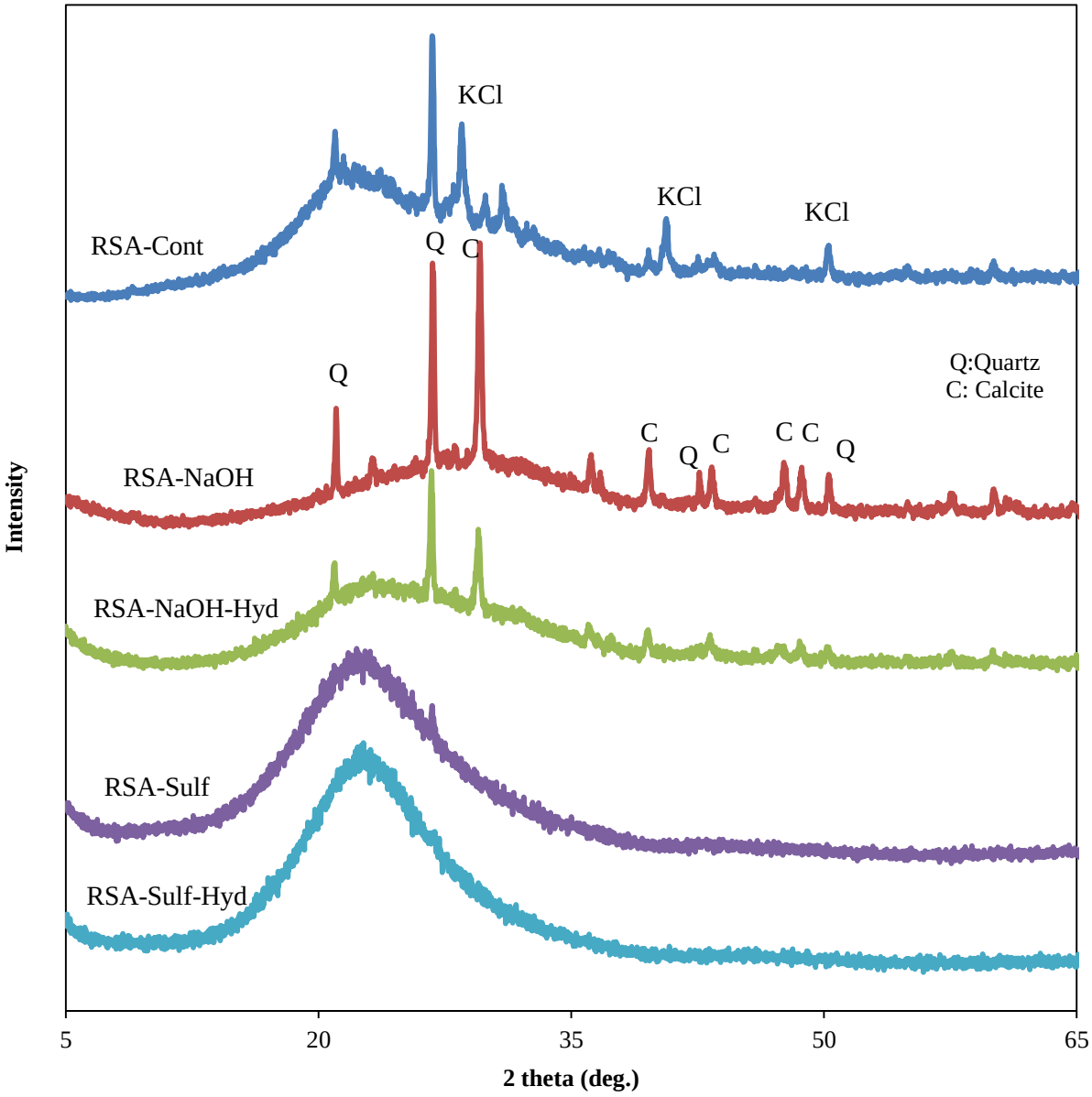

Figure 5.7: XRD pattern of rice straw ash at different stages

The existence of crystalline phases, such as potassium chloride and calcium carbonate, in unpretreated ash samples, CSA-Cont, WSA-Cont, RSA-Cont, could be explained by the existence of these phases in the biomass before burning. The existence of crystalline phases, namely calcite, in NaOH pretreated ash samples could be because the

NaOH pretreatment did not remove these phases out of the biomass, as seen in Table 5.1. Although enzymatic hydrolysis removed some Ca, P, and Mg out of the NaOH pretreated biomass, it could not lead to amorphous ash. The increase of crystalline phases in NaOH pretreated ash samples as compared to unpretreated samples could be associated with the removal of silicon (Si) out the biomass by the NaOH pretreatment. As Si content of the biomass decreases, so does silica content of the biomass ash, thus leading to higher percentages of other mineral phases. In addition, the calcite phase may be encased by silica in the biomass; therefore, dissolving silica exposes calcite XRD peaks.

Amorphous silica content of agricultural residue ash is an important factor in the reactivity of ARA in concrete materials. Reduction in amorphous silica content of the ash decreases its reactivity in cementitious systems. When sulfuric acid pretreatment is used for bioethanol production, the HLR could be used to produce reactive SCMs. However, as the NaOH pretreated biomass ash contains crystalline phases, its reactivity in concrete could be lower than that of sulfuric acid pretreated biomass ash. Additionally, when NaOH pretreatments are used for bioethanol production, the ash from HLR, or bioethanol byproduct, could be less reactive in concrete. Thus, while selecting pretreatment methods for bioethanol production, it is worth considering their impact on bioethanol byproduct and use for concrete applications. If sulfuric acid and NaOH pretreatments have similar impacts on bioethanol production, sulfuric acid should be utilized because bioethanol byproduct can be a potential resource for reactive SCM production for concrete use.

5.4 Conclusions:

The impact of NaOH and dilute sulfuric acid pretreatments, as well as enzymatic hydrolysis, on properties of three types of agricultural residue ash, namely corn stover ash, wheat straw ash, and rice straw ash, was studied. The primary disadvantage of NaOH pretreatment was that it did not remove the crystalline phases out of the biomass, making the subsequent ash less reactive in concrete. Contrary to NaOH pretreatments, sulfuric acid pretreatments improved ash properties for concrete application by removing crystalline phases from the biomass. Additionally, sulfuric acid pretreatment was effective in removing phosphorous, which can poison cement hydration, out of the biomass. Because of high alkalinity, NaOH pretreatment was not effective in removing calcium, phosphorous, and magnesium out of the biomass, leading to a crystallized ash. However, enzymatic hydrolysis removed some of these elements. Therefore, if NaOH and sulfuric acid pretreatments have similar impacts on bioethanol production, the consideration of sulfuric acid pretreatment provides greater opportunity for the utilization of bioethanol byproducts for reactive SCM production for concrete use.

5.5 Acknowledgements:

Financial support for this study was supported by the National Science Foundation (NSF) under award # CMMI-103093. The authors are thankful to Dr. Praveen Vadlani and Anne Rigdon from Grain Science and Industry Department for their assistance in enzymatic hydrolysis. The help of Antoine Borden is appreciated.

Chapter 6 - Impact of Rice Straw Ash on Air Entraining Agent Adsorption

Abstract:

Microscopic air bubbles are purposely entrained in concrete to impart freeze-thaw durability. Some supplementary cementitious materials (SCMs) contain carbon that adsorbs air entraining agents (AEA), thus increasing the AEA dosage required for a specified air content of concrete needed to protect concrete structures from freeze-thaw damage. The impact of rice straw ash (RSA) as a new SCM on AEA adsorption was studied by means of a foam index (FI) test. Six RSA samples with different surface areas and carbon contents were prepared. No correlation was found between carbon content and AEA adsorption. Although RSA samples with high surface area showed higher FI compared to RSA samples with lower surface area, no direct correlation was found between surface area and FI. At a cement replacement level of 20% or lower, pretreated RSA samples had higher FI compared to those containing same percentages of silica fume, but similar to a Class F fly ash. The type of unburned carbon in SCMs and availability of SCM surface area for AEA adsorption were found to affect AEA adsorption in concrete.

6.1 Introduction:

Air content of concrete has a major impact on freeze-thaw durability of concrete structures. Microscopic air bubbles in concrete can provide locations for ice to form without causing large stresses on concrete pore walls during a freezing event. Concrete made without air-entraining chemical admixtures can contain 1-3% air voids, called entrapped air, resulting from imperfect consolidation or large air bubbles introduced during mixing. Air entraining agents (AEA), or chemical surfactants, are used in concrete to stabilize and entrain very small air bubbles and to increase concrete air content to a desired level. The AEA dosage required to obtain a desired percentage of air content depends on the combination of materials used.

The foam index test has been used to determine AEA adsorption by fly ash and other supplementary cementitious materials (SCMs) in cementitious systems [6.1] [6.2]. The test measures AEA adsorption in cementitious slurry and determines the amount of AEA needed to stabilize the foam layer at the top surface of the slurry. Results of foam index have been shown to have good correlation with AEA adsorption in concrete [6.1]. Concrete containing fly ash typically requires a higher dosage of AEA compared to concrete without fly ash [6.1] [6.3]. The increase in AEA dosage due to fly ash addition has been attributed to unburned carbon content, alkali content, and the ash surface area [6.1] [6.4]. Particle size distribution of unburned carbon in the fly ash has been shown to influence AEA dosage, as well [6.2]. Air entraining agents are not as effective at stabilizing air bubbles in low pH solutions [6.4]. Besides chemical and physical properties of the fly ash, the impact of the ash on cement pore solution chemistry may also increase the AEA dosage requirement in cementitious systems.

Although many researchers have studied the impact of fly ash on air content and AEA dosage in concrete, the influence of agricultural residue ash on the AEA dosage has not been

investigated. Physicochemical properties of RSA are different than those of the fly ash. Depending on the production method of RSA, it can have very high internal porosity, surface area and amorphous silica content and low unburned carbon content [6.5]. Because of the high surface area, RSA could adsorb relatively higher amounts of AEA compared to fly ash, leading to an increase in the AEA dosage requirement in concrete containing RSA.

This study investigated the impact of RSA on AEA adsorption using the foam index test. To compare the impact of surface area and carbon content of the ash on AEA adsorption, RSA samples with different surface areas and carbon contents were used. Unpretreated and dilute hydrochloric acid pretreated rice straw ash samples were prepared using various burning conditions to create RSA with different carbon contents. The impact of RSA on AEA adsorption was compared with that of fly ash and silica fume samples. The silica fume was chosen because it had similar chemical composition but different surface area compared to RSA. A Class F fly ash was chosen for comparison purposes.

6.2 Materials and methods:

6.2.1 Materials:

An ASTM C 150 [6.6] Type I/II portland cement was used for this study. Rice straw (RS) was obtained from Missouri Rice Research Farm, Glennonville, Missouri. Reagent grade HCl was obtained and diluted to 0.1 N for RS pretreatments. A high-grade saponified rosin air entraining admixture was used. A Class F fly ash and undensified silica fume were used [6.7] [6.8]. Chemical composition of portland cement, rice straw ash samples, silica fume, and fly ash used in this study are shown in Table 6.1.

6.2.2 Methods:

6.2.2.1 Rice straw ash (RSA) preparation:

Rice straw was pretreated with 0.1N HCl. To pretreat the rice straw, 250g of straw were immersed in 3100±100 mL of solution in a 4000 mL glass jar. The sample was stored undisturbed at 80^{o}C for 24 hours. The rice straw was then rinsed twice with 2500 mL of distilled water and dried at 80^{o}C. A programmable electric muffle furnace was used to heat biomass samples to a predetermined temperature and hold time. To prepare RSA, 200g of rice straw were burned in each batch. A stainless steel cage with two wire mesh shelves was used to hold the biomass during burning. A stainless steel pan was placed below the cage to catch any ash that fell through the mesh. The rice straw was burned at 500^{o}C for one, two, or four hours or at 650^{o}C for one hour. Finally, the ash was ground for one hour at 85 revolutions per minute (rpm) in a laboratory ball mill.

Table 6.1: Material chemical compositions

Sample ID	Chemical composition						
	SiO_2(%)	Al_2O_3(%)	Fe_2O_3(%)	CaO (%)	MgO(%)	K_2O(%)	Na_2O(%)
Portland cement	19.66	4.71	3.26	62.74	1.03	0.56	0.12
RSA-Cont-650/1	79.1	0.34	0.82	11.6	2.54	5.18	0.5
RSA-HCl80-650/1	88.2	0.47	0.74	9.48	0.56	0.31	0.17
RSA-HCl80-500/2	85.7	1.4	1.02	10.73	0.6	0.34	0.23
Fly Ash	55.6	24	4.2	8.1	2.1	1.1	0.7
Silica Fume (SF)	96.96	0.13	0.05	0.43	0.96	0.38	0.08

A total of six RSA samples were used. Two of the samples were unpretreated ash; one burned at 500^{o}C for two hours (RSA-Cont-500/2), and the other burned at 650^{o}C for one hour (RSA-Cont-650/1). Three RSA samples were pretreated and burned at 500^{o}C for one hr (RSA-

HCl80-500/1), two hrs (RSA-HCl80-500/2), and four hrs (RSA-HCl80-500/4). One RSA sample, RSA-HCl80-650/1, was pretreated and burned at 650^{o}C for one hour. Chemical composition of rice straw ash samples is shown in Table 6.1. Because RSA-HCl80-500/1, RSA-HCl80-500/2, and RSA-HCl80-500/4 were all obtained from the same source and pretreatment and differed only in time of burning, they had similar chemical compositions.

6.2.2.2 Foam index test:

An ASTM sand equivalent shaker, shown in Figure 6.1, was used to ensure consistent shaking from sample to sample [6.9]. 10 g of cementitious materials were mixed in 20 mL of deionized water in a 50 mL plastic centrifuge tube. Height of the tube was 115 mm with a diameter of 27 mm. The tube was shaken for 30 sec, followed by a 30-second rest period. Twenty µl of 5% air-entraining agent solution was added to the mixture, and the mixture was shaken for 10 sec. The tube was left undisturbed for 15 seconds. A shaking speed of 172 cycles per min was used. At this time, if a stable foam layer at the water-air interface was observed, the volume of AEA was recorded as the foam index. If, however, a stable foam layer was absent, another 20 µl of 5% AEA solution was added and the procedure continued until a stable foam layer was reached and recorded. To determine the impact of ash samples on the foam index, 10%, 20%, 30%, 40%, or 50% of the cement was replaced by the ash with a constant water volume.

Figure 6.1: Test setup

6.2.2.3 Determination of the solution pH:

To determine the impact of rice straw ash, fly ash, or silica fume on the pH of the solution, 10%, 20%, 30%, 40%, or 50% of the cement was replaced by each SCM. The samples were shaken for 60 seconds, followed by a 60-second rest period, and then an additional 60 seconds of shaking. After the sample was left undisturbed for 120 seconds, the sample was filtered through a 25µm Whatman filter paper. The pH of the filtrate was then measured using an Accumet AB150 pH meter.

6.3 Results and discussion:

The loss on ignition (LOI) and surface area of rice straw ash (RSA), silica fume, and fly ash samples are shown in Table 6.2. Foam index values for samples containing various amounts of RSA are shown in Figure 6.2. Repeatability of foam index values was found to be within ±20 µL. Increasing amounts of SCM percentage in the sample increased foam index values for all samples. For RSA percentages greater than 50%, the foam index test was inconclusive. For 60% cement replacement by RSA-HCl80-500/2, RSA-HCl80-500/4, or RSA-HCl80-650/1, a stable foam layer could not be detected up to the addition of 800 µL of 5% AEA solution.

Table 6.2: LOI and surface area of RSA and SF

Sample ID	LOI (wt%)	BET (m^2/g)
RSA-HCl80-500/1	3.67	185
RSA-HCl80-500/2	2.25	181
RSA-HCl80-500/4	1.21	196
RSA-Cont-500/2	7.24	17
RSA-HCl80-650/1	0.80	134.5
RSA-Cont-650/1	3.08	10
Silica Fume (SF)	1.6	9
Fly ash (type F)	0.5	1

Note: Each data reported is the average of two tests

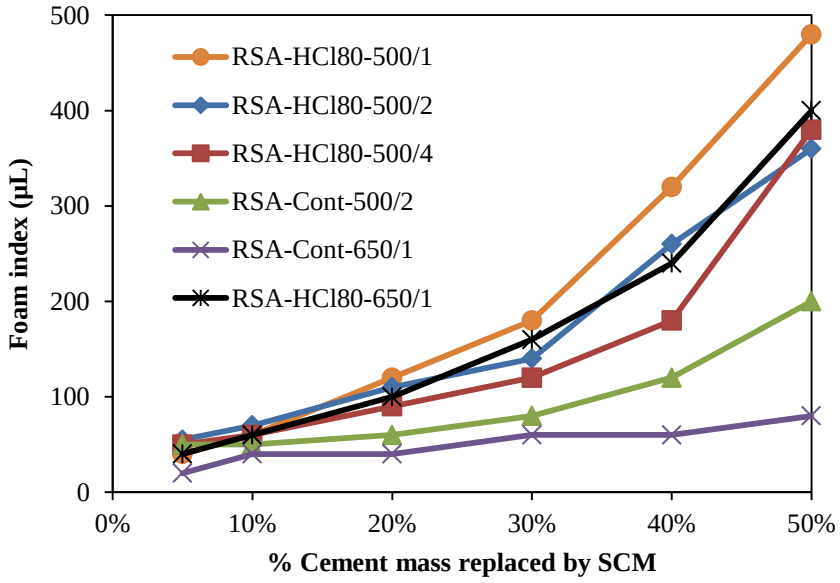

Figure 6.2: Foam index form samples containing rice straw ash samples

Higher unburned carbon content (LOI) did not necessarily result in higher FI values, and no correlation was revealed between LOI and the foam index, as shown in Figure 6.3. RSA-Cont-650/1 sample had higher LOI as compared to RSA-HCl80-650/1; however, at a given ash percentage, the latter sample had much higher FI values compared to the former sample.

Additionally, RSA-Cont-500/2 had higher LOI compared to RSA-HCl80-500/2 yet FI values of RSA-Cont-500/2 were much lower than that of the RSA-HCl80-500/2 sample. Similarly, although the fly ash sample had lower LOI compared to the RSA-HCl80-500/4 sample, for cement replacement levels of 10% to 40%, the fly ash sample had higher FI values than the latter sample, as shown in Figure 6.4. Although RSA-HCl80-500/4 had lower LOI than RSA-HCl80-500/1, the latter sample had higher FI. The type of unburned carbon appeared to be more important than the LOI in AEA adsorption.

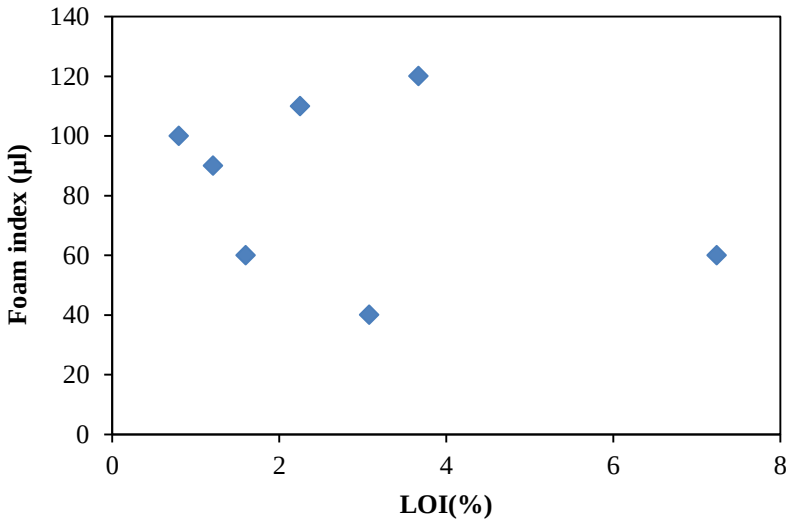

Figure 6.3: Correlation between LOI and foam index at 20% SCM replacement

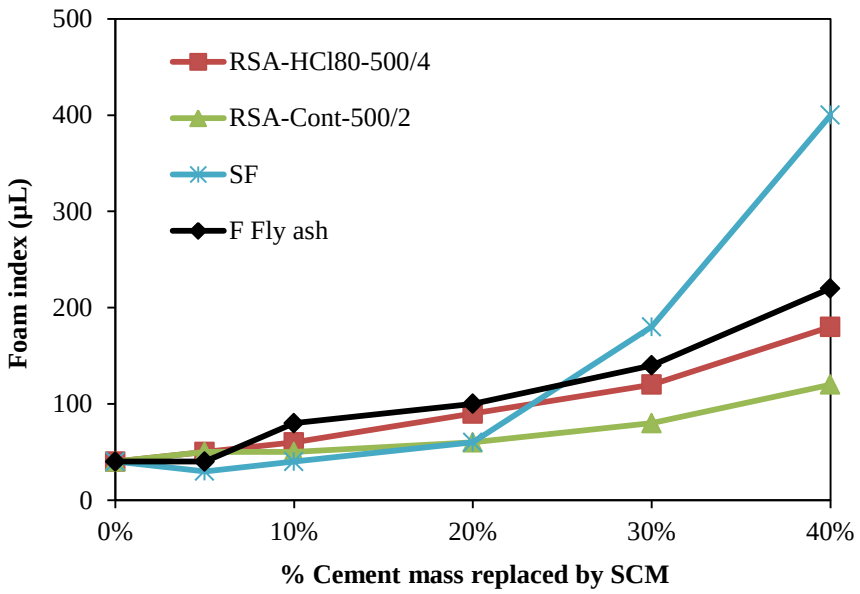

Figure 6.4: Foam index for silica fume and fly ash

Figure 6.4 compares foam index values of pretreated and unpretreated RSA samples with those of silica fume (SF). Up to 20% cement replacement, foam index values of silica fume were lower as compared to the RSA samples. However, at higher percentages, the FI values of silica fume were much higher than those of the RSA samples. Therefore, although silica fume had much lower surface are than pretreated RSA, the silica fume showed higher FI compared to RSA samples at cement replacement levels higher than 20%. The correlation between FI and surface area for 20% SCM dosage is shown in Figure 6.5. Increase in surface area increased the FI. However, for similar surface areas, different FI were observed. RSA-HCl80-650/1 had a lower surface area and LOI than RSA-HCl80-500/4, but had higher FI. Although RSA-HCl80-500/2 had a slightly smaller surface area compared to RSA-HCl80-500/4, RSA-HCl80-500/2 showed higher FI. Therefore, AEA adsorption capacity of SCM not only depends on surface area and

LOI, but also on the type of surface area and unburned carbon as well as availability of the surface area for AEA adsorption.

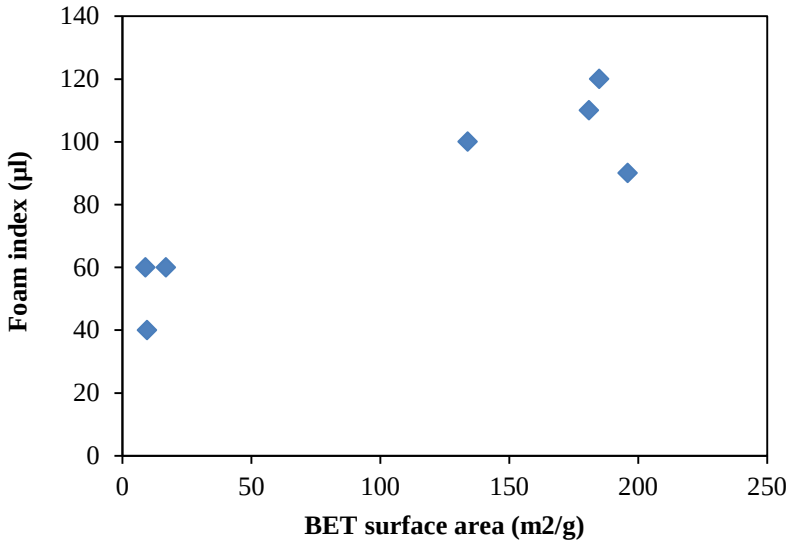

Figure 6.5: Correlation between ash surface area and foam index at 20% SCM replacement

Table 6.3 shows the impact of RSA-HCl80-500/4 and silica fume samples on the pH of the solution and its influence on the foam index. As the cement amount in the solution was reduced, the pH of the solution also decreased, as shown in Figure 6.6. The pH value of a sample containing 1g of cement and no SCM was 12.26, while the pH value of a sample containing 10g of cement with no SCM was 13.29. For samples containing cement only, pH values between 12.65 and 13.29 had similar foam index values. However, the foam index of the sample containing one gram of cement (no ash added) was 140µL, whereas the foam index of the sample containing 10g of cement was only 40µL. The increase of foam index for the sample containing 1g of cement compared to the sample containing 10g of cement could be attributed to the low pH and/or to the low amount of solid surfaces in the former sample [6.4].

Table 6.3: Ash impact on the pH of the solution

OPC (g)	RSA-HCl80-500/4 (g)	SF (g)	pH	FI (µL)
0	0	0	6.77	---
1	0	0	12.26	140
2	0	0	12.65	40
4	0	0	12.93	40
6	0	0	13.04	40
8	0	0	13.2	50
10	0	0	13.29	40
8	2	0	12.68	90
6	4	0	12.48	180
4	6	0	12.15	>800
8	0	2	13.12	60
6	0	4	12.96	400
4	0	6	12.66	>800

The impact of silica fume on the solution alkalinity (pH) is shown in Figure 6.7. Silica fume reduced the pH of the solution. The addition of silica fume and RSA also reduced the pH of the solution. However, for a given cement replacement level, RSA showed higher pH reduction than silica fume. The solution pH of the sample containing 60% of RSA-HCl80-500/4 was 12.15, whereas the pH was 12.66 for silica fume at this replacement level. Although samples containing silica fume had a higher pH than those containing RSA, foam index values of samples containing silica fume were higher than those containing RSA, as shown in Table 6.3. As long as the solution pH remains greater than 12, it seems that the pH does not significantly affect the air entraining admixture demand. A minimum water-cement ratio does seem to be important as there

likely is an interaction between the charged cement surface, bubbles created during shaking, and stabilization of those bubbles.

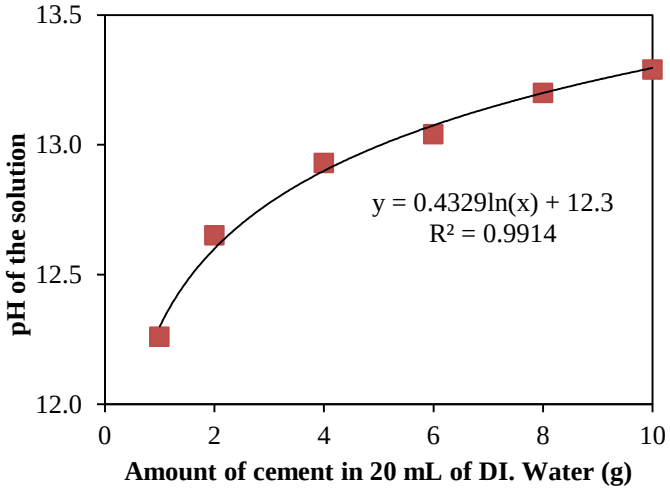

Figure 6.6: Relationship between cement content and solution pH

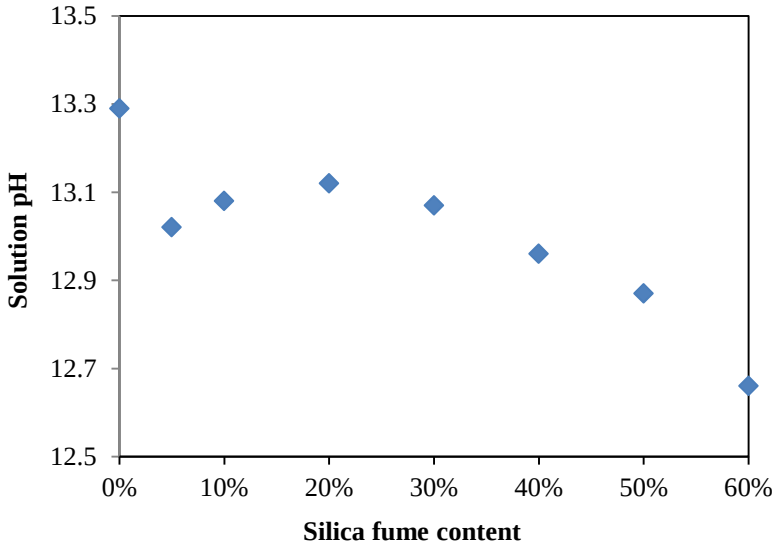

Figure 6.7: Impact of silica fume on the pH of the solution

6.4 Conclusions:

The impact of rice straw ash (RSA) on air entraining agents (AEA) was studied using the foam index test. Results indicated that, when mixed in cementitious systems, RSA adsorbs AEA. At a cement replacement percentage lower than 20%, RSA showed an increase in foam index

compared to that of silica fume. For a given SCM, no correlation was found between foam index and LOI. Although an increase in surface area was associated with an increase in foam index and air-entrainment demand as well, the foam index did not correlate with the material surface area. Different SCMs having similar LOI and surface areas do not have a similar impact on AEA adsorption, possibly due to differences in carbon type and, most significantly, ability of the surface area to adsorb AEA.

6.5 Acknowledgements:

Financial support for this study was provided by the National Science Foundation (NSF) under award # CMMI-103093. Authors are thankful to Antoine Borden for his help in performing foam index experiments.

Chapter 7 - Agricultural Residue Ash as a Substitute for Silica Fume

Abstract:

Silica fume (SF) is a commonly used supplementary cementitious material (SCM) in concrete. It is used to produce high strength, high performance, and durable concrete. However, availability of another highly reactive SCM for making high performance concrete would be beneficial to the concrete industry as silica fume is costly and is not widely available. This study investigated agricultural residue ash, specifically pretreated wheat straw ash (WSA) and rice straw ash (RSA), as potential SCM sources for making high strength concrete. WSA and RSA had much higher surface areas but slightly lower silica contents as compared to the silica fume. Hydration kinetics and mortar strength experiments showed RSA and WSA to have similar reactivity to silica fume. Although surface area is believed to increase early hydration as it provides nucleation sites for calcium silicate hydrate precipitation, the high surface area of WSA and RSA did not increase early hydration as compared to silica fume. This could be because it is not just the surface area that determines the reaction rate but also surface area location and availability during hydration process. Other phases on the WSA and RSA surface could also slow down silica dissolution and reduce the effectiveness of surface area in hydration reaction.

7.1 Introduction:

Silica fume (SF) is being used in concrete to produce high strength, high performance, and durable concrete [7.1] [7.2] [7.3]. It is well established that, when used as partial replacement of cement in concrete, silica fume increases compressive strength, reduces permeability, improves sulfate resistance, and helps mitigate alkali-silica expansion of concrete [7.4]. The improved strength, performance, and durability of concrete containing silica fume has been attributed to reduction in the interfacial transition zone (ITZ), porosity reduction of the paste matrix, and the pozzolanic reaction and space filling of silica fume [7.5] [7.6]. High amorphous silica content makes silica fume an especially well-suited material for making high strength concrete. Silica fume is an industrial byproduct of the silicone metal industry and is not available in large quantities worldwide; this increase the cost of silica fume, especially in locations where it is not produced. Alternative SCMs that could be used to produce high strength concrete would benefit the concrete industry.

Agricultural residue ash (ARA), such as rice husk ash (RHA), rice straw ash (RSA), and wheat straw ash (WSA), are other SCMs that have high amorphous content and surface area. Because ARAs can be produced at low cost, they are of great interest to the concrete industry, especially in developing regions. ARA can be made with a high surface area and high amorphous silica content, making them highly reactive pozzolanic materials [7.7] [7.8] [7.9] [7.10]. Although WSA and RSA can have similar chemical compositions to those of the silica fume, they can have higher surface area and calcium content than silica fume [7.8]. The high surface area of ARA has been attributed to their internal porosity [7.10]. Surface area provides nucleation sites for calcium silicate hydrate (C-S-H) precipitation which plays an essential role in the hydration process of cementitious systems [7.11].

This study aimed to test the hypothesis that the increased surface area of SCMs containing high percentages of amorphous silica will lead to a corresponding higher increase in early reactivity and strength gain. WSA and RSA with high surface are and amorphous content was produced. The reactivity and strength gain rates of WSA and RSA were compared with those of silica fume to test this hypothesis. Pozzolanic behavior of WSA, RSA, and silica fume was determined by measuring the impact of each material on heat of hydration, calcium hydroxide (CH) consumption, and chemical shrinkage of paste samples, and compressive strength of mortar cubes. The Chappelle test [7.12] was also used as an index test for material pozzolanic reactivity with calcium hydroxide solution.

7.2 Materials and methods:

7.2.1 Materials:

An ASTM C 150 [7.13] Type I portland cement and undensified silica fume were utilized for this study. Cement and silica fume chemical and physical properties are shown in Table 7.1 and Table 7.2, respectively. Standard graded sand [7.14] was used for the mortar experiments. Wheat straw (WS) was purchased from a local farm in Manhattan, Kansas, and rice straw (RS) was obtained from Missouri Rice Research Farm, Glennonville, Missouri. One N reagent grade HCl was obtained and diluted to 0.1 N for use in the study. Reagent grade calcium oxide (CaO) and ACS grade zinc oxide and phenolphthalein were used for performing the Chappell test.

7.2.2 Methods:

7.2.2.1 Biomass ash preparation:

In order to produce WSA and RSA with high amorphous content, high surface area, and low loss on ignition (LOI), the biomass (wheat straw and rice straw) was pretreated with 0.1N

HCl at 80^{o}C. 250 g of biomass was immersed in 3100±100 mL of 0.1N HCl solution in a 4000 mL glass jar. The sample was stored undisturbed at a constant temperature of 80^{o}C for 24 hrs. The biomass was then rinsed twice, each time with 2500 mL of distilled water, and dried at 80^{o}C in an oven. To prepare the ash (WSA or RSA), a programmable electric muffle furnace was used to heat the biomass. 200 g of dried biomass was ashed in each batch. A stainless steel cage with two wire mesh shelves was used to hold the biomass during burning, and a stainless steel pan was placed below the cage to catch any ash that fell through the mesh. Finally, the ash was ground for one hour at 85 revolutions per minute (rpm) in a laboratory ball mill. WSA was prepared by burning the pretreated wheat straw at 650°C for one hour and was called (WSA-650). Two types of RSA were prepared: (RSA-650) was obtained by burning pretreated rice straw at 650°C for one hour, and (RSA-500) was prepared by burning pretreated rice straw at 500°C for two hours. Properties of WSA and RSA samples are shown in Table 7.2.

7.2.2.2 Silica fume and biomass ash characterization:

Particle-size distribution and internal surface area of silica fume, WSA, and RSA samples were determined using a laser diffractometer and BET nitrogen adsorption respectively. LOI was determined by measuring mass loss after heating one gram of dry materials (SF, WSA or RSA) to 900°C for three hrs. Chemical composition of ash samples and silica fume was determined using x-ray fluorescence (XRF). To determine crystalline phases of the materials, x-ray diffraction (XRD) analysis was performed (Cu Kα radiation with λ=1.5046Å). A step size of 0.02° 2θ /4s and a scan range of 5°–70° 2θ was used. The Rietveld analysis [7.15] [7.16] [7.17] was performed to obtain the amorphous content of the WSA, RSA, and silica fume. Sample preparation for Rietveld refinement analysis included mixing 1.8g of SCM with 0.2 g of zinc oxide as an internal standard in ethanol to create a slurry. This was followed by hand grinding in

a ceramic mortar for approximately two min., followed by drying in a fume hood for 20 min. The Rietveld algorithm optimizes the model function by minimizing the weighted sum of squared difference between observed and computed intensity values [7.18]. The refinement process of each SCM sample was evaluated with R-factor refinement criteria, including R-pattern (Rp), R-weighted pattern (Rwp) and R-expected (Rexp) [7.19]. A commercial software was used to perform the Rietveld refinement until the best fit was obtained.

Table 7.1: Cement properties

Chemical compositions (%)		Bogue compounds (%)	
SiO_2	19.36	C_3S	62.76
Al_2O_3	5.13	C_2S	8.16
Fe_2O_3	2.53	C_3A	9.31
CaO	63.17	C_4AF	7.70
MgO	1.03	Blain Surface area: 386 m^2/kg	
K_2O	0.88		
Na_2O	0.086	LOI (%):	2.7
SO_3	3.22		

Table 7.2: SCM properties

Sample ID	Chemical compositions (%)							BET surface area (m^2/g)	LOI (%)
	SiO_2	Al_2O_3	Fe_2O_3	CaO	MgO	K_2O	Na_2O		
WSA-650	86.5	0.28	1.13	9.73	0.78	1.54	0.1	65	1.2
RSA-650	88.2	0.47	0.74	9.48	0.56	0.31	0.17	134	0.8
RSA-500	85.7	1.4	1.02	10.73	0.6	0.34	0.23	200	2.2
Silica Fume (SF)	96.96	0.13	0.05	0.43	0.96	0.38	0.08	8.9	1.6

7.2.2.3 Pozzolanic reactivity measurements:

Pozzolanic reactivity of WSA, RSA, and silica fume was measured by several experimental procedures. The Chapelle test [7.12] was used to measure pozzolanic reactivity of the materials. In this test, 2 g of calcium oxide was mixed with 1 g of sample in 250 mL of deionized water in a 500 mL Erlenmeyer glass flask. The flask was placed on a stirring–heating plate for 16 hrs at 90°C. At the end of 16 hrs, the slurry was cooled to 23°C by placing the flask in cold water. 60 g of sucrose was mixed with 250 ml of deionized water, added to the slurry, and stirred for 15 min. The resulting solution was filtered through a 1.1 µm diameter filter paper. Five drops of 0.1% phenolphthalein and 25 mL of filtrate were then titrated with 0.1N HCl. The total volume of 0.1N HCl solution needed for titration was recorded as V_b for the blank sample (no WSA, RSA, or silica fume added) and V_m for samples containing SCMs (WSA, RSA, and silica fume). Titration results were then used to determine the amount of calcium hydroxide (mg) fixed by the pozzolanic materials using Eq. 7.1:

$$Ca(OH)_2 \ \ fixed = 2\frac{(V_b - V_m)}{V_b}\frac{74}{56}1000 \qquad \text{Eq. 7.1}$$

Pozzolanic reactivity was also determined by measuring the heat of hydration of cement paste samples containing WSA, RSA, or silica fume. 10% cement by weight was replaced with WSA, RSA, or silica fume when used. A 0.45 water-cementitious material ratio (w/cm) was used. Paste samples were mixed with a vertical laboratory mixer [7.20]. Distilled water was added to the cementitious material and mixed at 500 rpm for 90 seconds, followed by a 120 second rest period, and then mixed at 2000 rpm for 120 seconds. Paste samples of approximately 30 g each were used in an eight-channel isothermal calorimeter at 23°C.

Calcium hydroxide (CH) content of paste samples was measured at various ages to determine CH consumption by the pozzolanic reaction. To obtain CH content of paste samples,

samples were cast in 1l ml polystyrene vials. Hydration was stopped at 7, 28, and 90 days of hydration by means of solvent exchange with isopropanol. Samples approximately 2mm thick were cut and placed in isopropanol for seven days. After this period, the samples were dried in a vacuum for at least three days. CH content was measured using a thermogravimetric analyzer (TGA) to heat the dried samples at 20°C/min up to 800°C in a nitrogen environment [7.21].

Chemical shrinkage of paste samples were measured in accordance with procedure A of ASTM C1608. Approximately 6 g of paste sample was cast in a 26 ml polystyrene vial. The vial was then filled with water. A capillary tube was inserted through the center of a rubber stopper, and the stopper was then inserted into the vial. The capillary tube was partially filled by distilled water, and a few drops of red oil were added in the tube. The decrease in water level in the tube was monitored by taking pictures with an automatic webcam. The images taken were then analyzed suing Shrinkage Suite developed by Bishnoi [7.22] . The average of three replicate samples was used for chemical shrinkage results.

Mortar cube compressive strength was measured according to ASTM C 109 [7.23] with a sand to cementitious material ratio of 2.75. To keep the w/cm of paste and mortar samples identical, w/cm for all mortar samples was also 0.45. WSA, RSA, or silica fume was used at 10% replacement level by mass of cement. Mortar cube compressive strength was tested at 7, 28, and 91 days with results reported as the average of three mortar cubes.

7.3 Results:

7.3.1 Materials characteristics:

Particle size distribution of cement (OPC), WSA, RSA, and silica fume samples is shown in Figure 7.1. Agglomeration was the most likely cause of large particle size seen in silica fume. Chemical and physical properties of WSA-650, RSA-650, RSA-500, and silica fume are shown

in Table 7.2. All ash samples (WSA-650, RSA-650, and RSA-500) had similar chemical composition. Silica (SiO_2) content of silica fume was approximately 10% higher compared to ash samples; however, CaO content of ash samples was approximately 9% higher than that of silica fume. The ash samples had much higher surface area than silica fume. Among the ash samples, WSA-650 had the lowest (65 m^2/g) surface area, and RSA-500 had the highest (200 m^2/g) surface area which was more than 20 times larger than that of the silica fume. High surface area of the ash samples has been attributed to internal porosity [7.10].

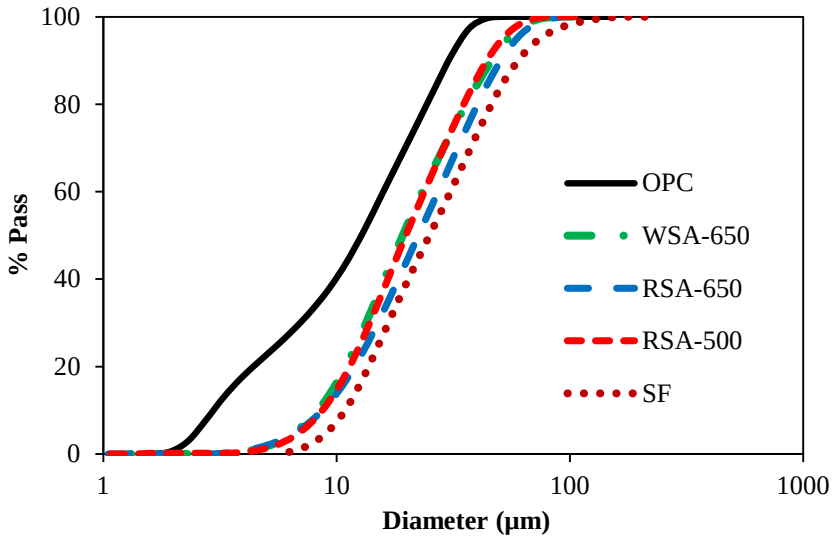

Figure 7.1: Particle size distribution

The XRD data for WSA-650, RSA-650, RSA-500, and silica fume samples are shown in Figure 7.2. WSA-650 showed very low crystalline phases, similar to silica fume. RSA-650- and RSA-500 showed some crystalline quartz. Table 7.3 shows Rietveld refinement results. The RSA samples had the lowest amorphous content, whereas the WSA and silica fume samples were made up of over 99% amorphous content.

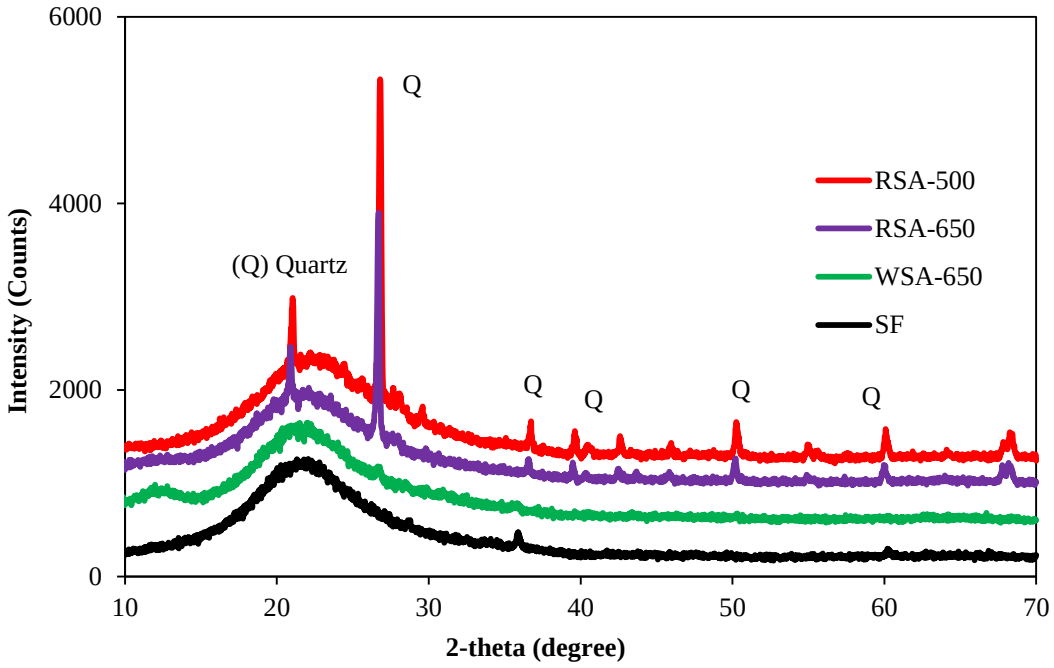

Figure 7.2: XRD plots for WSA, RSA, and SF

Table 7.3: Rietveld refinement data

Minerals	RSA-650	RSA-500	WSA-650	SF
Quartz (mass %)	4.2	11.8	0.7	0.1
Amorphous (mass %)	95.8	88.2	99.3	99.9

7.3.2 Chappelle test:

Results from the Chappelle test showed that silica fume fixed/consumed more CH than ash samples, as shown in Figure 7.3. Silica fume fixed 18.8% more CH than that which was fixed by the RSA-650 sample. The high surface area of ash samples did not appear to increase CH fixation during the Chappelle test. This is most likely because the high temperature and alkalinity in the Chappelle test provides only an index of the total potential reactive material in the SCM rather than the reactivity rate of the SCM. The accuracy of the Chappelle test in

determining the pozzolanic reactivity of materials is also limited because of the extreme conditions in the test and because the pozzolanic reaction in cementitious systems is more complex than that provided by the test solution. This is evidenced by the crystalline quartz results which fixed 202 mg of CH in the Chappelle test.

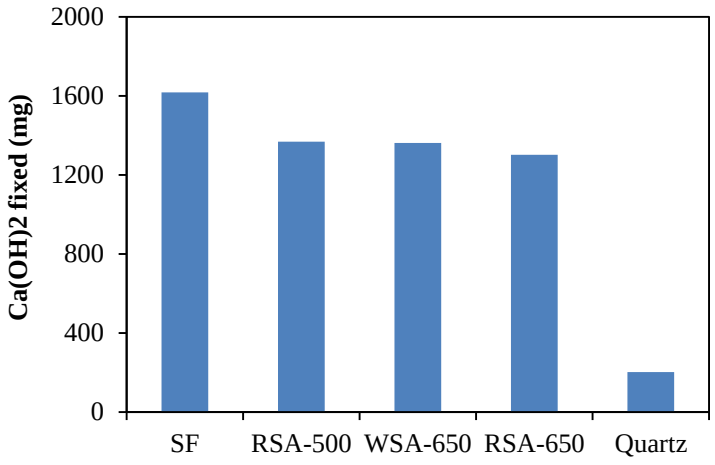

Figure 7.3: Chappelle test results

7.3.3 Reaction Kinetics

Silica fume and ash samples increased the heat of hydration produced by cement, as illustrated in Figure 7.4. Ash samples (WSA-650, RSA-650 and RSA-500) and silica fume shortened the induction period, possibly because of the high surface area of samples that can act as nucleation sites, thus accelerating the hydration [7.11] [7.24]. Peaks from silicate and aluminate hydration were slightly larger for samples containing silica fume than those containing ash samples. However, cement paste samples containing WSA or RSA showed similar total heat of hydration to silica fume containing sample.

Chemical shrinkage per gram of dry cement is also a measure of the paste reaction kinetics complementary to isothermal calorimetry, shown for the paste samples experiments in Figure 7.5. Samples containing SCMs (RSA-650, RSA-500, WSA-650, and silica fume) had

higher chemical shrinkage, per gram of dry cement, as compared to control (OPC) samples. However, paste samples containing SCMs showed similar chemical shrinkage to each other.

Calcium hydroxide (CH) of cement paste samples at different ages is shown in Figure 7.6. At three and seven days, the CH content of paste samples containing ash samples (OPC+WSA-650, OPC+RSA-650, and OPC+RSA500) was slightly lower than those containing silica fume, whereas for the rest of the hydration period (28, 91, and 180 days) the CH content of silica fume containing paste samples was lower than those containing ash samples.

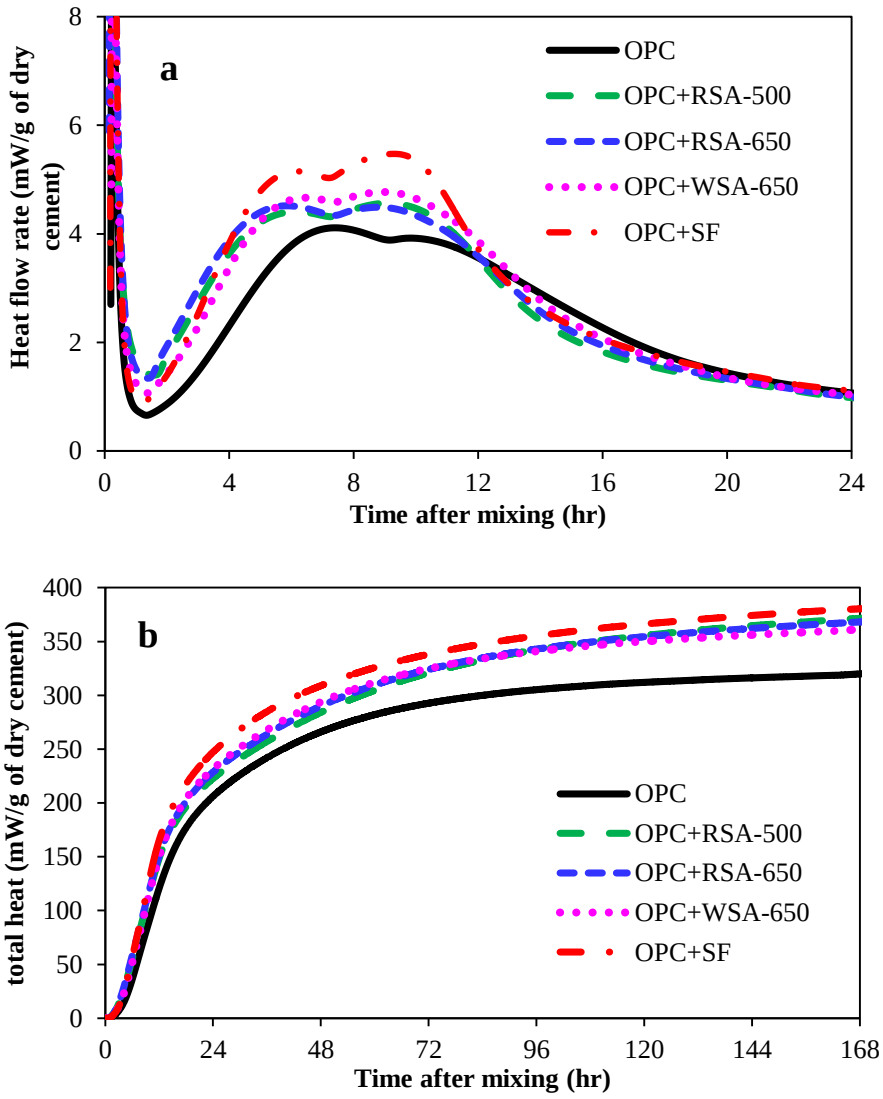

Figure 7.4: Heat of hydration of paste samples: a) heat flow rate, b) cumulative heat of hydration

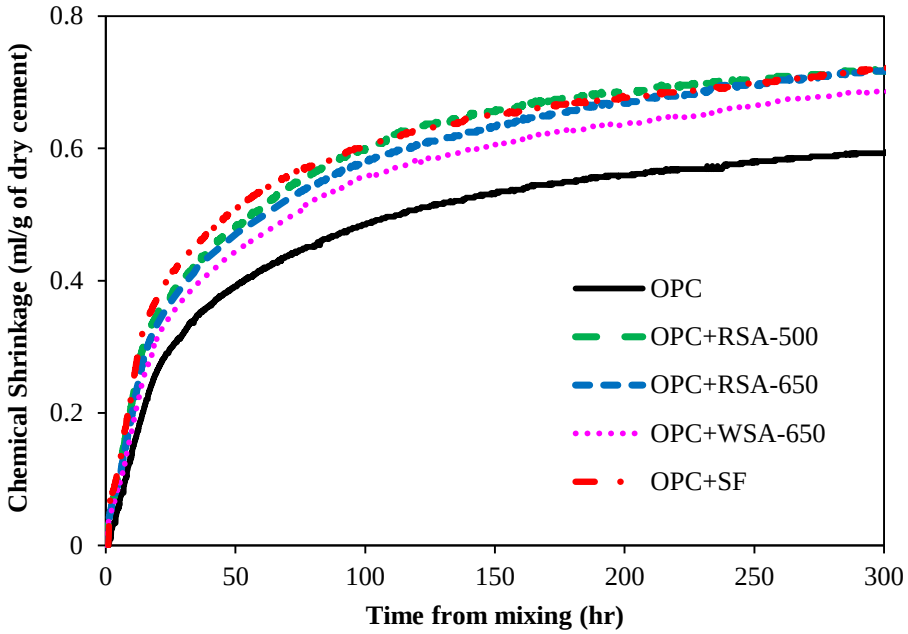

Figure 7.5: Chemical shrinkage of paste samples

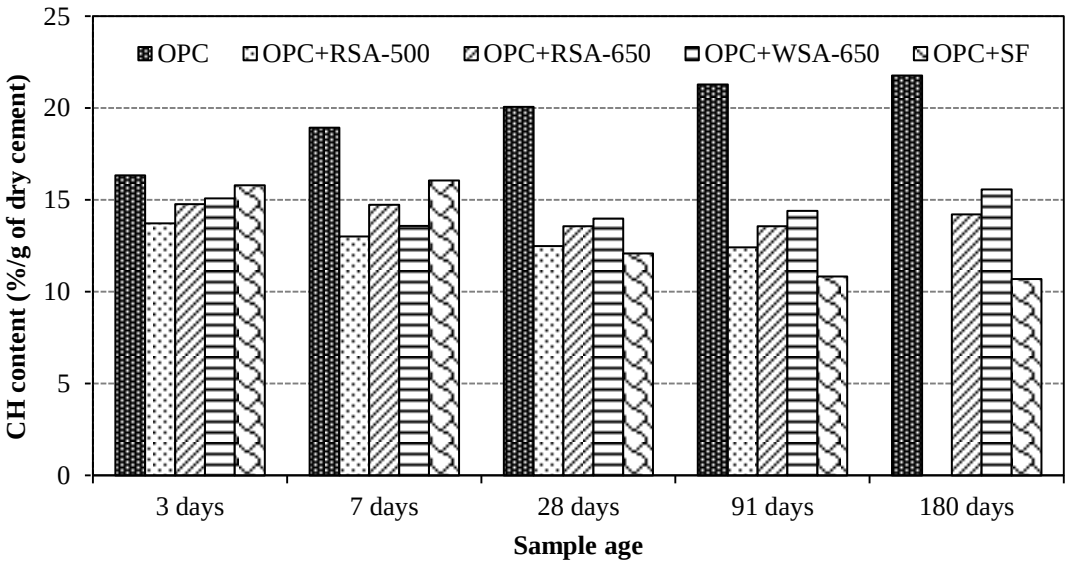

Figure 7.6: Calcium hydroxide (CH) content of cement paste samples

7.3.4 Compressive strength:

Compressive strength data for mortar samples is shown in Figure 7.7. At a given age, samples containing either RSA or silica fume had higher compressive strength than control

(OPC) samples. At a given age, compressive strength of samples containing RSA was similar to those containing silica fume. High surface area of RSA samples did not significantly increase early compressive strength of mortar samples containing RSA.

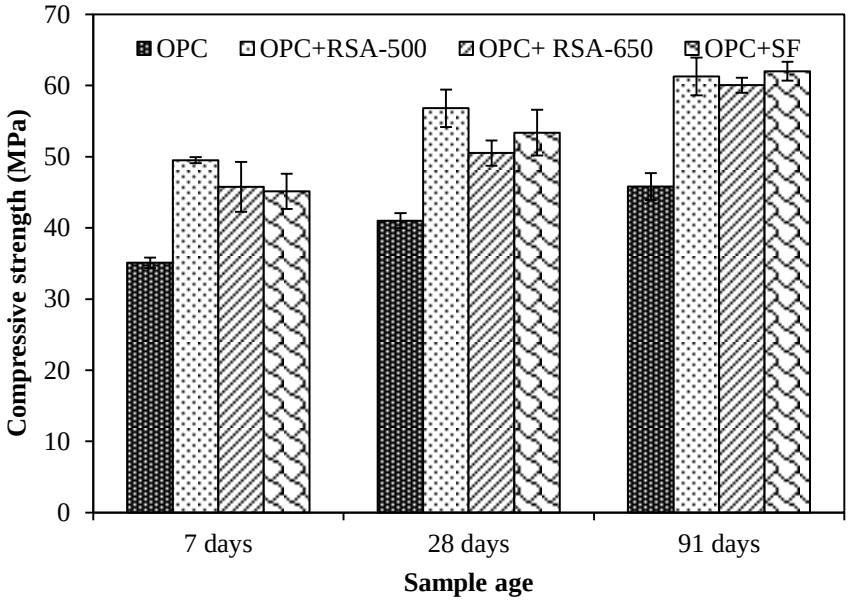

Figure 7.7: Mortar cube compressive strength

7.4 Discussion:

WSA and RSA showed similar pozzolanic behavior to that of the silica fume. Although SCMs with high surface area are believed to increase early reaction of cementitious systems, the higher surface area of WSA and RSA did not increase the early hydration because paste samples containing WSA and RSA revealed similar induction period and total heat of hydration when compared to silica fume. This result could be because surface area of WSA and RSA was not available for C-S-H precipitation. Availability of surface area of ash in cement hydration could be limited by various factors. Ash samples are not spherical and have complex shape and structure [7.10]. Consequently, dissolution of small amounts of silica from ash may dramatically reduce the surface area. It is also possible that availability of surface area is less in WSA and

RSA because internal pores can be diffusion controlled. Pozzolanic reactivity of WSA and RSA will also be affected by reactivity of their silica phase which, subsequently, could be reduced by calcium oxide in the ash, thus potentially decreasing pozzolanic reactivity of ash samples. In addition, if carbon and potassium or other impurities precipitate on the surface of ash, it could prevent the surface area from participating in the nucleation process of calcium silicate hydrate. Besides limited surface area availability of ash samples, silica fume could provide enough surface area for nucleation process. These factors effectively result in similar hydration kinetics for ash samples to silica fume.

Larger silicate and aluminate hydration peaks and higher early (3 and 7 days of age) CH content of paste samples containing silica fume, as compared to those containing WSA or RSA could be attributed to water sorption by ash samples. WSA and RSA could have higher sorption capacity than silica fume because of higher internal porosity and surface area. Sorption of water by WSA and RSA reduces available water for cement reaction, thus reducing CH content of paste samples. Water encased in pores within ash samples is available for hydration once a demand is presented. Availability of water at later ages could be the cause of high CH content of samples containing WSA and RSA after 28 days of hydration, as shown in Figure 7.6. Release of water from pores increases cement hydration and CH content of paste samples.

7.5 Conclusions:

Pozzolanic reactivity of dilute acid pretreated wheat straw ash (WSA) and rice straw ash (RSA) prepared at either 650°C or 500°C was compared to that of silica fume to investigate the hypothesis that higher surface area independent of silica source and structure leads to higher early pozzolanic reaction was tested. Results showed that although WSA and RSA samples had much higher surface area than silica fume, pozzolanic reactivity of all samples was similar.

Cement paste samples containing 10% silica fume showed similar heat of hydration, chemical shrinkage, and calcium hydroxide (CH) content to those containing 10% WSA or RSA. Additionally, at a given age of hydration, mortar samples containing 10% silica fume and those containing 10% RSA had similar compressive strength, proving that the high surface area of WSA and RSA samples had negligible influence on early pozzolanic reactivity. This shows that it is not just the surface area of amorphous silica but also availability of surface area that can be affected by shape and composition of SCMs that controls early cement reaction.

7.6 Acknowledgements:

Funding for this study was provided by the National Science Foundation under award # CMMI-103093. The authors are thankful to Sarah Taylor Lange for her help in performing the Rietveld refinement analysis.

Chapter 8 - Conclusions and Recommendations

8.1 Conclusions:

Impacts of bioethanol pretreatment methods on pozzolanic properties of agricultural residue ashes (ARA), namely corn stover ash (CSA), wheat straw ash (WSA), and rice straw ash (RSA) were investigated. Additionally, suitability of bioethanol byproduct for reactive supplementary cementitious materials (SCMs) production was explored. Findings of this research are as follows:

6- Distilled water and dilute acid pretreatments increased amorphous silica content and surface area and reduced the carbon content of ash samples. This was attributed to the removal of calcium (Ca), potassium (K), phosphorous (P), and magnesium (Mg) out of the biomass by pretreatments. Dilute acid pretreatment was more effective than distilled water pretreatment in removing these elements. In an oxygen-limited environment, potassium traps carbon during combustion leading to high carbon content of resulting ash. Decrease of surface area of the ash was attributed to carbon entrapment during burning, while increase in amorphous content of the ash was attributed to removal of crystalline phases by pretreatments.

7- Distilled water and dilute acid pretreated ash samples showed improved pozzolanic reactivity compared to unpretreated ash samples. This result was attributed to the increase in amorphous content and surface area of ash samples. Increased ash surface area acts as nucleation sites for calcium silicate hydrate precipitation, leading to increased cement hydration. Additionally, removing phosphorous from biomass ash greatly contributed to improved pozzolanic behavior of biomass ash. 20% replacement of portland cement by

pretreated ash samples in mortar samples increased compressive strength, even at seven days, compared to those without ash.

8- The study showed that sodium hydroxide pretreatment was not as effective as dilute acid pretreatment in improving pozzolanic properties of ARA. Sodium hydroxide pretreatment did not remove all crystalline phases out of the biomass. More importantly, sodium hydroxide pretreatment did not leach out phosphorous from the biomass.

9- Byproducts of bioethanol production were shown to be potential resources for producing reactive supplementary cementitious materials (SCMs). Enzymatic hydrolysis was found to enhance reactivity biomass byproducts further than pretreatments when burned for use in concrete. When dilute acid pretreatments are used for bioethanol production, byproducts should be better candidates for reactive SCM production as compared to sodium hydroxide pretreatments.

10- Wheat straw ash and rice straw ash pretreated with dilute acid revealed similar pozzolanic behavior to that of silica fume; however, these ash samples had slightly higher capacity than silica fume for adsorbing air entraining agents in concrete. Care should be taken when using pretreated agricultural residue ash for making high performance concrete in freeze-thaw environments.

8.2 Recommendations for future research:

Although several aspects of agricultural residue ash (ARA) were studied in this research, further research is needed to successfully implement partial replacement of portland cement by ARA in concrete. The following factors should be integrated into future research programs:

- The influence of ARA on concrete durability is needed for use in freezing and thawing environments. Although this research showed that ARA adsorbs slightly

more air entraining agent than silica fume, further research is needed to demonstrate how ARA influences air void size and distribution and freeze-thaw performance in hardened concrete.

- Because of a porous shape and high surface area, ARA reduces concrete workability, an important property of fresh concrete. Further research is needed to investigate methods to improve rheological properties of concrete containing ARA.
- Because of high internal porosity, the use of pretreated ARA could provide internal curing for concrete, which was not studied in this research.
- Although the chemical similarity of ARA and silica fume suggests they should have similar properties in regards to alkali-silica reaction in concrete, this assumption should be verified through experimental means.
- In alkali-activated cement and concrete, silicon ions play an important role in polymerization. Because pretreated ARA has a high surface area and amorphous silica content, incorporation of ARA in alkali-activated concrete could improve properties of alkali-activate cement by providing silicon source and C-S-H seeding. Further research is needed.
- During this research, agricultural residue ash was prepared at controlled burning conditions using a programmable electrical muffle furnace. Because agricultural residues are commonly used in boilers for energy generation, it is important to study the impact of pretreatments on pozzolanic behavior of agricultural residue ash under boiler burning conditions.

- This study investigated the potential use of bioethanol byproduct in concrete materials. However, only corn stover bioethanol byproducts were studied. Other biomass, such as sorghum, could respond differently to pretreatment and enzymatic hydrolysis as they have different physical and chemical properties. Further research is required to study potentiality of bioethanol byproducts from various sources of lignocellulosic materials for SCMs production.

This research answered many questions concerning utilization of agricultural residue and bioethanol byproducts for production of reactive supplementary cementitious materials for concrete use. Implementation of these materials in practice, however, needs further investigation.

Chapter 9 - References

[1.1] "Recycling Concrete," World Business Council for Sustainable Development-The Cement Sustainability Initiative, 2009.

[1.2] P. K. Metha and P. J. M. Monteiro, Concrete: Microstructures, properties, and materials, third ed., New York: McGraw-Hill Companies, Inc., 1993, pp. 3-20.

[1.3] N. R. M. C. Association, "Concrete CO2 Fact Sheet," National Ready Mixed Concrete Association, 2012.

[1.4] H. C. E. C. a. P. L. D. Mohammed Ba-Shammakh, "Analysis and Optimization of Carbon Dioxide Emission Mitigation Options in the Cement Industry," *American journal of environmental sciences,* vol. 4, no. 5, pp. 482-490, 2008.

[1.5] waob, "World Agricultural Supply and Demand Estimates," United States Department of Agricultural, 2011.

[1.6] H. Y. M. S. a. S. S. Qingge Feng, "Study on the pozzolanic properties of rice husk ash by hydrochloric acid pretreatment," *Cement and concrete research,* vol. 36, no. 3, pp. 521-526, 2004.

[1.7] A. Salas, S. Delvasto, R. M. d. Gutierrez and D. Lange, "Comparison of two processes for treating rice husk ash for use in high performance concrete," *Cement and Concrete Research,* vol. 39, pp. 773-778, 2009.

[1.8] H. Biricik, F. Akoz, I. Berkaty and A. Tulgar, "Study of pozzolanic properties of wheat straw ash," *Cement and Concrere Research,* vol. 29, no. 5, pp. 637-643, 1999.

[1.9] H. Biricik, F. Akoz, I. Berkaty and A. Tulgar, "Study of pozzolanic properties of wheat straw ash," *Cement and Concrete Research,* vol. 29, no. 5, pp. 637-643, 1999.

[1.10] A. El-Damatty and I. Hussain, "An economical solution fo the environmental problem resulting from disposal of rice straw," in *ERTEP*, Ghana, Africa, 2007.

[1.11] T. Francisco, J. Paul and R. AustriacoLilia, "compressive strenght of concrete blended with calcined rice straw ash," in *The 3rd ACF International Conference*, Ho Chi Minh, Vietnam, 2008.

[1.12] B. Lothenbach, K. Scrivener and R. Hooton, "Supplementary Cementitious Materials," *Cement and Concrete Research*, vol. 41, p. 1244–1256, 2011.

[1.13] C. Bellido, S. Bolado, M. Coca, S. Lucas, G. González-Benito and M. Teresa García-Cubero, "Effect of inhibitors formed during wheat straw pretreatment on ethanol fermentation by Pichia stipitis," *Bioresource Technology*, vol. 102, p. 10868–10874, 2011.

[1.14] B. C. Saha and M. A. Cotta, "Lime pretreatment, enzymatic saccharification and fermentation of rice hulls to ethanol," *BIOMAS S AND B I OENERGY,* vol. 32, p. 971 – 977, 2008.

[1.15] L. Shi, S. Yu, F.-C. Wang and J. Wang, "Pyrolytic characteristics of rice straw and its constituents catalyzed by internal alkali and alkali earth metals," *Fuel,* vol. 96, p. 586–594, 2012.

[1.16] Y. Zheng, Z. Pan and R. Zhang, "Overview of biomass pretreatment for cellulosic ethanol production," *International Journal of Agricultural and Biological Engineering,* vol. 2, no. 3, pp. 51-68, 2009.

[1.17] D. Chiaramonti, M. Prussi, S. Ferrero, L. Oriani, P. Ottonello, P. Torre and F. Cherchi,

"Review of pretreatment processes for lignocellulosic ethanol production, and development of an innovative method," *Biomass and Bioenergy,* vol. 46, pp. 25-35, 2012.

[1.18] M. Galbe and G. Zacchi, "Pretreatment: The key to efficient utilization of lignocellulosic materials," *Biomass and Bioenergy,* vol. 46, pp. 70-78, 2012.

[1.19] A. Kumar, L. Wang, Y. A. Dzenis, D. D. Jones and M. A. Hanna, "Thermogravimetric characterization of corn stover as gasification and pyrolysis feedstock," *Biomass and Bioenergy,* vol. 32, no. 5, p. 460–467, 2008.

[1.20] D. Mu, T. Seager, P. S. Rao and F. Zhao, "Comparative Life Cycle Assessment of Lignocellulosic Ethanol Production: Biochemical Versus Thermochemical Conversion," *Environmental Management,* vol. 46, pp. 565-578, 2010.

[1.21] a. Z. D. Zongjin Li, "Property improvement of Portland cement by incorporating with metakaolin and slag," *Cement and concrete research,* vol. 33, no. 4, pp. 579-584, 2003.

[1.22] J. W. Bullard, H. M. Jennings, R. A. Livingston, A. Nonat, G. W. Scherer, J. S. Schweitzer, K. L. Scrivener and J. J. Thomas, "Mechanisms of cement hydration," *Cement and Concrete Research,* vol. 41, p. 1208–1223, 2011.

[1.23] K. L. Scrivener and A. Nonat, "Hydration of cementitious materials, present and future," *Cement and Concrete Research,* vol. 41, p. 651–665, 2011.

[1.24] a. N. M. Al-Akhras, "Durability of metakaolin concrete to sulfate attack," *Cement and concrete research,* vol. 36, no. 9, pp. 1727-1734, 2006.

[1.25] X. Cong, S. Gong, D. Darwin and S. L. McCabe, "Role of Silica Fume in Compressive Strength of Cement Paste, Mortar, and Concrete," *ACI Materials Journal,* vol. 89, no. 4, pp. 375-387, 1992.

[1.26] R. D. Hooton, "Influence of Silica Fume Replacement of Cement on Physical Properties and Resistance to Sulfate Attack, Freezing and Thawing, and Alkali-Silica Reactivity," *ACI Materials Journal*, vol. 90, no. 2, pp. 143-151, 1993.

[1.27] A. Behnood and H. Ziari, "Effects of silica fume addition and water to cement ratio on the properties of high-strength concrete after exposure to high temperatures," *Cement and Concrete Composites*, vol. 30, pp. 106-112, 2008.

[1.28] Y.-S. Yoon, J.-P. Won, S.-K. Woo and Y.-C. Song, "Enhanced durability performance of fly ash concrete for concrete-faced rockfill dam application," vol. 32, no. 1, p. 23–30, 2002.

[1.29] N. M. Al-Akhras, "Durability of metakaolin concrete to sulfate attack," vol. 36, no. 9, p. 1727–1734, 2006.

[1.30] D. Roy, P. Arjunan and M. Silsbee, "Effect of silica fume, metakaolin, and low-calcium fly ash on chemical resistance of concrete," *Cement and Concrete Research*, vol. 31, no. 12, p. 1809–181, 2001.

[2.1] A. Salas, S. Delvasto, R. M. Gutierrez and D. Lange, "Comparison of two processes for treating rice husk ash for use in high performance concrete," Cement and Concrete Research, vol. 39, pp. 773-778, 2009.

[2.2] H. Y. M. S. a. S. S. Qingge Feng, "Study on the pozzolanic properties of rice husk ash by hydrochloric acid pretreatment," Cement and concrete research, vol. 36, no. 3, pp. 521-526, 2004.

[2.3] G. Nair, S. Jagadish and A. Fraaij, "Reactive pozzolanas from rice husk ash: An alternative to cement for rural housing," Cement and Concrete Research, vol. 36, no. 6,

pp. 1062-1071, 2006.

[2.4] S. Agarwal, "Pozzolanic activity of various siliceous materials," Cement and Concrete Research, vol. 36, no. 9, pp. 1735-1739, 2006.

[2.5] A. Sales and L. Sofia, "Use of Brazilian sugarcanebagasseash in concrete as sand replacement," Waste Management, vol. 30, no. 6, p. 1114–1122, 2010.

[2.6] N. V. Tuan, G. Ye, K. v. Breugel and O. Copuroglu, "Hydration and microstructure of ultra high performance concrete incorporating rice husk ash," Cement and Concrete Research, vol. 41, p. 1104–1111, 2011.

[2.7] Q. Feng, H. Yamamichi, M. Shoya and S. Sugita, "Study on the pozzolanic properties of rice husk ash by hydrochloric acid pretreatment.”," Cement and Concrete Research, vol. 34, no. 3, pp. 521-526, 2004.

[2.8] S. Wansom, S. Janjaturaphan and S. Sinthupinyo, "Characterizing pozzolanic activity of rice husk ash by impendence spectroscopy," Cement and Concrete Research, vol. 40, no. 12, pp. 1714-1722, 2010.

[2.9] S. Chandrasekhar, P. Pramada and J. Majeed, "Effect of calcination temperature and heating rate on the optical properties and reactivity of rice husk ash," Journal of Materials Science, vol. 41, no. 23, pp. 7926-7933, 2006.

[2.10] Y. Zheng, Z. Pan and R. Zhang, "Overview of biomass pretreatment for cellulosic ethanol production," International Journal of Agricultural and Biological Engineering, vol. 2, no. 3, pp. 51-68, 2009.

[2.11] B. Saha, L. Iten, M. Cotta and Y. Wu, "Dilute acid pretreatment, enzymatic saccharification and fermentation of wheat straw to ethanol," Process Biochemistry, vol.

40, no. 12, pp. 3693-3700, 2005.

[2.12] N. Mosier, C. Wyman, B. Dale, R. Elander, Y. Lee, M. Holtzapple and M. Ladisch, "Features of promising technologies for pretreatment of lignocellulosic biomass," Bioresources Technology, vol. 96, no. 6, pp. 673-686, 2005.

[2.13] B. Jenkins, J. Mannapperuma and R. Bakker, "Biomass leachate treatment by reverse osmosis," Fuel Processing Technology, vol. 81, no. 3, pp. 223-246, 2003.

[2.14] H. Biricik, F. Akoz, I. Berkaty and A. Tulgar, "Study of pozzolanic properties of wheat straw ash," Cement and Concrete Research, vol. 29, no. 5, pp. 637-643, 1999.

[2.15] N. Al-Akhras and B. Abu-Alfoul, "Effect of wheatstrawash on mechanical properties of autoclaved mortar," Cement and Concrete Research, vol. 32, no. 6, pp. 859-863, 2002.

[2.16] T. Francisco, J. Paul and R. AustriacoLilia, "compressive strenght of concrete blended with calcined rice straw ash," in The 3rd ACF International Conference, Ho Chi Minh, Vietnam, 2008.

[2.17] A. El-Damatty and I. Hussain, "An economical solution fo the environmental problem resulting from disposal of rice straw," in ERTEP, Ghana, Africa, 2007.

[2.18] ASTM, "Standard Specification for Portland Cement," C150, p. 10 pp., 2009.

[2.19] S. Sinthaworn and P. Nimityongskul, "Effects of temperature and alkaline solution on electrical conductivity measurements of pozzolanic activity," Cement and Concrete Research, vol. 33, no. 5, pp. 622-627, 2011.

[2.20] S. Sinthaworn and P. Nimityongskul, "Quick monitoring of pozzolanic reactivity of waste ashes," Waste Management, vol. 25, no. 9, pp. 1526-1531, 2009.

[2.21] J. Paya, M. Borrachero, J. Monzo and E. Peris-Mora, "Enhanced conductivity

measurement techniques for evaluation of fly ash pozzolanic activity," Cement and Concrete Research, vol. 31, no. 1, pp. 41-49, 2001.

[2.22] K. Riding, D. Silva and K. Scrivener, "Early age strength of blend cement systems by CaCl2 and diethanol-isopropanolmine," Cement and Concrete Research, vol. 40, no. 6, pp. 935-946, 2010.

[2.23] ASTM, "Standard Test Method for Compressive Strength of Hydraulic Cement Mortars," C109, p. 10 pp, 2008.

[2.24] ASTM, "Standard Practice for Estimating Concrete Strength by the Maturity Method," C1074, p. 10 pp, 2010.

[2.25] A. Muthadhi and S. Kothandaraman, "Optimum production condiction for reactive rice husk ash," Materials and Structures, vol. 43, no. 9, pp. 1303-1315, 2010.

[2.26] S. Genieva, S. Turmanova and L. Vlaev, "Utilization of rice husks and the products of its thermal degradation as fillers in polymer composites," 2011.

[2.27] J. Bullard, H. Jennings, R. Livingston, A. Nonat, G. Scherer, J. Schweitzer, K. Scrivener and J. Thomas, "Mechanisms of cement hydration," Cement and Concrete Research, vol. 41, no. 12, pp. 1208-1223, 2011.

[2.28] K. Scrivener and A. Nonat, "Hydration of cementitious materials, present and future," Cement and Concrete Research, vol. 41, no. 7, pp. 651-665, 2011.

[3.1] H. Goyal, D. Seal and S. R.C., "Bio-fuels from thermochemical conversion of renewable resources: A review," Renewable & Sustainable Energy Reviews, vol. 12, pp. 504-517, 2008.

[3.2] D. Humbird, R. Davis, L. Tao, D. Kinchin, A. Aden, P. Schoen, J. Lukas, B. Olthof, M.

Worley, D. Sexton and D. Duggeon, "Process Design and Economics for Biochemical Conversion of Lignocellulosic Biomass to Ethanol," National Renewable Engergy Labratory, Golden, CO, 2011.

[3.3] B. C. Saha, L. B. Iten, M. A. Cotta and V. Y. Wu, "Dilute acid pretreatment, enzymatic saccharification and fermentation of wheat straw to ethanol," Process Biochemistry, vol. 40, pp. 3693-3700, 2005.

[3.4] N. Al-Akhras and B. Abu-Alfoul, "Effect of wheatstrawash on mechanical properties of autoclaved mortar," Cement and Concrete Research, vol. 32, no. 6, pp. 859-863, 2002.

[3.5] F. F. Ataie and K. A. Riding, "Thermochemical Pretreatments for Agricultural Residue Ash Production for Concrete," Journal of Materials in Civil Engineering, 2012.

[3.6] Q. Feng, H. Yamamichi, M. Shoya and S. Sugita, "Study on the pozzolanic properties of rice husk ash by hydrochloric acid pretreatment.”," Cement and Concrete Research, vol. 34, no. 3, pp. 521-526, 2004.

[3.7] A. El-Damatty and I. Hussain, "An economical solution fo the environmental problem resulting from disposal of rice straw," in ERTEP, Ghana, Africa, 2007.

[3.8] D. Mourant, Z. Wang, M. He, S. Wang, M. Garcia-Perez, K. Ling and C.-Z. Li, "Mallee wood fast pyrolysis: Effects of alkali and alkaline earth metallic species on the yield and composition of bio-oil," Fuel, vol. 90, no. 9, p. 2915–2922, 2011.

[3.9] A. Bridgwater, "Review of fastpyrolysis of biomass and product upgrading," Biomass and Bioenergy, vol. 38, p. 68–94, 2012.

[3.10] H. Wang, R. Srinivasan, F. Yu, P. Steele, Q. Li and B. Mitchell, "Effect of Acid, Alkali, and Steam Explosion Pretreatments on Characteristics of Bio-Oil Produced from

Pinewood," Energy Fuels, vol. 25, no. 8, p. 3758–3764, 2011.

[3.11] D. Nutalapati, R. Gupta, B. Moghtaderi and T. Wall, "Assessing slagging and fouling during biomass combustion: A thermodynamic approach allowing for alkali/ash reactions," Fuel Processing Technology, vol. 88, pp. 1044-1052, 2007.

[3.12] Y. Zheng, Z. Pan and R. Zhang, "Overview of biomass pretreatment for cellulosic ethanol production," International Journal of Agricultural and Biological Engineering, vol. 2, no. 3, pp. 51-68, 2009.

[3.13] A. Salas, S. Delvasto, R. M. Gutierrez and D. Lange, "Comparison of two processes for treating rice husk ash for use in high performance concrete," Cement and Concrete Research, vol. 39, pp. 773-778, 2009.

[3.14] P. Alvira, E. Tomas-Pejo, M. Ballesteros and M. Negro, "Pretreatment technologies for an efficient bioethanol production process based on enzymatic hydrolysis: A review," Bioresource Technology, vol. 101, pp. 4851-4861, 2010.

[3.15] M. Ballesteros, J. Oliva, M. Negro, P. Manzanares and I. Ballesteros, "Ethanol from lignocellulosic materials by a simultaneous saccharification and fermentation process (SFS) with Kluyveromyces marxianus CECT 10875," Process Biochemistry, vol. 39, pp. 1843-1848, 2004.

[3.16] N. Dowe and J. McMillan, "SSF Experimental Protocols-Lignocellulosic Biomass Hydrolysis and Fermentation," NREL, Golden, CO, 2008.

[3.17] A. Standard, "Standard Specification for Portalnd Cement," ASTM International, West Conshohocken, PA, 2009.

[3.18] A. Standard, "C778-12 Standard Specification for Standard Sand," ASTM International,

West Conshohocken, PA, 2012.

[3.19] K. Riding, D. Silva and K. Scrivener, "Early age strength of blend cement systems by CaCl2 and diethanol-isopropanolmine," Cement and Concrete Research, vol. 40, no. 6, pp. 935-946, 2010.

[3.20] A. Standard, "ASTM C109-Standard Test Method for Compressive Strength of Hydraulic Cement Mortars," ASTM International, West Conshohocken, PA, 2008.

[3.21] L. L. Baxter, T. R. Milesb, T. R. J. Miles, B. M. Jenkins, T. Milne, D. Dayton, R. W. Bryers and L. L. Oden, "The behavior of inorganic material in biomass-fired power boilers: field and laboratory experiences," Fuel Processing Technology, vol. 54, no. 1-3, pp. 47-78, 1998.

[3.22] K. Scrivener and A. Nonat, "Hydration of cementitious materials, present and future," Cement and Concrete Research, vol. 41, no. 7, pp. 651-665, 2011.

[4.1] Q. Feng, H. Yamamichi, M. Shoya and S. Sugita, "Study on the pozzolanic properties of rice husk ash by hydrochloric acid pretreatment," Cement and Concrete Research, vol. 34, no. 3, pp. 521-526, 2004.

[4.2] H. Biricik, F. Akoz, I. Berkaty and A. Tulgar, "Study of pozzolanic properties of wheat straw ash," Cement and Concrere Research, vol. 29, no. 5, pp. 637-643, 1999.

[4.3] F. F. Ataie and K. A. Riding, "Thermochemical Pretreatments for Agricultural Residue Ash Production for Concrete," Journal of Materials in Civil Engineering, 2012.

[4.4] A. Bridgwater, "Review of fast pyrolysis of biomass and product upgrading," Biomass and Bioenergy, vol. 38, p. 68–94, 2012.

[4.5] H. Wang, R. Srinivasan, F. Yu, P. Steele, Q. Li and B. Mitchell, "Effect of Acid, Alkali,

and Steam Explosion Pretreatments on Characteristics of Bio-Oil Produced from Pinewood," Energy Fuels, vol. 25, no. 8, p. 3758–3764, 2011.

[4.6] Y. Eom, K.-H. Kim, J.-Y. Kim, S.-M. Lee, H.-M. Yeo and I.-G. Choi, "Characterization of primary thermal degradation features of lignocellulosic biomass after removal of inorganic metals by diverse solvents," Bioresource Technology, vol. 102, p. 3437–3444, 2011.

[4.7] Y. Eom, J.-Y. Kim, T.-S. Kim, S.-M. Lee, D. Choi, I.-G. Choi and J.-W. Choi, "Effect of essential inorganic metals on primary thermal degradation of lignocellulosic biomass," Bioresource Technology, vol. 104, pp. 687-694, 2012.

[4.8] D. J. Nowakowski and J. M. Jones, "Uncatalysed and potassium-catalysedpyrolysis of the cell-wall constituents of biomass and their model compounds," Journal of Analytical and Applied Pyrolysis, vol. 83, no. 1, pp. 12-25, 2008.

[4.9] H. Yang, R. Yan, H. Chen, C. Zheng, D.-H. Lee and D.-T. Liang, "In-Depth Investigation of Biomass Pyrolysis Based on Three Major Components: Hemicellulose, Cellulose and Lignin," Energy Fuels, vol. 20, no. 1, p. 388–393, 2006.

[4.10] Q. Liu, Z. Zhong, S. Wang and Z. Luo, "Interactions of biomass components during pyrolysis: A TG-FTIR study," Journal of Analytical and Applied Pyrolysis, vol. 90, pp. 213-318, 2012.

[4.11] N. Mosier, C. Wyman, B. Dale, R. Elander, Y. Lee, M. Holtzapple and M. Ladisch, "Features of promising technologies for pretreatment of lignocellulosic biomass," Bioresources Technology, vol. 96, no. 6, pp. 673-686, 2005.

[4.12] X. Wei, U. Schnell and K. R. Hein, "Behaviour of gaseous chlorine and alkali metals

during biomass thermal utilisation," Fuel, vol. 84, p. 841–848, 2005.

[4.13] K. Davidson, B. Stojkova and J. Pettersson, "Alkali emission from birchwood particles during rapid pyrolysis," Energy Fuels, vol. 16, p. 1033–1099, 2002.

[5.1] B. Yang and C. E. Wyman, "Pretreatment: the key to unlocking low-cost cellulosic ethanol," biofuels bioproducts and biorefining, vol. 2, pp. 26-40, 2007.

[5.2] M. Galbe and G. Zacchi, "Pretreatment: The key to efficient utilization of lignocellulosic materials," Biomass and Bioenergy, vol. 46, pp. 70-78, 2012.

[5.3] D. Chiaramonti, M. Prussi, S. Ferrero, L. Oriani, P. Ottonello, P. Torre and F. Cherchi, "Review of pretreatment processes for lignocellulosic ethanol production, and development of an innovative method," Biomass and Bioenergy, vol. 46, pp. 25-35, 2012.

[5.4] C. Bellido, S. Bolado, M. Coca, S. Lucas, G. González-Benito and M. Teresa García-Cubero, "Effect of inhibitors formed during wheat straw pretreatment on ethanol fermentation by Pichia stipitis," Bioresource Technology, vol. 102, p. 10868–10874, 2011.

[5.5] B. C. Saha and M. A. Cotta, "Lime pretreatment, enzymatic saccharification and fermentation of rice hulls to ethanol," BIOMAS S AND B I OENERGY, vol. 32, p. 971 – 977, 2008.

[5.6] L. Shi, S. Yu, F.-C. Wang and J. Wang, "Pyrolytic characteristics of rice straw and its constituents catalyzed by internal alkali and alkali earth metals," Fuel, vol. 96, p. 586–594, 2012.

[5.7] I. Kim and J.-I. Han, "Optimization of alkaline pretreatment conditions for enhancing glucose yield of rice straw by response surface methodology," Biomass and Bioenergy, vol. 46, pp. 2 1 0 -2 1 7, 2012.

[5.8] A. Kumar, L. Wang, Y. A. Dzenis, D. D. Jones and M. A. Hanna, "Thermogravimetric characterization of corn stover as gasification and pyrolysis feedstock," Biomass and Bioenergy, vol. 32, no. 5, p. 460–467, 2008.

[5.9] D. Mu, T. Seager, P. S. Rao and F. Zhao, "Comparative Life Cycle Assessment of Lignocellulosic Ethanol Production: Biochemical Versus Thermochemical Conversion," Environmental Management, vol. 46, pp. 565-578, 2010.

[5.10] Y. Zheng, Z. Pan and R. Zhang, "Overview of biomass pretreatment for cellulosic ethanol production," International Journal of Agricultural and Biological Engineering, vol. 2, no. 3, pp. 51-68, 2009.

[5.11] Q. Feng, H. Yamamichi, M. Shoya and S. Sugita, "Study on the pozzolanic properties of rice husk ash by hydrochloric acid pretreatment," Cement and Concrete Research, vol. 34, no. 3, pp. 521-526, 2004.

[5.12] F. F. Ataie and K. A. Riding, "Thermochemical Pretreatments for Agricultural Residue Ash Production for Concrete," Journal of Materials in Civil Engineering, 2012.

[5.13] U. Kaur, H. S. Oberoi, V. K. Bhargav, R. Sharma-Shivappa and S. S. Dhaliwal, "Ethanol production from alkali- and ozone-treated cotton stalks using thermotolerant Pichia kudriavzevii HOP-1," Industrial Crops and Products, vol. 37, p. 219– 226, 2012.

[5.14] D. J. SCHELL, J. FARMER, M. NEWMAN and J. D. MCMILLAN, "Dilute–Sulfuric Acid Pretreatment of Corn Stover in Pilot-Scale Reactor," Applied Biochemistry and Biotechnology, vol. 105, pp. 69-85, 2003.

[5.15] Y. Sun and J. J. Cheng, "Dilute acid pretreatment of rye straw and bermudagrass for ethanol production," Bioresource Technology, vol. 96, p. 1599–1606, 2005.

[5.16] F. Domingues, J. Queiroz, J. Cabral and L. Fonseca, "The influence of culture conditions on mycelial structure and cellulase production by Trichoderma reesei Rut C-30," Enzyme and Microbial Technology, vol. 26, p. 394–401, 2000.

[5.17] J. Xu, J. J. Cheng, R. R. Sharma-Shivappa and J. C. Burns, "Sodium Hydroxide Pretreatment of Switchgrass for Ethanol Production," Energy and Fuels, vol. 24, p. 2113–2119, 2010.

[5.18] H. A. CURRIE and C. C. PERRY, "Silica in Plants: Biological, Biochemical and Chemical Studies," Annals of Botany: Oxford Journals, vol. 100, p. 1383–1389, 2007.

[5.19] H. He, T. M. Bleby, E. J. Veneklaas, H. Lambers and J. Kuo, "Morphologies and elemental compositions of calcium crystals in phyllodes and branchlets of Acacia robeorum," Annals of Botany: Oxford Journals, pp. 1-10, 2011.

[5.20] M. A. Webb, "Cell-Mediated Crystallization of Calcium Oxalate in Plants," The Plant Cell, vol. 11, p. 751–761, 199.

[5.21] N. Palmer and M. V. Palmer, "Geochemistry of capillary seepage in Mammoth Cave," in Proc. of the 4th Mammoth Cave Science Conference, Mammoth Cave , KY, 1995.

[5.22] K. B. Krauskopf and D. K. Bird, Introduction To Geochemistry, 3rd ed., McGraw-Hill, 1994, p. Chapter 4.

[5.23] R. K. Iler, The Chemistry of Silica: Solubility, Polymerization, Colloid and Surface Properties and Biochemistry of Silica, Wiley-Interscience, 1979, pp. 3-100.

[5.24] P. Y. Duggirala, "Formation of Calcium Carbonate Scale and Control Strategies in Continuous Digesters," Nalco Company.

[5.25] P. SIPPONEN and M. HÄRKÖNEN, "Hypochlorhydric stomach: a risk condition for

calcium malabsorption and osteoporosis," Scandinavian Journal of Gastroenterology, vol. 45, p. 133–138, 2010.

[5.26] N. P. Rao, Urinary Tract Stone Disease, Springer, 2011, p. 21.

[5.27] J. C. Lieske, "mayo medica llaboratories," Feb. 2010. [Online]. Available: http://www.mayomedicallaboratories.com/articles/hottopics/transcripts/2010/2010-2a-kidney-stones/2a-24.html. [Accessed 19 June 2013].

[5.28] D. J. Nowakowski and J. M. Jones, "Uncatalysed and potassium-catalysedpyrolysis of the cell-wall constituents of biomass and their model compounds," Journal of Analytical and Applied Pyrolysis, vol. 83, no. 1, pp. 12-25, 2008.

[5.29] Y. Eom, J.-Y. Kim, T.-S. Kim, S.-M. Lee, D. Choi, I.-G. Choi and J.-W. Choi, "Effect of essential inorganic metals on primary thermal degradation of lignocellulosic biomass," Bioresource Technology, vol. 104, pp. 687-694, 2012.

[6.1] M. T. Ley, N. J. Harris, K. J. Folliard and K. C. Hover, "Investigation of Air-Entraining Admixture Dosage in Fly Ash Concrete," ACI Materials Journal, vol. 105, no. 5, pp. 494-498, 2008.

[6.2] I. Kulaots, A. Hsu, R. H. Hurt and E. M. Suuberg, "Size distribution of unburned carbon in coal fly ash and its implications," Fuel, vol. 83, pp. 223-230, 2004.

[6.3] J. P. Blatrus and R. B. LaCount, "Measurement of adsorption of air-entraining admixture on fly ash in concrete and cement," Cement and Concrete Research, vol. 31, pp. 819-824, 2001.

[6.4] I. Kulaots, A. Hsu, R. H. Hurt and E. M. Suuberg, "Adsorption of surfactants on unburned carbon in fly ash and development of a standardized foam index test," Cement and

Concrete Research, vol. 33, pp. 2091-2099, 2003.

[6.5] F. F. Ataie and K. A. Riding, "Thermochemical Pretreatments for Agricultural Residue Ash Production for Concrete," Journal of Materials in Civil Engineering, 2012.

[6.6] ASTM, "Standard Specification for Portland Cement," C150, p. 10 pp., 2009.

[6.7] ASTM C 618, Standard Specification for Coal Fly Ash and Raw or Calcined Natural Pozzolan for Use in Concrete, West Conshohocken, PA: ASTM International, 2005, p. 3 pp..

[6.8] ASTM C 1240, Standard Specification for Silica Fume Used in Cementitious Mixtures, West Conshohocken, PA: ASTM International, 2012, p. 3 pp..

[6.9] A. Standard, "D2419-09- Standard Test Method for Sand Equivalent Value of Soils and Fine Aggregate," ASTM International, West Conshohocken, PA, 2009.

[7.1] W. Zhang, Y. Zhang, L. Liu, G. Zhang and Z. Liu, "Investigation of the influence of curing temperature and silica fume content on setting and hardening process of the blended cement paste by an improved ultrasonic apparatus," Construction and Building Materials, vol. 33, pp. 32-40, 2012.

[7.2] E.-H. Kadri and R. Duval, "Hydration heat kinetics of concrete with silica fume," Construction and Building Materials, vol. 23, p. 3388–3392, 2009.

[7.3] A. Behnood and H. Ziari, "Effects of silica fume addition and water to cement ratio on the properties of high-strength concrete after exposure to high temperatures," Cement and Concrete Composites, vol. 30, pp. 106-112, 2008.

[7.4] R. D. Hooton, "Influence of Silica Fume Replacement of Cement on Physical Properties and Resistance to Sulfate Attack, Freezing and Thawing, and Alkali-Silica Reactivity,"

ACI Materials Journal, vol. 90, no. 2, pp. 143-151, 1993.

[7.5] X. Cong, S. Gong, D. Darwin and S. L. McCabe, "Role of Silica Fume in Compressive Strength of Cement Paste, Mortar, and Concrete," ACI Materials Journal, vol. 89, no. 4, pp. 375-387, 1992.

[7.6] S. Caliskan, "Aggregate/mortar interface: influence of silica fume at the micro- and macro-level," Cement and Concrete Composites, vol. 23, p. 557–564, 2003.

[7.7] Q. Feng, H. Yamamichi, M. Shoya and S. Sugita, "Study on the pozzolanic properties of rice husk ash by hydrochloric acid pretreatment.”," Cement and Concrete Research, vol. 34, no. 3, pp. 521-526, 2004.

[7.8] F. F. Ataie and K. A. Riding, "Thermochemical Pretreatments for Agricultural Residue Ash Production for Concrete," Journal of Materials in Civil Engineering, 2012.

[7.9] A. Salas, S. Delvasto, R. M. d. Gutierrez and D. Lange, "Comparison of two processes for treating rice husk ash for use in high performance concrete," Cement and Concrete Research, vol. 39, pp. 773-778, 2009.

[7.10] N. V. Tuan, G. Ye, K. v. Breugel, A. L. Fraaij and B. D. Dai, "The study of using rice husk ash to produce ultra high performance concrete," Construction and Building Materials, vol. 25, p. 2030–2035, 2011.

[7.11] B. Lothenbach, K. Scrivener and R. Hooton, "Supplementary Cementitious Materials," Cement and Concrete Research, vol. 41, p. 1244–1256, 2011.

[7.12] R. Largent, "Estimation de l’activite pouzzolanique," Bull Liaison Lab Pont, Pont Chaussee, vol. 93, pp. 61-65, 1978.

[7.13] A. Standard, "Standard Specification for Portalnd Cement," ASTM International, West

Conshohocken, PA, 2009.

[7.14] A. Standard, "C778-12 Standard Specification for Standard Sand," ASTM International, West Conshohocken, PA, 2012.

[7.15] H. Rietveld, "Line profiles of neutron powder-diffraction peaks for structure refinement," Acta Crystallographica, vol. 22, pp. 151-152., 1967.

[7.16] H. Rietveld, "A profile refinement method for nuclear and magnetic structures," Journal of Applied Crystallography, vol. 2, pp. 65-71, 1969.

[7.17] R. Chancey, P. Stutzman, M. Juenger and D. Fowler, "Comprehensive phase characterization of crystalline and amorphous phases of a Class F fly ash," vol. 40, pp. 146-156, 2010.

[7.18] B. Toby, "R-factors in Rietveld analysis: How good is good enough?," Powder Diffraction, vol. 21, no. 1, pp. 67-70, 2006.

[7.19] W. I. F. David, "Powder Diffraction:Least-Squares and Beyond," J. Res. Natl. Inst. Stand. Technol., vol. 109, pp. 107-123, 2004.

[7.20] K. Riding, D. Silva and K. Scrivener, "Early age strength of blend cement systems by CaCl2 and diethanol-isopropanolmine," Cement and Concrete Research, vol. 40, no. 6, pp. 935-946, 2010.

[7.21] N. V. Tuan, G. Ye, K. v. Breugel and O. Copuroglu, "Hydration and microstructure of ultra high performance concrete incorporating rice husk ash," Cement and Concrete Research, vol. 41, p. 1104–1111, 2011.

[7.22] S. Bishnoi, "Automated Chemical Shrinkage Test and Shrinkage Suite Software," 2009.

[7.23] A. Standard, "ASTM C109-Standard Test Method for Compressive Strength of Hydraulic

Cement Mortars," ASTM International, West Conshohocken, PA, 2008.

[7.24] K. Scrivener and A. Nonat, "Hydration of cementitious materials, present and future," Cement and Concrete Research, vol. 41, no. 7, pp. 651-665, 2011.